

Technical Bases for Inspection Requirements for PWR Steam Generator Class 1 Nozzle-to-Vessel Welds and Class 1 and Class 2 Vessel Head, Shell, Tubesheet-to-Head, and Tubesheet-to-Shell Welds

2019 TECHNICAL REPORT

Technical Bases for Inspection Requirements for PWR Steam Generator Class 1 Nozzle-to-Vessel Welds and Class 1 and Class 2 Vessel Head, Shell, Tubesheet-to- Head, and Tubesheet-to-Shell Welds

3002015906

EPRI Project Managers
R. Grizzi
A. Cinson

All or a portion of the requirements of the EPRI Nuclear
Quality Assurance Program apply to this product.

YES



ELECTRIC POWER RESEARCH INSTITUTE

3420 Hillview Avenue, Palo Alto, California 94304-1338 • PO Box 10412, Palo Alto, California 94303-0813 • USA
800.313.3774 • 650.855.2121 • askepri@epri.com • www.epri.com

DISCLAIMER OF WARRANTIES AND LIMITATION OF LIABILITIES

THIS DOCUMENT WAS PREPARED BY THE ORGANIZATION NAMED BELOW AS AN ACCOUNT OF WORK SPONSORED OR COSPONSORED BY THE ELECTRIC POWER RESEARCH INSTITUTE, INC. (EPRI). NEITHER EPRI, ANY MEMBER OF EPRI, ANY COSPONSOR, THE ORGANIZATION BELOW, NOR ANY PERSON ACTING ON BEHALF OF ANY OF THEM:

(A) MAKES ANY WARRANTY OR REPRESENTATION WHATSOEVER, EXPRESS OR IMPLIED, (I) WITH RESPECT TO THE USE OF ANY INFORMATION, APPARATUS, METHOD, PROCESS, OR SIMILAR ITEM DISCLOSED IN THIS DOCUMENT, INCLUDING MERCHANTABILITY AND FITNESS FOR A PARTICULAR PURPOSE, OR (II) THAT SUCH USE DOES NOT INFRINGE ON OR INTERFERE WITH PRIVATELY OWNED RIGHTS, INCLUDING ANY PARTY'S INTELLECTUAL PROPERTY, OR (III) THAT THIS DOCUMENT IS SUITABLE TO ANY PARTICULAR USER'S CIRCUMSTANCE; OR

(B) ASSUMES RESPONSIBILITY FOR ANY DAMAGES OR OTHER LIABILITY WHATSOEVER (INCLUDING ANY CONSEQUENTIAL DAMAGES, EVEN IF EPRI OR ANY EPRI REPRESENTATIVE HAS BEEN ADVISED OF THE POSSIBILITY OF SUCH DAMAGES) RESULTING FROM YOUR SELECTION OR USE OF THIS DOCUMENT OR ANY INFORMATION, APPARATUS, METHOD, PROCESS, OR SIMILAR ITEM DISCLOSED IN THIS DOCUMENT.

REFERENCE HEREIN TO ANY SPECIFIC COMMERCIAL PRODUCT, PROCESS, OR SERVICE BY ITS TRADE NAME, TRADEMARK, MANUFACTURER, OR OTHERWISE, DOES NOT NECESSARILY CONSTITUTE OR IMPLY ITS ENDORSEMENT, RECOMMENDATION, OR FAVORING BY EPRI.

THE FOLLOWING ORGANIZATION, UNDER CONTRACT TO EPRI, PREPARED THIS REPORT:

Structural Integrity Associates, Inc.

THE TECHNICAL CONTENTS OF THIS PRODUCT WERE **NOT** PREPARED IN ACCORDANCE WITH THE EPRI QUALITY PROGRAM MANUAL THAT FULFILLS THE REQUIREMENTS OF 10 CFR 50, APPENDIX B. THIS PRODUCT IS **NOT** SUBJECT TO THE REQUIREMENTS OF 10 CFR PART 21.

NOTE

For further information about EPRI, call the EPRI Customer Assistance Center at 800.313.3774 or e-mail askepri@epri.com.

Electric Power Research Institute, EPRI, and TOGETHER...SHAPING THE FUTURE OF ELECTRICITY are registered service marks of the Electric Power Research Institute, Inc.

Copyright © 2019 Electric Power Research Institute, Inc. All rights reserved.

ACKNOWLEDGMENTS

The following organization, under contract to the Electric Power Research Institute (EPRI), prepared this report:

Structural Integrity Associates, Inc.
5215 Hellyer Ave., Suite 210
San Jose, CA 95138

Principal Investigators

N. Cofie
C. Lohse
D. Dedhia
D. J. Shim
M. Fong
D. Somasundaram
S. Chesworth

This report describes research sponsored by EPRI.

The following EPRI subject matter expert performed independent technical reviews of this report:

G. Stevens, Technical Executive

This publication is a corporate document that should be cited in the literature in the following manner:

Technical Bases for Inspection Requirements for PWR Steam Generator Class 1 Nozzle-to-Vessel Welds and Class 1 and Class 2 Vessel Head, Shell, Tubesheet-to-Head, and Tubesheet-to-Shell Welds. EPRI, Palo Alto, CA: 2019. 3002015906.

ABSTRACT

Welds in pressurized water reactor (PWR) steam generators (SGs) are subjected to periodic examination under American Society of Mechanical Engineers (ASME) Code, Section XI. Through the Electric Power Research Institute, the power industry has undertaken a study to determine whether the inspection requirements for these components can be optimized based on operating history, the results of in-service examinations performed to date, and flaw tolerance evaluations. This report focuses on the Class 1 nozzle-to-vessel welds and the Class 1 and Class 2 vessel head, shell, tubesheet-to-head, and tubesheet-to-shell welds in SGs. These welds are listed under the following examination categories in Tables IWB-2500-1 and IWC-2500-1 of ASME Code, Section XI: Class 1, Category B-B, pressure-retaining welds in vessels other than reactor vessels; Class 1, Category B-D, full penetration welded nozzles in vessels; and Class 2, Category C-A, pressure-retaining welds in pressure vessels.

The objectives of this report are to evaluate the current examination requirements for the subject welds and establish the technical bases for various alternative inspection scenarios. The report includes a review of previous related projects, a review of inspection history and results, a survey of components in the industry, selection of representative components and operating transients for stress analysis, evaluation of potential degradation mechanisms, and a flaw tolerance evaluation consisting of probabilistic and deterministic fracture mechanics analyses. Based on the evaluations performed in this report, the technical bases are provided for various ASME Code, Section XI inspection schedules for these PWR steam generator welds. The evaluations show that once pre-service inspection has been performed, no other inspections are required to maintain plant safety for up to 80 years of operation.

Keywords

American Society of Mechanical Engineers (ASME) Boiler and Pressure Vessel Code,
Section XI

Nozzle-to-vessel weld

Tubesheet-to-shell weld

Vessel head weld

Vessel shell weld

Volumetric examination

Deliverable Number: 3002015906

Product Type: Technical Report

Product Title: Technical Bases for Inspection Requirements for PWR Steam Generator Class 1 Nozzle-to-Vessel Welds and Class 1 and Class 2 Vessel Head, Shell, Tubesheet-to-Head, and Tubesheet-to-Shell Welds

PRIMARY AUDIENCE: In-service inspection program engineers for nuclear utilities

SECONDARY AUDIENCE: Technical staff for nuclear utilities and regulators

KEY RESEARCH QUESTION

Utilities would benefit by optimizing their examinations of the components of the steam generators (SGs) of pressurized water reactors (PWRs) in a way that does not compromise plant safety or reliability. Based on the operating history of a specific set of such components combined with flaw tolerance evaluations, can technical bases be established for various inspection scenarios defined in American Society of Mechanical Engineers (ASME) Code, Section XI?

RESEARCH OVERVIEW

Factors considered in establishing the technical bases for a variety of inspection scenarios for PWR SG components consisted of operating history, inspection results to date, and flaw tolerance evaluations involving probabilistic and deterministic fracture mechanics analyses considering potential applicable degradation mechanisms (corrosion fatigue, mechanical fatigue, and thermal fatigue).

KEY FINDINGS

- The entire industry was surveyed to collect the number of examinations performed and the associated examination results for Item Nos. B2.31, B2.32, B2.40, B3.130, C1.10, C1.20, and C1.30, including the PWR SG components evaluated in this report. The survey results showed that out of a combined total of 1,374 examinations performed on Item Nos. B2.31, B2.32, B2.40, B3.130, C1.10, C1.20, and C1.30 components, two PWR units reported flaws in Item No. B2.40 components and two PWR units reported flaws in Item No. C1.20 components that exceeded ASME Code, Section XI acceptance standards and required flaw evaluation for acceptability. None of the flaws was considered service-induced.
- A degradation mechanism evaluation was performed for the PWR SG Item Nos. B2.31, B2.32, B2.40, B3.130, C1.10, C1.20, and C1.30 components. The only potentially significant degradation mechanisms for these components are corrosion fatigue, mechanical fatigue, and thermal fatigue. These mechanisms were therefore considered in the fracture mechanics evaluation for these components.

- Probabilistic fracture mechanics evaluations were performed and showed that a regulatory safety goal of 10^{-6} failures per year would be met for various inspection scenarios. This was supplemented by deterministic fracture mechanics evaluations that showed that the components are very flaw-tolerant.
- The current ASME Code, Section XI inspection schedules for the PWR SG Item Nos. B2.31, B2.32, B2.40, B3.130, C1.10, C1.20, and C1.30 components can be revised without compromising plant safety.

WHY THIS MATTERS

Establishing the technical bases for alternative inspection scenarios for a specific set of PWR SG components—based on operating history, inspection results to date, and evaluation of potentially significant degradation mechanisms—provides the benefit of possible optimization of these examinations in the future, potentially reducing the health and safety risks to personnel, promoting improved as-low-as-reasonably-achievable (ALARA) practices, and decreasing overall inspection burdens, all without adversely impacting the safe operations of nuclear facilities.

HOW TO APPLY RESULTS

This report develops technical bases for various inspection scenarios using inputs that are designed to evaluate the applicable range of conditions experienced at operating reactors. Section 9 defines how to apply these technical bases to a given plant based on key criteria that determine whether the results of these analyses bound actual plant operation.

LEARNING AND ENGAGEMENT OPPORTUNITIES

- Industry advisors have contributed to the review of this report.

EPRI CONTACT: Robert Grizzi, Program Manager, rgrizzi@epri.com

PROGRAMS: Nuclear Power, P41 and Nondestructive Evaluation, P41.04.01

IMPLEMENTATION CATEGORY: Technical Basis Reference

Together...Shaping the Future of Electricity®

Electric Power Research Institute

3420 Hillview Avenue, Palo Alto, California 94304-1338 • PO Box 10412, Palo Alto, California 94303-0813 USA

800.313.3774 • 650.855.2121 • askepri@epri.com • www.epri.com

© 2017 Electric Power Research Institute (EPRI), Inc. All rights reserved. Electric Power Research Institute, EPRI, and TOGETHER...SHAPING THE FUTURE OF ELECTRICITY are registered service marks of the Electric Power Research Institute, Inc.

ACRONYMS, ABBREVIATIONS, AND SYMBOLS

2-D	two-dimensional
3-D	three-dimensional
ANO-1	Arkansas Nuclear One, Unit 1
ASME	American Society of Mechanical Engineers
B&W	Babcock & Wilcox
BWR	boiling water reactor
BWRVIP	BWR Vessel and Internals Project
CC	Code Case
CE	Combustion Engineering
CRD	control rod drive
DFM	deterministic fracture mechanics
EAF	environmental assisted fatigue
ECSCC	external chloride stress corrosion cracking
EFPY	effective full power years
EPRI	Electric Power Research Institute
FAC	flow-accelerated corrosion
FCG	fatigue crack growth
FEA	finite-element analysis
FEM	finite-element model
FSAR	Final Safety Analysis Report
HX	heat exchanger
IGSCC	intergranular stress corrosion cracking
IN	Information Notice (NRC)
ISI	in-service inspection
K	applied stress intensity factor

K _{IC}	fracture toughness
MIC	microbiologically influenced corrosion
MRP	Materials Research Project (EPRI)
MS	main steam
NPS	nominal pipe size
NRC	U.S. Nuclear Regulatory Commission
NSSS	nuclear steam supply system
OD	outside diameter
OTSG	once-through steam generator
PDI	Performance Demonstration Initiative
PFM	probabilistic fracture mechanics
POD	probability of detection
PSI	pre-service inspection
PVRUF	Pressure Vessel Research User's Facility
PWHT	post-weld heat treatment
PWR	pressurized water reactor
PWSCC	primary water stress corrosion cracking
RCP	reactor coolant pump
RG	Regulatory Guide (NRC)
RI-ISI	risk-informed in-service inspection
RPV	reactor pressure vessel
RSG	replacement steam generator
R/t	radius-to-thickness (ratio)
SCC	stress corrosion cracking
SE	Safety Evaluation (NRC)
SG	steam generator
TASCS	thermal stratification, cycling, and striping
TGSCC	transgranular stress corrosion cracking
V&V	verification and validation
xLPR	extremely low probability of rupture
W	Westinghouse

UNITS CONVERSION FACTORS

$$1 \text{ in.} = 2.54 \text{ cm} = 25.4 \text{ mm}$$

$$1^{\circ}\text{F} = 1.8^{\circ}\text{C} + 32$$

$$1^{\circ}\text{F}\Delta = 1.8^{\circ}\text{C}\Delta$$

$$1 \text{ psi} = 6,895 \text{ Pa} = 6.895 \times 10^{-3} \text{ MPa}$$

$$1 \text{ BTU} = 1,055 \text{ J}$$

$$1 \text{ lb} = 0.454 \text{ kg}$$

$$1 \text{ ft} = 30.48 \text{ cm} = 304.8 \text{ mm}$$

$$1 \text{ ksi} = 6.895 \text{ MPa}$$

$$1 \text{ ksi}\sqrt{\text{in.}} = 1.099 \text{ MPa}\sqrt{\text{m}}$$

CONTENTS

ABSTRACT	V
EXECUTIVE SUMMARY	VII
ACRONYMS, ABBREVIATIONS, AND SYMBOLS.....	IX
UNITS CONVERSION FACTORS.....	XI
1 INTRODUCTION	1-1
1.1 Background	1-1
1.2 Objective	1-10
2 REVIEW OF PREVIOUS RELATED PROJECTS.....	2-1
2.1 Nozzle-to-Vessel Welds	2-1
2.2 Vessel Shell Welds.....	2-3
2.3 Related Work	2-4
2.4 Concluding Remarks.....	2-5
3 REVIEW OF INSPECTION HISTORY AND EXAMINATION EFFECTIVENESS	3-1
3.1 Summary of Survey Results.....	3-1
3.2 Concluding Remarks.....	3-3
4 SURVEY OF COMPONENTS AND SELECTION OF REPRESENTATIVE COMPONENTS FOR ANALYSIS	4-1
4.1 Steam Generators and NSSS Suppliers	4-1
4.2 SG Operating Experience	4-5
4.3 Variation Among SG Designs.....	4-5
4.3.1 Dimensions.....	4-6
4.3.2 Design Pressures and Temperatures.....	4-7
4.3.3 ASME Code Design Considerations.....	4-8
4.4 Configurations with Impractical or Limited Exams.....	4-9

4.5 Selection of Components for Evaluation	4-9
4.5.1 SG Primary-Side Nozzles	4-9
4.5.2 SG Primary-Side Head	4-11
4.5.2.1 Item No. B2.31: Steam Generator (Primary Side) Head Circumferential Welds	4-11
4.5.2.2 Item No. B2.32: Steam Generator (Primary Side) Head Meridional Welds	4-12
4.5.2.3 Item No. B2.40: Steam Generator (Primary Side) Tubesheet-to-Head Welds	4-12
4.5.3 SG Secondary-Side Shell	4-12
4.5.3.1 Item No. C1.10: Class 2 Vessel Shell Circumferential Welds	4-12
4.5.3.2 Item No. C1.20: Class 2 Vessel Head Circumferential Welds	4-13
4.5.3.3 Item No. C1.30: Class 2 Vessel Tubesheet-to-Shell Welds	4-13
4.6 Conclusions	4-13
5 MATERIALS PROPERTIES, OPERATING LOADS, AND TRANSIENTS	5-1
5.1 Materials Selection and Properties	5-1
5.2 Operating Loads and Transients	5-5
5.2.1 Operating Conditions for PWR SG Vessel (Primary Side) Welds (Item Nos. B2.31, B2.32, and B2.40)	5-8
5.2.2 Operating Conditions for SG Inlet Nozzle-to-Vessel Welds (Item No. B3.130)	5-10
5.2.3 Operating Conditions for PWR SG Vessel (Secondary Side) Welds (Item Nos. C1.10, C1.20, and C1.30)	5-11
6 EVALUATION OF POTENTIAL DEGRADATION MECHANISMS	6-1
6.1 Degradation Mechanisms	6-1
6.2 Degradation Mechanism Evaluation	6-2
6.2.1 Intergranular Stress Corrosion Cracking	6-2
6.2.2 Transgranular Stress Corrosion Cracking	6-2
6.2.3 External Chloride Stress Corrosion Cracking	6-3
6.2.4 Primary Water Stress Corrosion Cracking	6-3
6.2.5 Corrosion Fatigue	6-3
6.2.6 Microbiologically Influenced Corrosion	6-4
6.2.7 Pitting	6-4
6.2.8 Crevice Corrosion	6-4
6.2.9 Erosion-Cavitation	6-4
6.2.10 Erosion	6-5

6.2.11 Flow-Accelerated Corrosion	6-5
6.2.12 Corrosion/Wastage	6-5
6.2.13 Galvanic Corrosion	6-6
6.2.14 Thermal Stratification, Cycling, and Striping.....	6-6
6.2.15 Thermal Transients.....	6-6
6.2.16 Mechanical Fatigue	6-6
6.3 Conclusions.....	6-7
7 COMPONENT STRESS ANALYSIS	7-1
7.1 Stress Analysis for PWR SG Inlet Nozzle-to-Vessel Welds (Item No. B3.130).....	7-2
7.1.1 Finite-Element Model.....	7-2
7.1.2 Pressure/Thermal Stress Analysis	7-3
7.1.2.1 Internal Pressure Loading Analysis	7-3
7.1.2.2 Thermal Heat Transfer Analyses	7-5
7.1.2.3 Thermal Stress Analyses	7-7
7.1.3 Stress Analysis Results	7-9
7.2 Stress Analysis for PWR SG Vessel Welds (Item Nos. B2.31, B2.32, B2.40, C1.10, C1.20, and C1.30)	7-20
7.2.1 Finite-Element Model.....	7-20
7.2.2 Pressure/Thermal Stress Analysis	7-20
7.2.2.1 Internal Pressure Loading Analysis	7-20
7.2.2.2 Thermal Heat Transfer Analyses	7-20
7.2.2.3 Thermal Stress Analyses	7-23
7.2.3 Stress Analysis Results	7-23
8 DETERMINISTIC AND PROBABILISTIC FRACTURE MECHANICS EVALUATION	8-1
8.1 Overview of Technical Approach.....	8-1
8.2 DFM Evaluation.....	8-3
8.2.1 Technical Approach.....	8-3
8.2.2 Design Inputs.....	8-3
8.2.2.1 Geometry	8-3
8.2.2.2 Initial Crack Size and Shape.....	8-3
8.2.2.3 Applied Stresses	8-4
8.2.2.3.1 Operating Transient Stresses	8-4
8.2.2.3.2 Weld Residual Stresses	8-4
8.2.2.4 Fracture Mechanics Models.....	8-4

8.2.2.5 Fracture Toughness.....	8-5
8.2.2.6 Fatigue Crack Growth Law	8-6
8.2.2.7 Summary of Design Inputs.....	8-6
8.2.3 Results of DFM Evaluation	8-7
8.3 PFM Evaluation	8-8
8.3.1 Technical Approach.....	8-8
8.3.1.1 Treatment of Uncertainties	8-9
8.3.1.2 Sampling Method	8-9
8.3.2 Details of Analysis Methodology and Inputs.....	8-10
8.3.2.1 Component Geometry.....	8-10
8.3.2.2 Initial Flaw Distribution and Number of Flaws per Weld	8-10
8.3.2.3 Probability of Detection Curve	8-11
8.3.2.4 Applied Stresses	8-12
8.3.2.5 Fracture Mechanics Models.....	8-12
8.3.2.6 Fatigue Crack Growth	8-12
8.3.2.7 Fracture Toughness.....	8-13
8.3.2.8 Inspection Schedule Scenarios.....	8-13
8.3.2.9 Acceptance Criterion.....	8-14
8.3.2.10 Limitations and Assumptions	8-14
8.3.3 Computer Software Application	8-14
8.3.3.1 Software Development	8-14
8.3.3.2 Software Verification and Validation	8-15
8.3.3.2.1 Software Testing	8-15
8.3.3.2.2 Benchmarking	8-16
8.3.4 Base Case, Sensitivity Analysis, and Sensitivity Studies	8-17
8.3.4.1 Base-Case Evaluation	8-17
8.3.4.1.1 Effect of Various In-Service Inspection Scenarios	8-19
8.3.4.2 Sensitivity Analyses	8-20
8.3.4.3 Sensitivity Studies.....	8-22
8.3.4.3.1 Sensitivity to Fracture Toughness.....	8-22
8.3.4.3.2 Sensitivity to Stresses	8-26
8.3.4.3.3 Sensitivity to Initial Crack Depth Distribution.....	8-30
8.3.4.3.4 Sensitivity to Number of Flaws.....	8-32
8.3.4.3.5 Sensitivity to the Distribution of Number of Flaws.....	8-34
8.3.4.3.6 Sensitivity to Crack Size Distribution.....	8-35

8.3.4.3.7 Sensitivity to Crack Growth Rate	8-35
8.3.4.3.8 Sensitivity to POD Curves	8-36
8.3.4.3.9 Sensitivity to Inspection Schedules Using Two Different PODs.....	8-38
8.3.4.3.10 Sensitivity to Number of Realizations.....	8-39
8.3.4.3.11 Sensitivity Study to Determine Combined Effect of Important Parameters.....	8-40
8.3.5 Inspection Coverage.....	8-41
8.3.6 Summary of Sensitivity Studies	8-42
8.4 Concluding Remarks on PFM and DFM Evaluations	8-43
9 PLANT-SPECIFIC APPLICABILITY	9-1
9.1 Geometric Configurations.....	9-1
9.2 Materials Properties	9-1
9.3 Operating Transients.....	9-1
9.4 Criteria for Technical Basis Applicability	9-2
9.4.1 General.....	9-2
9.4.2 SG Primary Inlet Nozzle-to-Vessel Welds (Item B3.130)	9-2
9.4.3 PWR SG Vessel (Primary Side) Welds (Item Nos. B2.31, B2.32, and B2.40)	9-3
9.4.4 PWR SG Vessel (Secondary Side) Welds (Item Nos. C1.10, C1.20, and C1.30).....	9-3
10 SUMMARY AND CONCLUSIONS	10-1
11 REFERENCES	11-1

LIST OF FIGURES

Figure 1-1 ASME Code, Section XI, Figure IWB-2500-3, Spherical Vessel Head Circumferential and Meridional Weld Joints (Item Nos. B2.31 and B2.32)	1-2
Figure 1-2 ASME Code, Section XI, Figure IWB-2500-6, Typical Tubesheet-to-Head Weld Joints (Item No. B2.40)	1-3
Figure 1-3 ASME Code, Section XI, Figure IWB-2500-7, Nozzle in Shell or Head (Item No. B3.130).....	1-4
Figure 1-4 ASME Code, Section XI, Figure IWB-2500-7, Nozzle in Shell or Head (Item No. B3.130).....	1-5
Figure 1-5 ASME Code, Section XI, Figure IWB-2500-7, Nozzle in Shell or Head (Item No. B3.130).....	1-6
Figure 1-6 ASME Code, Section XI, Figure IWB-2500-7, Nozzle in Shell or Head (Item No. B3.130).....	1-7
Figure 1-7 ASME Code, Section XI, Figure IWC-2500-1, Vessel Circumferential Welds (Item Nos. C1.10 and C1.20)	1-8
Figure 1-8 ASME Code, Section XI, Figure IWC-2500-2, Typical Tubesheet-to-Shell Circumferential Welds (Item No. C1.30).....	1-9
Figure 4-1 Westinghouse U-tube SG	4-2
Figure 4-2 CE U-tube SG.....	4-3
Figure 4-3 B&W OTSG	4-4
Figure 4-4 CE SG inlet nozzle-to-vessel (Item No. B3.130) weld geometry selected for evaluation	4-10
Figure 4-5 B&W SG inlet nozzle-to-vessel (Item No. B3.130) weld geometry selected for evaluation	4-11
Figure 7-1 2-D finite-element model and mesh for PWR SG inlet nozzle (CE design)	7-2
Figure 7-2 2-D finite-element model and mesh for PWR SG inlet nozzle (B&W design).....	7-3
Figure 7-3 Applied boundary conditions and unit internal pressure for PWR SG inlet nozzle (CE design).....	7-4
Figure 7-4 Applied boundary conditions and unit internal pressure for PWR SG inlet nozzle (B&W design).....	7-4
Figure 7-5 Applied thermal boundary conditions for thermal transient analyses for PWR SG inlet nozzle (CE design)	7-6
Figure 7-6 Applied thermal boundary conditions for thermal transient analyses for PWR SG inlet nozzle (B&W design)	7-7
Figure 7-7 Applied mechanical boundary conditions for thermal stress analyses for PWR SG inlet nozzle (CE design)	7-8

Figure 7-8 Applied mechanical boundary conditions for thermal stress analyses for PWR SG inlet nozzle (B&W design)	7-8
Figure 7-9 Stress contours due to unit internal pressure for PWR SG inlet nozzle (CE design)	7-10
Figure 7-10 Stress contours due to unit internal pressure for PWR SG inlet nozzle (B&W design)	7-11
Figure 7-11 Temperature contour for heatup/cooldown transient for PWR SG inlet nozzle (CE design)	7-12
Figure 7-12 Stress contours for heatup/cooldown transient for PWR SG inlet nozzle (CE design)	7-13
Figure 7-13 Temperature contour for heatup/cooldown transient for PWR SG inlet nozzle (B&W design)	7-14
Figure 7-14 Stress contours for heatup/cooldown transient for PWR SG inlet nozzle (B&W design)	7-15
Figure 7-15 Path location for PWR SG inlet nozzle (CE design)	7-16
Figure 7-16 Path location for PWR SG inlet nozzle (B&W design)	7-17
Figure 7-17 Through-wall stress distribution at Path P1(N) for PWR SG inlet nozzle (CE design)	7-18
Figure 7-18 Through-wall stress distribution at Path P2(N) for PWR SG inlet nozzle (B&W design)	7-19
Figure 7-19 3-D finite-element model and mesh for the PWR SG	7-21
Figure 7-20 Applied thermal boundary conditions for thermal transient analyses for the PWR SG	7-22
Figure 7-21 Applied mechanical boundary conditions and pressure for thermal stress analyses for the PWR SG	7-23
Figure 7-22 Temperature contour for the plant loading transient for the PWR SG	7-24
Figure 7-23 Stress contours for the plant loading transient for the PWR SG	7-25
Figure 7-24 Path locations for the PWR SG	7-26
Figure 7-25 Through-wall stress distribution at Path P4 for the PWR SG	7-27
Figure 7-26 Through-wall stress distribution at Path P9 for the PWR SG	7-28
Figure 7-27 Through-wall stress distribution at Path P11 for the PWR SG	7-29
Figure 7-28 Through-wall stress distribution at Path P12 for the PWR SG	7-30
Figure 8-1 Weld residual stress distribution	8-4
Figure 8-2 Semielliptical axial crack in a cylinder model	8-5
Figure 8-3 Semielliptical circumferential crack in a cylinder model	8-5
Figure 8-4 ASME Section XI fracture toughness curve for vessels versus experimental data points	8-6
Figure 8-5 PFM overall technical approach	8-9
Figure 8-6 POD curve for vessels from BWRVIP-108	8-11
Figure 8-7 Carbon steel POD curve for all pipe section thicknesses used to develop Section XI Appendix L	8-12

Figure 8-8 Curve fit for FCG at R-ratio of 0.7 from BWRVIP-108 and comparison to the ASME Code, Section XI FCG law	8-36
Figure 8-9 POD curves for sensitivity study	8-37
Figure 8-10 Sensitivity of inspection schedule and POD curves on probability of rupture	8-39
Figure 8-11 Summary of key sensitivity studies	8-43

LIST OF TABLES

Table 2-1 Code examination requirements and alternative requirements for weld item nos. in the scope of this evaluation	2-6
Table 3-1 Summary of survey results for Item No. B2.31	3-4
Table 3-2 Summary of survey results for Item No. B2.32	3-4
Table 3-3 Summary of survey results for Item No. B2.40	3-4
Table 3-4 Summary of survey results for Item No. B3.130	3-5
Table 3-5 Summary of survey results for Item No. C1.10	3-5
Table 3-6 Summary of survey results for Item No. C1.30	3-6
Table 4-1 Units with Relief Request by Item No.	4-9
Table 4-2 Relevant dimensions of SG components selected for evaluation	4-12
Table 4-3 Summary of SG geometrical parameters for the various SG designs	4-13
Table 4-4 Variation of R/t ratios for various SG designs	4-14
Table 5-1 Materials used in stress analysis	5-2
Table 5-2 Materials properties for SA-533 Gr. B Cl. 1	5-2
Table 5-3 Materials properties for SA-508 Cl. 2	5-3
Table 5-4 Materials properties for SA-516 Gr. 70	5-4
Table 5-5 Material properties for SA-240 Type 304	5-5
Table 5-6 Summary of reactor coolant system design transients for ANO-1 compared to MRP-393 cycles	5-7
Table 5-7 Thermal transients for stress analysis of the PWR SG primary-side head welds	5-9
Table 5-8 Thermal transients for stress analysis of the B&W SG primary inlet nozzle	5-11
Table 5-9 Thermal transients for stress analysis of the PWR SG secondary-side vessel welds	5-12
Table 8-1 Previous ISI projects that evaluated inspection requirements	8-2
Table 8-2 Summary of DFM design inputs	8-6
Table 8-3 Results of the DFM evaluation	8-7
Table 8-4 Inspection schedule scenarios	8-13
Table 8-5 Random variables and their associated distributions	8-15
Table 8-6 Benchmarking inputs	8-16
Table 8-7 Comparison of cumulative probability of leak between PROMISE and VIPERNOZ for benchmarking	8-17
Table 8-8 PFM base-case inputs	8-17

Table 8-9 Probability of rupture and probability of leakage for base case	8-19
Table 8-10 Probability of rupture and probability of leakage for 80 years for PSI followed by combinations of 10-year ISIs and/or 20- or 30-year ISIs for Path SGPTH-P4A	8-20
Table 8-11 Results of sensitivity analysis for Path SGPTH-P4A	8-21
Table 8-12 Results of sensitivity analysis with random stress multiplier for Path SGPTH-P4A	8-21
Table 8-13 Sensitivity of toughness on probability of rupture for 80 years	8-23

1

INTRODUCTION

1.1 Background

Welds in pressurized water reactor (PWR) steam generators (SGs) are subjected to periodic examination under American Society of Mechanical Engineers (ASME) Code, Section XI [1]. Through the Electric Power Research Institute (EPRI), the power industry has undertaken a study to determine whether the inspection requirements for these components can be optimized based on the operating history and the results of in-service examinations performed to date. The first part of this study, documented in the EPRI report *Technical Bases for Inspection Requirements for PWR Steam Generator Feedwater and Main Steam Nozzle-to-Shell Welds and Nozzle Inside Radius Sections* [2], focused on PWR SG feedwater and main steam nozzle-to-shell welds and nozzle inside radius sections.

This report is a continuation of that study and focuses on the Class 1 nozzle-to-vessel welds and the Class 1 and Class 2 vessel head, shell, tubesheet-to-head, and tubesheet-to-shell welds in SGs. These welds are listed under the following categories in Tables IWB-2500-1 and IWC-2500-1 of ASME Code, Section XI:

- Class 1, Category B-B, pressure-retaining welds in vessels other than reactor vessels
- Class 1, Category B-D, full penetration welded nozzles in vessels
- Class 2, Category C-A, pressure-retaining welds in pressure vessels

Specifically, the welds to be evaluated are listed under the following item numbers:

- Item No. B2.31 – steam generators (primary side), head welds, circumferential
- Item No. B2.32 – steam generators (primary side), head welds, meridional
- Item No. B2.40 – steam generators (primary side), tubesheet-to-head weld
- Item No. B3.130 – steam generators (primary side), nozzle-to-vessel welds
- Item No. C1.10 – shell circumferential welds
- Item No. C1.20 – head circumferential welds
- Item No. C1.30 – tubesheet-to-shell weld

The preceding item numbers all require volumetric examination. Item Nos. B2.31 and B2.32 require examination of one weld per head during each inspection interval. Item No. B3.130 requires examination of all nozzles with full penetration welds to the vessel shell (or head) and integrally cast nozzles during each inspection interval. Item Nos. B2.40, C1.10, C1.20, and C1.30 require examination of specified welds during each inspection interval.

Typical PWR SG Class 1 nozzle-to-vessel weld and Class 1 and Class 2 vessel head, shell, tubesheet-to-head, and tube-sheet to shell weld configurations and associated examination surfaces and volumes are provided in ASME Code, Section XI, Figures IWB-2500-3, IWB-2500-6, IWB-2500-7, IWC-2500-1, and IWC-2500-2, which are reproduced in Figures 1-1 through 1-8.

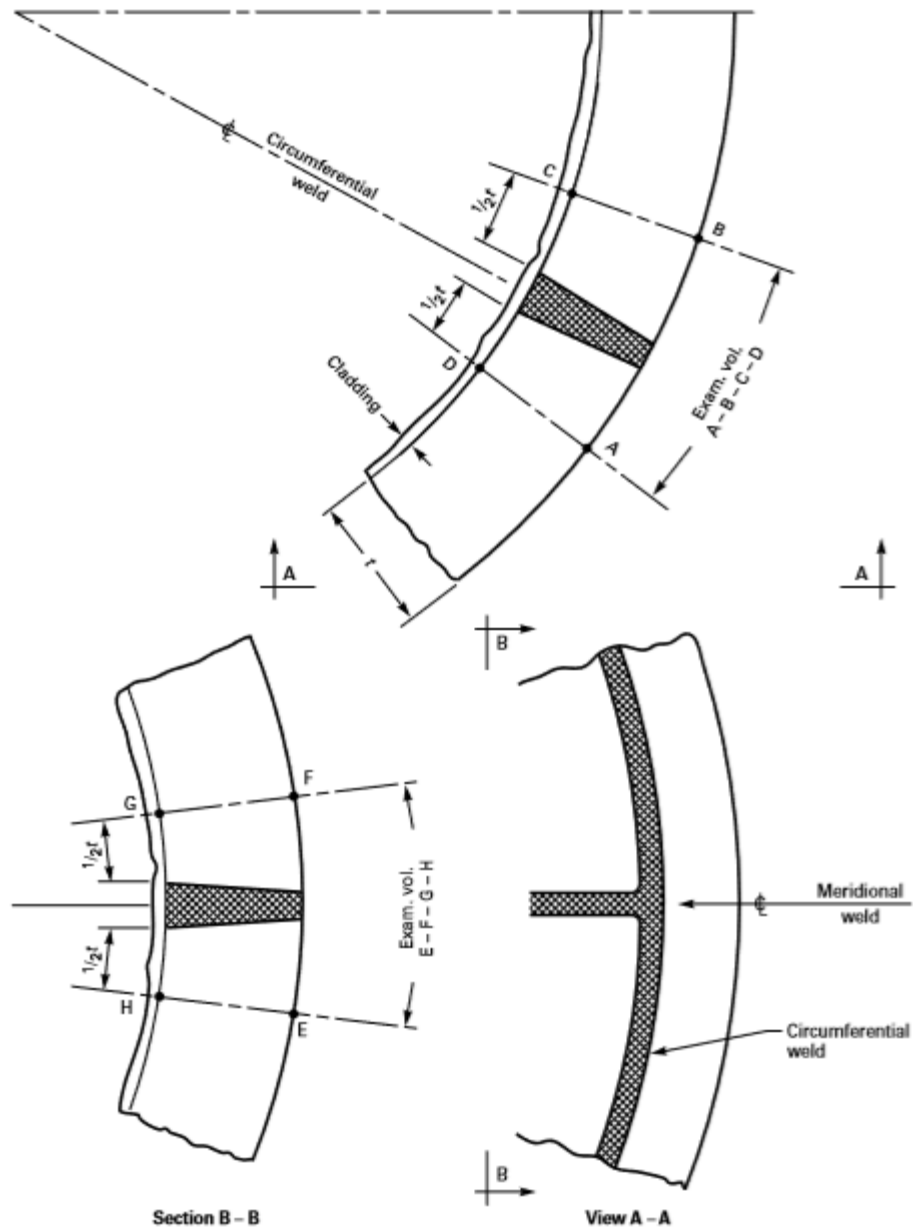


Figure 1-1
ASME Code, Section XI, Figure IWB-2500-3, Spherical Vessel Head Circumferential and Meridional Weld Joints (Item Nos. B2.31 and B2.32)

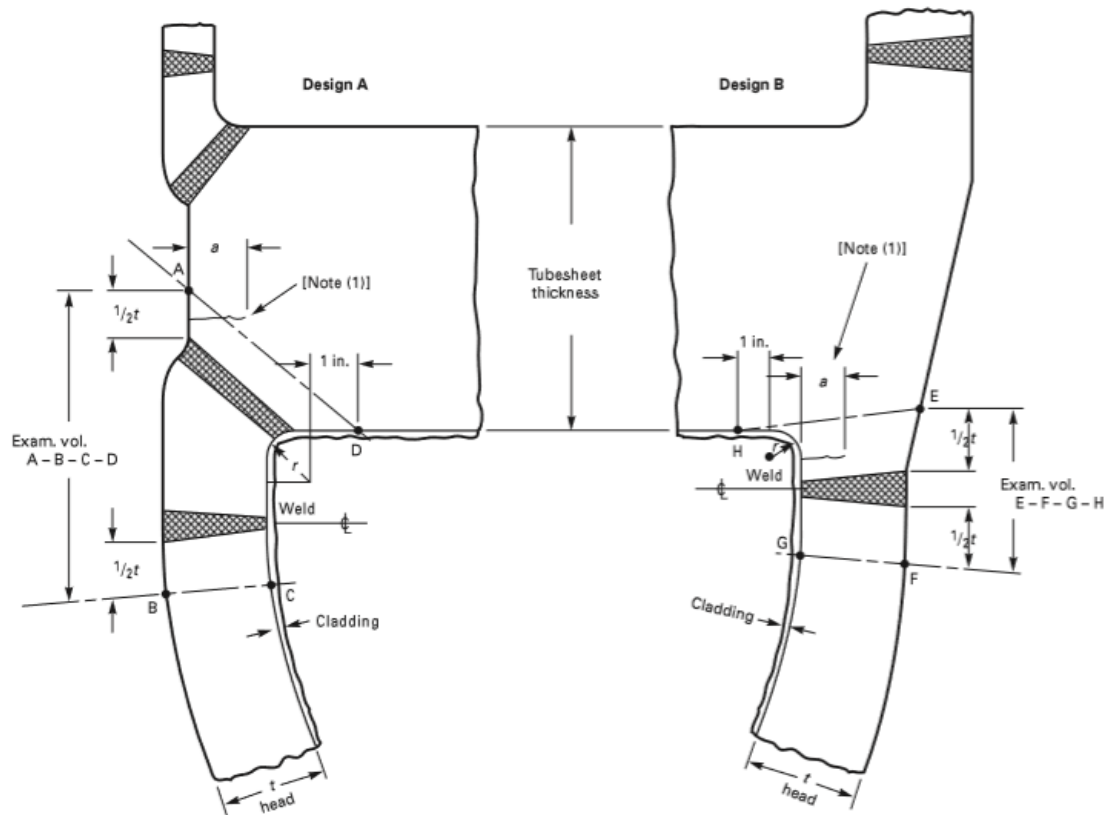


Figure 1-2
ASME Code, Section XI, Figure IWB-2500-6, Typical Tubesheet-to-Head Weld Joints
(Item No. B2.40)

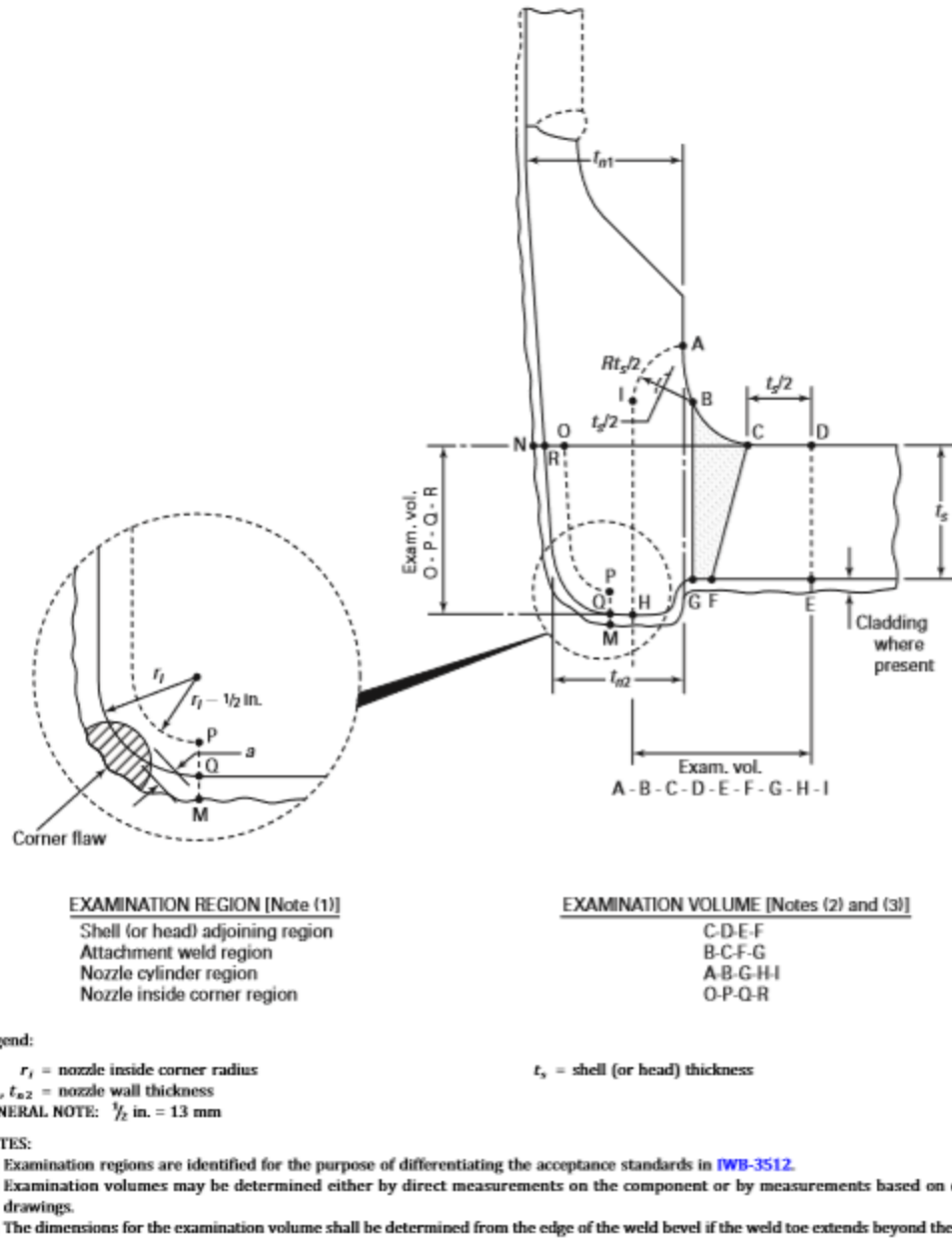


Figure 1-3
ASME Code, Section XI, Figure IWB-2500-7(a), Nozzle in Shell or Head (Item No. B3.130)

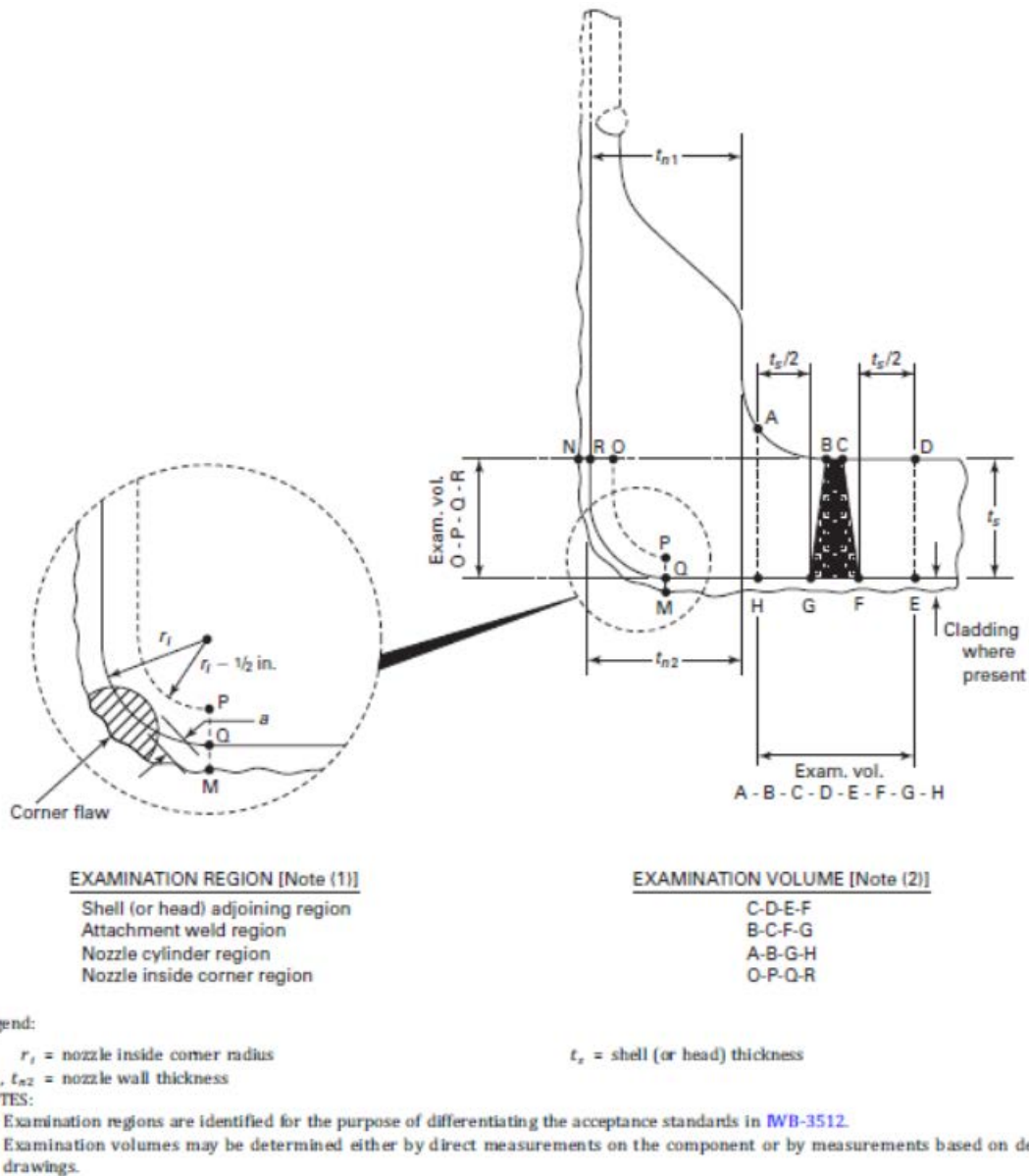


Figure 1-4
ASME Code, Section XI, Figure IWB-2500-7(b), Nozzle in Shell or Head (Item No. B3.130)

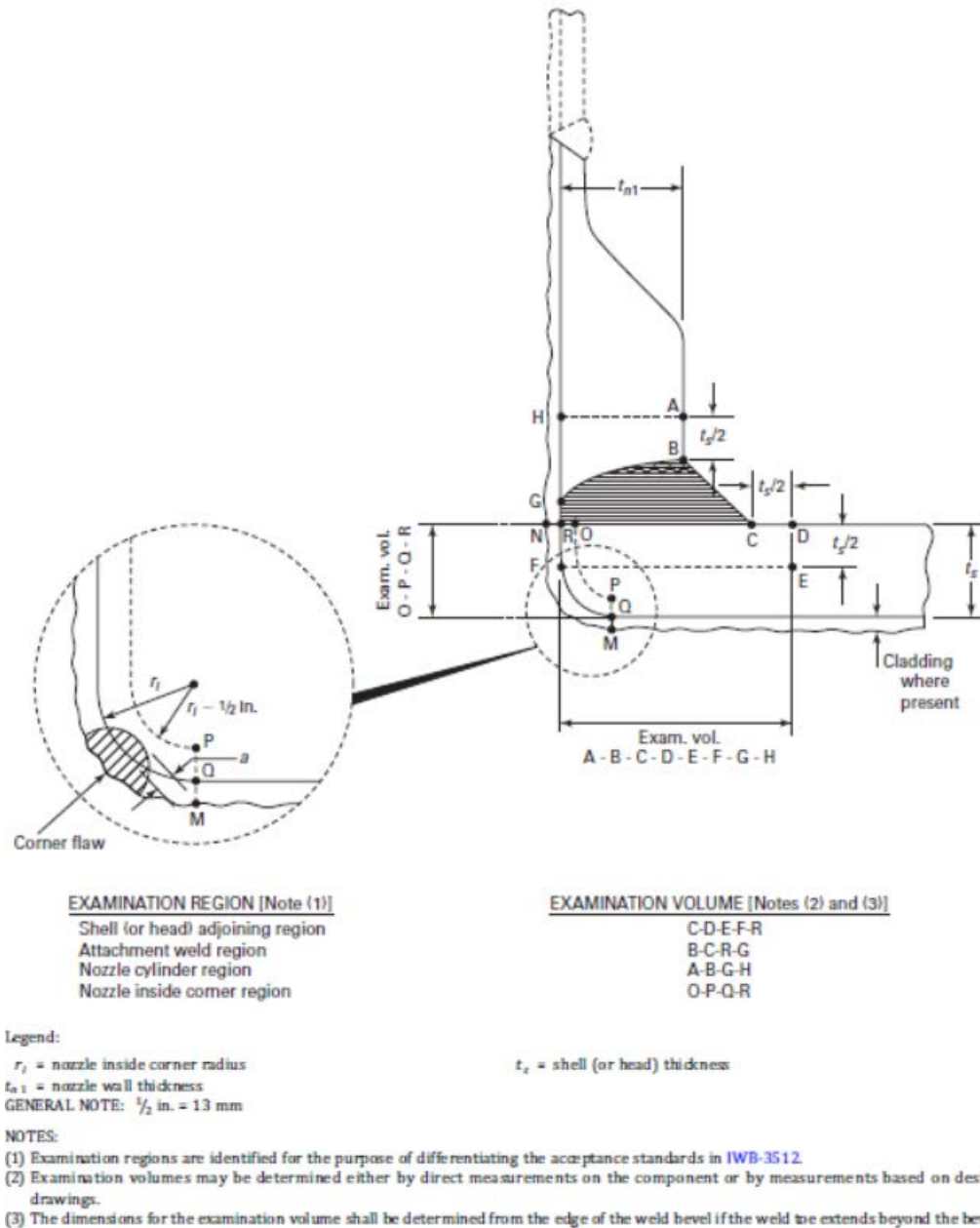


Figure 1-5
ASME Code, Section XI, Figure IWB-2500-7(c), Nozzle in Shell or Head (Item No. B3.130)

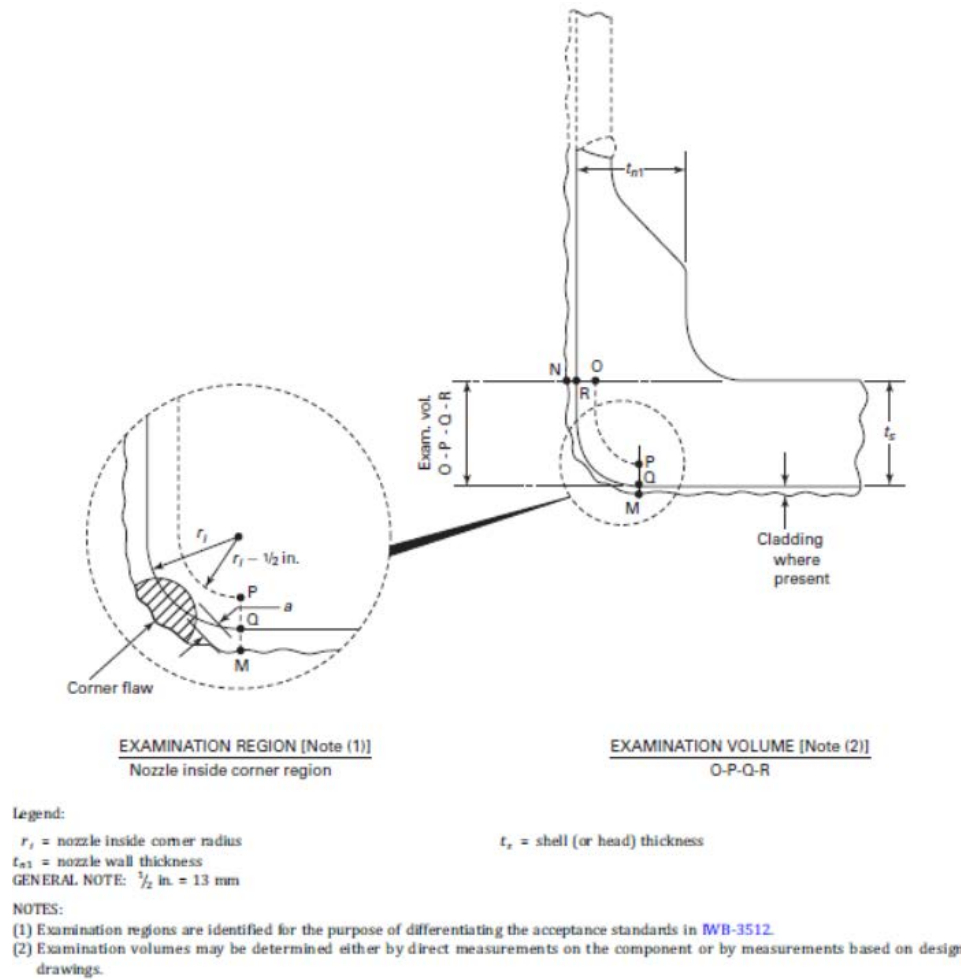
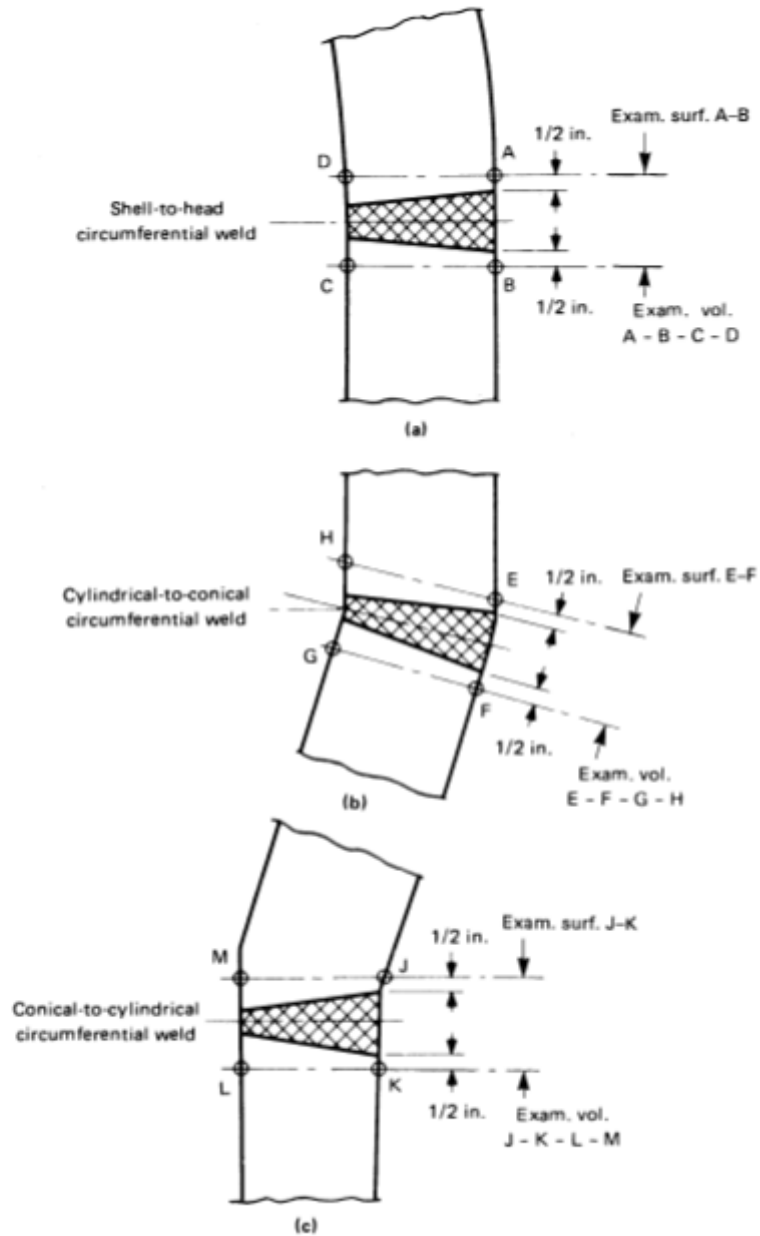


Figure 1-6
ASME Code, Section XI, Figure IWB-2500-7(d), Nozzle in Shell or Head (Item No. B3.130)



GENERAL NOTE: $1/2$ in. = 13 mm

Figure 1-7
ASME Code, Section XI, Figure IWC-2500-1, Vessel Circumferential Welds (Item Nos. C1.10 and C1.20)

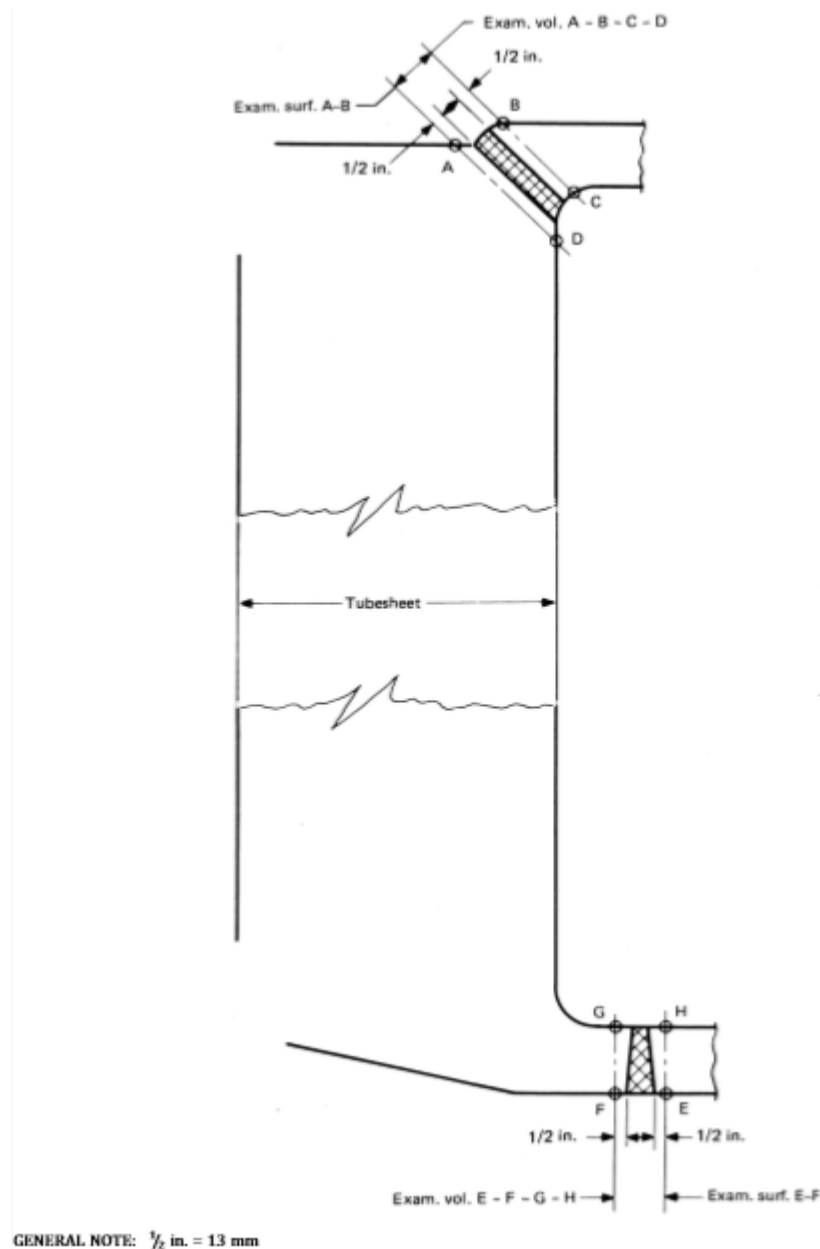


Figure 1-8
ASME Code, Section XI, Figure IWC-2500-2, Typical Tubesheet-to-Shell Circumferential Welds (Item No. C1.30)

Numerous examinations of these components have been performed by all plants in the U.S. fleet and other international plants that follow ASME Code, Section XI, and many years of operating history now exist. This field experience serves as the impetus behind researching the potential for establishing the technical bases for the inspection requirements of these components.

1.2 Objective

The objective of this report is to evaluate the examination requirements for the listed PWR SG components and provide the technical bases for various examination scenarios for these components. To accomplish this objective, this report addresses various topics and is organized in the following sequence:

- Section 2, Review of Previous Related Projects
- Section 3, Review of Inspection History and Examination Effectiveness
- Section 4, Survey of Components and Selection of Representative Components for Analysis
- Section 5, Materials Properties, Operating Loads, and Transients
- Section 6, Evaluation of Potential Degradation Mechanisms
- Section 7, Component Stress Analysis
- Section 8, Probabilistic and Deterministic Fracture Mechanics Evaluation
- Section 9, Plant-Specific Applicability
- Section 10, Summary and Conclusions

2

REVIEW OF PREVIOUS RELATED PROJECTS

This report focuses on the Class 1 nozzle-to-vessel welds and the Class 1 and Class 2 vessel head, shell, tubesheet-to-head, and tubesheet-to-shell welds of PWR SGs. Previous projects related to nozzle-to-vessel welds are covered in Section 2.1, and those related to vessel shell welds are covered in Section 2.2. Other previous projects covering related components are described in Section 2.3.

2.1 Nozzle-to-Vessel Welds

There have been several industry initiatives to provide alternative examination requirements for nozzles in lieu of the requirements in ASME Code, Section XI [1]. Some have been related to nozzle-to-vessel welds, whereas others have been related to other components. Most previous initiatives have focused on Class 1 nozzles, where the basis for alternative examination requirements has relied on plant operating experience and the results of nondestructive examinations performed on the relevant Code item, as well as supplementary deterministic and/or probabilistic flaw tolerance evaluations.

Currently, Class 1 nozzle-to-vessel welds in ASME Code, Section XI include the following:

- Item No. B3.90, reactor vessel nozzle-to-vessel welds
- Item No. B3.110, pressurizer nozzle-to-vessel welds
- Item No. B3.130, steam generator (primary side) nozzle-to-vessel welds
- Item No. B3.150, heat exchanger (primary side) nozzle-to-vessel welds

In 2002, the EPRI BWR Vessel and Internals Project (BWRVIP) undertook a study to optimize the inspection requirements for boiling water reactor (BWR) vessel nozzle-to-vessel welds (Item No. B3.90 for BWRs). This work is documented in BWRVIP-108 [3] and provided the justification for the reduction of nozzle-to-vessel weld examinations from 100% to a 25% sample of each nozzle type every 10 years. The feedwater and control rod drive (CRD) return line nozzles were excluded from that study. The justification was based on an industry survey of examination results to date, which found no records of indications in the inspection results. A selection process was then used to identify a sampling of nozzles to use in deterministic and probabilistic fracture mechanics evaluations to evaluate the safety implications of reducing the examination population from 100% to 25%. The results of the analyses supported the alternative inspection criteria of a 25% sample of each nozzle type. In the safety evaluation of BWRVIP-108 [4], the U.S. Nuclear Regulatory Commission (NRC) stated that licensees who plan to request relief from the current ASME Code, Section XI requirements should demonstrate plant-specific applicability of the conclusions of BWRVIP-108 to their unit(s) by demonstrating that several general and nozzle-specific criteria are met.

As a result of the NRC conditions placed on BWRVIP-108, the BWRVIP initiated a follow-on study that resulted in BWRVIP-241 [5]. The intent of this study was to determine the extent to which the NRC conditions could be addressed to permit greater applicability to the BWR fleet without the need for a relief request. The results of this follow-on study concluded that not all BWR nozzles satisfy the NRC conditions and, as such, some require a plant-specific evaluation. Two of the criteria set forth by the NRC in Reference [4] were modified as a result of this study. The NRC issued a safety evaluation for BWRVIP-241 [6], accepting the modifications in Reference [5] to the original criteria established in Reference [4] but still requiring that plant-specific applicability be demonstrated against the modified criteria. The work performed in BWRVIP-108 and BWRVIP-241 provided the technical basis for ASME Code Case N-702 [7]. This Code Case was conditionally approved for use in NRC Regulatory Guide (RG) 1.147, Revision 17 [8], where the NRC requested that applicability of the Code Case be demonstrated to the criteria in Section 5.0 of the NRC safety evaluation of BWRVIP-108 [4] and Section 5.0 of the NRC's safety evaluation of BWRVIP-241 [6].

The PWR Owner's Group also undertook a study to optimize the inspection requirements for PWR reactor vessel nozzle-to-vessel welds (Item No. B3.90 for PWRs) [9]. A different approach was used in this study compared to the approach used by the BWRVIP for BWR nozzles, in that extension of the inspection interval was sought rather than a reduction in the inspection sample size. Based on operating experience, results of a survey of examination findings to date, and the results of deterministic and probabilistic fracture mechanics evaluations, the NRC granted extension of the inspection interval from 10 years to 20 years for PWR reactor vessel nozzle-to-vessel welds. The probabilistic approach used elements of Code Case N-691 [10], which provides guidelines for risk-informed application to extend PWR inspection intervals. Three pilot plants (representing the nuclear steam supply system [NSSS] designs from Westinghouse [W], Combustion Engineering [CE], and Babcock & Wilcox [B&W]) were used in the study. In the safety evaluation [11], the NRC concluded that the methodology in Reference [9] can be applied to other PWR plants by confirming the applicability of parameters in Appendix A of Reference [9] on a plant-specific basis. The study in Reference [9] did not result in any changes to ASME Code, Section XI requirements. However, because the 10-year inspection interval is required by Section XI, IWB-2412, as regulated in 10 CFR 50.55(a), licensees must submit an Exemption Request for NRC approval to extend the inspection interval of PWR reactor vessel nozzle-to-vessel welds from 10 years to 20 years.

Recognizing the difficulties involved in volumetric examination of regenerative and residual heat exchangers (because these components were not designed for such examinations), ASME published Code Case N-706 in November 2005 to allow visual (VT-2) examinations in lieu of the volumetric examinations for these heat exchangers. This Code Case applies to PWR heat exchangers fabricated from stainless steel for Examination Categories B-B, B-D, and B-J in Table IWB-2500-1 of ASME Code, Section XI, and Examination Categories C-A, C-B, and C-F-1 in Table IWC-2500-1 of ASME Code, Section XI. This includes Class 1 Item No. B3.150 and Class 2 Item Nos. C2.21 and C2.32. The Code Case was revised in 2007 to N-706-1 [12], and the technical basis is provided in Reference [13], which relied on deterministic and probabilistic fracture mechanics evaluations. Code Case N-706-1 is unconditionally approved for use per NRC RG 1.147, Revision 17 [8] and is currently being used by most U.S. utilities for the examination of stainless steel heat exchangers in PWRs. (Note: The preceding Code Case N-706-1 [12] discussion is also relevant to the vessel shell welds covered in Section 2.2.)

2.2 Vessel Shell Welds

There have been several industry initiatives to provide alternative examination requirements for vessels in lieu of the requirements in ASME Code Section XI. Some of these initiatives have been specifically related to the reactor pressure vessel (RPV) shell welds, whereas others have been related to other plant components. Of those related to the RPV shell welds, all have focused on Class 1 welds. The basis for the alternative examination requirements for Class 1 RPV shell welds has relied on plant operating experience and the results of nondestructive examinations performed on the relevant Code item, as well as supplementary deterministic and/or probabilistic flaw tolerance evaluations. These initiatives are described in more detail in the following.

There have been two major studies regarding the RPV shell welds (ASME Item Nos. B1.10, B1.20, and B1.30), which set precedent to the current effort. In 1995, the EPRI BWRVIP published the results in BWRVIP-05 [14] that optimized the inspection requirements for the BWR RPV shell welds. This study was limited to circumferential and longitudinal shell welds (Category B-A welds, Item Nos. B1.11 and B1.12). It did not address other vessel shell welds, such as head welds (Item Nos. B1.21 and B1.22), shell-to-flange welds (Item No. B1.30), and head-to-flange welds (Item No. B1.40). The results of that work provided the justification for eliminating the examination of the circumferential shell welds in BWR RPVs.

The justification was based on conducting an industry survey of examination results to date (which found no records of service-induced defects in the inspection results), in conjunction with deterministic and probabilistic fracture mechanics evaluations, to determine the safety implication of eliminating the examination of the shell circumferential welds. Initially, 50% examination of the axial weld was also sought in BWRVIP-05, but after the review process, the NRC finally requested that 100% examination of the axial welds be performed. Due to the very long review process, the NRC issued interim technical guidance in Information Notice (IN) 97-63 [15] that the staff would consider Relief Requests for augmented examinations of the BWR RPV circumferential shell welds during the fall 1997 or spring 1998 outages in accordance with 10 CFR 50.55a(a)(3)(i), 10CFR50.55a(a)(3)(ii), and 10 CFR 50.55a(g)(6)(ii)A(5) from BWR licensees who were scheduled to perform inspections. In May 1998, the NRC staff issued IN 97-63, Supplement 1 [16], extending the period of the Relief Requests to the fall 1998 and spring 1999 outage seasons. The final Safety Evaluation (SE) [17] for BWRVIP-05 was issued by the NRC on July 28, 1998, concluding that a near-term safety concern was not created by eliminating the examination of the BWR RPV shell circumferential welds due to various conservatisms in the calculation for axial welds, including use of peak end-of-license fluence levels for all postulated flaws and the assumption of flaw density and flaw location. The final SE included agreement between the industry and the NRC to inspect 100% of the axial welds and only portions of the circumferential welds at their intersections with the axial welds.

Following this SE, the NRC issued Generic Letter 98-05 [18] informing all BWRs that they can request permanent relief from the in-service inspection requirements of 10 CFR 50.55a(g) for the volumetric examination of circumferential RPV welds. On March 7, 2000, the NRC issued a supplement to the initial SE [19] addressing the high conditional failure probability levels for axial welds in BWR RPVs determined in the staff SE [17]. The staff concluded in this supplement that the RPV failure frequency due to failure of the limiting axial welds in the BWR fleet was below 5×10^{-6} per reactor-year, given the assumptions of flaw density and flaw distribution/location. The supplement made it clear that the results of the study applied only to

the initial 40-year license period of BWR plants, and that any consideration of BWR axial welds for license renewal would require a plant-specific treatment by the license renewal applicant. The 40-year life for the work in BWRVIP-05 was extended to 60 years based on studies performed in BWRVIP-74-A [20]. A probabilistic fracture mechanics study was performed in Reference [21] to determine the implication of the failure probability of a BWR RPV operating beyond 60 years. The results of this study confirmed the results of the original analysis in BWRVIP-05 that the conditional probability of failure for the circumferential welds is orders of magnitude less than of the axial welds, and, therefore, examinations of the circumferential welds are not necessary for up to 72 effective full power years (EFPY).

Similarly, work performed by the PWR Owners Group in Reference [9] also included the shell weld items listed in Table IWB-2500-1 of ASME Code, Section XI for Category B-A and B-D welds. As a result of that study, the NRC granted extension of the inspection interval from 10 years to 20 years for PWR RPV shell welds.

2.3 Related Work

In addition to the initiatives described in Section 2.1 and Section 2.2 to optimize examinations of nozzle-to-vessel welds and vessel shell welds, respectively, several other efforts have been conducted by the industry and cognizant ASME Section XI Code Committees to support optimizing the inspections of related plant components. These efforts are summarized as follows:

- Code Case N-560-2 [22] was approved by ASME in March 2000 and provides alternative inspection requirements for Class 1, Category B-J piping welds. This Code Case permits a reduction in the examination population of Category B-J welds from 25% to 10% using risk-informed principles. The technical basis for this Code Case is provided in EPRI TR-112657, Rev. B-A [23]. This Code Case is not approved for use by the NRC and is listed in NRC RG 1.193, Revision 5 [24], but it has been used extensively by the U.S. industry through Relief Requests to the NRC.
- Code Cases N-577-1 [25] and N-578-1 [26] were approved by ASME in March 2000, and they provide alternative examination requirements for Class 1, 2, and 3 piping welds based on risk-informed principles. The use of these Code Cases has led to significant reductions in examinations of such piping welds. The technical bases for these Code Cases are provided in WCAP-14572 [27] and EPRI TR-112657, Rev. B-A [23], respectively. These Code Cases are not approved for use by the NRC and are listed in RG 1.193, Revision 5 [24], but they have been used extensively by the industry through Relief Requests to the NRC.
- Code Case N-716-1 [28] was approved by ASME in January 2013 and provides alternative piping classification and examination requirements for Class 1, 2, 3, and non-Class piping welds, as well as for Category C-A, C-B, C-D, and C-G components. The technical basis for this Code Case is provided in References [29] and [30]. This Code Case was unconditionally approved for use and incorporated into Revision 17 of NRC RG 1.147 [8].
- Code Case N-613-2 [31] was approved by ASME in December 2010 and provides alternatives to the examination volume requirements in Figures 2500-7(a), (b), (c), and (d) of ASME Code Section XI for the ultrasonic examination of reactor vessel nozzle-to-vessel shell welds and nozzle inside radius sections. It is unconditionally approved for use in NRC

RG 1.147, Revision 17 [8]. This Code Case results in a significant reduction in the examination volume for Category B-D nozzle welds by reducing the inspection volume of adjacent material from half the shell thickness to ½ in. This has resulted in a significant reduction in both qualification and scanning times.

- EPRI TR-3002007626 [32], published in April 2016, provides the technical basis for alternative inspection requirements for the reactor vessel threads-in-flange examination (ASME Code Section XI, Examination Category B-G-1, Item No. B6.40). Since then, at least four utilities have sought relief and received NRC approval for using this alternative [33–36]. EPRI TR-3002007626 provided the technical basis for ASME Code Case N-864 [37], which was published by ASME in July 2017. The Code Case has not yet been reviewed by the NRC for inclusion in their Code Case RGs.
- EPRI TR-3002012966 [38], published in April 2018, provides the technical basis for alternative inspection requirements for the accessible areas of the reactor vessel interior (ASME Section XI Examination Category B-N-1). This EPRI report provided the basis for ASME Code Case N-885 [39], which was published by ASME in December 2018 to provide alternative requirements for Table IWB-2500-1, Examination Category B-N-1, for the interior of the reactor vessel; B-N-2, welded core support structures and interior attachments to reactor vessels; and B-N-3, removable core support structures. The Code Case has not yet been reviewed by the NRC for inclusion into their Code Case RGs.
- EPRI TR-3002014590 [2], published in April 2019, provides the technical basis for alternative inspection requirements for PWR steam generator feedwater and main steam nozzle-to-shell welds and nozzle inside radius sections (ASME Section XI Examination Category C-B). To date, that work has not been published in any ASME Code actions.

2.4 Concluding Remarks

Section 2.1 covers previous projects related to nozzle-to-vessel welds. No previous projects have developed alternative requirements for the PWR SG Item No. B3.130 components in the scope of this evaluation, which, according to ASME Code Section XI, require a volumetric examination of all welds during each interval.

Section 2.2 covers previous projects related to vessel shell welds. No previous projects have developed alternative requirements for the PWR SG Item Nos. B2.31, B2.32, B2.40, C1.10, C1.20, and C1.30 components in the scope of this evaluation. (Note: As discussed in Section 2.3, PWR stainless steel heat exchanger Item Nos. C1.10, C1.20, and C1.30 components now use Code Case N-706-1 as an alternative.)

The current ASME Code Section XI examination requirements for the SG primary- and secondary-side components evaluated in this report are summarized in Table 2-1. Table 2-1 also provides a summary of alternative requirements. As previously noted, alternative requirements have been developed only for PWR stainless steel heat exchanger components.

Table 2-1

Code examination requirements and alternative requirements for weld item nos. in the scope of this evaluation

Code Item No.	Current Code Requirements			Alternative Requirements				
	Exam Method	Exam Sample	Exam Frequency	Alternative to Code		Exam Method	Exam Sample	Exam Frequency
B2.31	Volumetric	All welds first interval, one weld per head in successive intervals	Every interval	None		NA	NA	NA
B2.32	Volumetric	All welds first interval, one weld per head in successive intervals	Every interval	None		NA	NA	NA
B2.40	Volumetric	All vessels first interval, one vessel in successive intervals	Every interval	None		NA	NA	NA
B3.130	Volumetric	All welds	Every interval	None		NA	NA	NA
C1.10	Volumetric	Cylindrical-shell-to-conical-shell-junction welds and shell (or head)-to-flange welds	Every interval	PWR SS HXs	N-706-1	VT-2	All Vessels	Every Interval
				All Others	None	NA	NA	NA
C1.20	Volumetric	Head-to-shell weld	Every interval	PWR SS HXs	N-706-1	VT-2	All Vessels	Every Interval
				All Others	None	NA	NA	NA
C1.30	Volumetric	Tubesheet-to-shell weld	Every interval	PWR SS HXs	N-706-1	VT-2	All Vessels	Every Interval
				All Others	None	NA	NA	NA

3

REVIEW OF INSPECTION HISTORY AND EXAMINATION EFFECTIVENESS

As part of this project, a survey was conducted to collect the number of examinations performed and associated examination results for Item Nos. B2.31, B2.32, B2.40, B3.130, C1.10, C1.20, and C1.30 for U.S. and international nuclear units. The PWR SG nozzle-to-vessel and vessel shell weld components evaluated in this report are addressed by these item numbers. The survey was conducted between April 2017 and September 2017. Responses were obtained from a total of 69 U.S. and 5 international units. The data gathered from this survey covered plant designs fabricated by Babcock & Wilcox, Combustion Engineering, Westinghouse, and General Electric. The following information was requested:

- Plant name.
- Total number of applicable components for the ASME Code Section XI Item and associated vessel description (for example, heat exchanger).
- Total number of in-service inspections (ISIs) performed on the subject component to date.
- Number of examinations containing flaws that exceeded ASME Code Section XI acceptance standards (that is, IWB-3500).
- Total number of flaws (across all examinations for the item).
- How were the flaws dispositioned that exceeded ASME Code Section XI acceptance standards?
- Estimated dose accumulated per examination (including any pre- and post-examination activities, such as insulation removal or scaffold erection).
- Did the examination have any impact on outage critical path?
- Were any Relief Requests submitted and/or approved for this item?
- Comments or any additional information.

3.1 Summary of Survey Results

The survey results for the in-scope SG nozzle-to-vessel and vessel shell weld components (that is, the components listed in Section 1.1) are provided in Reference [40] and summarized in Tables 3-1 through 3-7. The results for each component are as follows:

- Item No. B2.31 (steam generator [head] circumferential welds): The summary of results for Item No. B2.31 is shown in Table 3-1. This item applies only to PWRs, and Table 3-1 shows that it is present in all PWR designs except the Westinghouse three-loop and Westinghouse four-loop plants. Thirty examinations have been performed on this item to date for the plants

that responded to the survey, with no identified flaws that exceeded the acceptance criteria of ASME Code Section XI. Section XI, Table IWB-2500-1 requires volumetric examination of all welds for this item in every interval. No relief has been requested from the NRC to use alternative examination methods by any of the seven units with this item.

- Item No. B2.32 (steam generator [head] meridional welds): The summary of results for Item No. B2.32 is shown in Table 3-2. This item applies only to PWRs, and Table 3-2 shows that it is only present in one unit of the CE design. Thirteen examinations have been performed on this item to date for the plants that responded to the survey, with no identified flaws that exceeded the acceptance criteria of ASME Code Section XI. Section XI, Table IWB-2500-1, requires volumetric examination of all welds for this item in every interval. No relief has been requested from the NRC to use alternative examination methods by the one CE unit with this item.
- Item No. B2.40 (steam generator tubesheet-to-head welds): The summary of results for Item No. B2.40 is shown in Table 3-3. This item applies only to PWRs, and Table 3-3 shows that it is present in all PWR designs. To date, 183 examinations have been performed on this item for the plants that responded to the survey. Examinations at two units at a single plant site identified multiple flaws exceeding the acceptance criteria of ASME Code Section XI. The flaws were determined to be subsurface embedded fabrication flaws and not service-induced. A flaw evaluation was performed, and the flaws were found to be acceptable as-is. Section XI, Table IWB-2500-1, requires volumetric examination of all welds for this item in every interval. Several units sought relief from the NRC for examination of this item, some due to limited coverage.
- Item No. B3.130 (steam generator primary side nozzle-to-vessel welds): The summary of results for Item No. B3.130 is shown in Table 3-4. This item applies only to PWRs, and Table 3-4 shows that it is present in all PWR designs except the Westinghouse two-loop plants. To date, 135 examinations have been performed on this item for the plants that responded to the survey, with no identified flaws that exceeded the acceptance criteria of ASME Code Section XI. Section XI, Table IWB-2500-1, requires volumetric examination of all welds for this item in every interval. A few units sought relief from the NRC for examination of this item due to limited (less than essentially 100%) coverage resulting from geometric limitations or permanent obstructions in the examination area.
- Item No. C1.10 (vessel shell circumferential welds): The summary of results for Item No. C1.10 is shown in Table 3-5. This item applies to both PWRs and BWRs (BWR components are not addressed in this report, but the related survey results are included for completeness). Table 3-5 shows that it is present in all PWR and BWR plant designs. To date, 445 examinations have been performed on this item for the plants that responded to the survey, with no identified flaws that exceeded the acceptance criteria of ASME Code Section XI. Section XI, Table IWC-2500-1, requires volumetric examination of all welds for this item in every interval. Most PWR heat exchanger welds now receive a VT-2 examination using Code Case N-706-1 in lieu of the volumetric exam required by Section XI. Some Item No. C1.10 components are no longer examined because they are included in the scope of the plant's risk-informed in-service inspection (RI-ISI) program and were not selected for examination.

- Item No. C1.20 (vessel head circumferential welds): The summary of results for Item No. C1.20 is shown in Table 3-6. This item applies to both PWRs and BWRs (BWR components are not addressed in this report, but the related survey results are included for completeness). Table 3-6 shows that it is present in all PWR and BWR plant designs. To date, 373 examinations have been performed on this item for the plants that responded to the survey. Two PWR units reported flaws exceeding the acceptance criteria of ASME Code, Section XI. In the first unit, a single flaw was identified and evaluated as an inner-diameter surface imperfection. Reference [41] indicates that this was a spot indication with no measurable through-wall depth. This indication is therefore not considered to be service-induced but rather fabrication-related. A flaw evaluation per IWC-3600 was performed for this flaw, and it was found to be acceptable for continued operation. In the second unit, multiple flaws were identified. As discussed in References [42] and [43], these flaws were most likely subsurface weld defects typical of thick vessel welds and not service-induced. A flaw evaluation per IWC-3600 was performed for these flaws, and they were found to be acceptable for continued operation. Section XI, Table IWC-2500-1, requires volumetric examination of all welds for this item in every interval. Most PWR heat exchanger welds now receive a VT-2 examination using Code Case N-706-1 in lieu of the volumetric exam required by Section XI. Some Item No. C1.20 components are no longer examined because they are included in the scope of the plant's RI-ISI program and were not selected for examination.
- Item No. C1.30 (vessel tubesheet-to-shell welds): The summary of results for Item No. C1.30 is shown in Table 3-7. This item applies to both PWRs and BWRs (BWR components are not addressed in this report, but the related survey results are included for completeness). Table 3-7 shows that these welds are present in all PWR and BWR plant designs. To date, 195 examinations have been performed on this item for the plants that responded to the survey, with no identified flaws that exceeded the acceptance criteria of ASME Code Section XI. Section XI, Table IWC-2500-1, requires volumetric examination of all welds for this item in every interval. Most PWR heat exchanger welds now receive a VT-2 examination using Code Case N-706-1 in lieu of the volumetric exam required by Section XI. Some Item No. C1.30 components are no longer examined because they are included in the scope of the plant's RI-ISI program and were not selected for examination.

3.2 Concluding Remarks

A survey was conducted to collect the number of examinations performed and the associated examination results for Item Nos. B2.31, B.2.32, B2.40, B3.130, C1.10, C1.20, and C1.30, including the PWR SG nozzle-to-vessel and vessel weld components evaluated in this report. The survey results are summarized in Tables 3-1 through 3-7. Out of a total of 1,374 examinations that have been performed on the preceding item numbers identified by the plants that responded to the survey, two PWR units reported flaws in Item No. B2.40 components and two PWR units reported flaws in Item No. C1.20 components that exceeded the acceptance criteria of ASME Code, Section XI. However, none of these flaws was considered service-induced, all of the flaws were evaluated and found to be acceptable without repair, and no other indications were identified in any in-scope components.

Table 3-1
Summary of survey results for Item No. B2.31 (SG [head] circumferential welds)

Plant Type	Total No. of Units in Survey	No. of Units with this Item	Total No. of Applicable Components	Total No. of Examinations	Total No. of Exams Containing Flaws that Exceed Section XI Acceptance Criteria
BWR	27	0	0	0	0
PWR W-2 Loop	4	1	1	6	0
PWR W-3 Loop	11	0	0	0	0
PWR W-4 Loop	20	0	0	0	0
PWR-CE	6	3	10	13	0
PWR B&W	6	3	10	11	0
Total	74	7	21	30	0

Table 3-2
Summary of survey results for Item No. B2.32 (SG [head] meridional welds)

Plant Type	Total No. of Units in Survey	No. of Units with this Item	Total No. of Applicable Components	Total No. of Examinations	Total No. of Exams Containing Flaws that Exceed Section XI Acceptance Criteria
BWR	27	0	0	0	0
PWR W-2 Loop	4	0	0	0	0
PWR W-3 Loop	11	0	0	0	0
PWR W-4 Loop	20	0	0	0	0
PWR-CE	6	1	10	13	0
PWR B&W	6	0	0	0	0
Total	74	1	10	13	0

Table 3-3
Summary of survey results for Item No. B2.40 (SG tubesheet-to-head welds)

Plant Type	Total No. of Units in Survey	No. of Units with this Item	Total No. of Applicable Components	Total No. of Examinations	Total No. of Exams that Exceed Section XI Acceptance Criteria
BWR	27	0	0	0	0
PWR W-2 Loop	4	4	7	46	Note 1
PWR W-3 Loop	11	9	27	35	0
PWR W-4 Loop	20	20	74	61	0
PWR-CE	6	6	11	18	0
PWR B&W	6	6	20	23	0
Total	74	45	139	183	Note 1

Note 1: Two PWR Westinghouse two-loop units at a single plant reported multiple subsurface embedded fabrication flaws. See Section 3.1 for details.

Table 3-4
Summary of survey results for Item No. B3.130 (SG primary side nozzle-to-vessel welds)

Plant Type	Total No. of Units in Survey	No. of Units with this Item	Total No. of Applicable Components	Total No. of Examinations	Total No. of Exams Containing Flaws that Exceed Section XI Acceptance Criteria
BWR	27	0	0	0	0
PWR W-2 Loop	4	0	0	0	0
PWR W-3 Loop	11	2	12	12	0
PWR W-4 Loop	20	1	8	14	0
PWR-CE	6	5	30	83	0
PWR B&W	6	2	8	26	0
Total	74	10	58	135	0

Table 3-5
Summary of survey results for Item No. C1.10 (vessel shell circumferential welds)

Plant Type	Total No. of Units in Survey	No. of Units with this Item	Total No. of Applicable Components	Total No. of Examinations	Total No. of Exams Containing Flaws that Exceed Section XI Acceptance Criteria
BWR	27	24	90	140	0
PWR W-2 Loop	4	4	12	37	0
PWR W-3 Loop	11	11	74	91	0
PWR W-4 Loop	20	16	169	102	0
PWR-CE	6	6	25	45	0
PWR B&W	6	6	42	30	0
Total	74	67	412	445	0

Table 3-6
Summary of survey results for Item No. C1.20 (vessel head circumferential welds)

Plant Type	Total No. of Units in Survey	No. of Units with this Item	Total No. of Applicable Components	Total No. of Examinations	Total No. of Exams that Exceed Section XI Acceptance Criteria
BWR	27	20	42	54	0
PWR W-2 Loop	4	4	15	42	Note 1
PWR W-3 Loop	11	11	66	108	0
PWR W-4 Loop	20	20	114	113	1
PWR-CE	6	6	16	33	0
PWR B&W	6	6	24	23	0
Total	74	67	277	373	Note 1

Note: A single PWR Westinghouse two-loop unit reported multiple flaws. See Section 3.1 and References [42] and [43] for details.

Table 3-6
Summary of survey results for Item No. C1.30 (vessel tubesheet-to-shell welds)

Plant Type	Total No. of Units in Survey	No. of Units with this Item	Total No. of Applicable Components	Total No. of Examinations	Total No. of Exams Containing Flaws that Exceed Section XI Acceptance Criteria
BWR	27	6	27	32	0
PWR W-2 Loop	4	4	7	13	0
PWR W-3 Loop	11	11	37	43	0
PWR W-4 Loop	20	20	84	46	0
PWR-CE	6	6	22	36	0
PWR B&W	6	6	36	25	0
Total	74	53	213	195	0

According to the survey results, Item Nos. B2.31, B2.32, and B3.130 are examined at only a few domestic plants. This can be partly attributed to the use of replacement steam generators (RSGs), many of which have integrally forged head nozzles that eliminate the welds associated with these examination items. Even though they represent a relatively small population, it was decided to evaluate these item numbers for completeness.

4

SURVEY OF COMPONENTS AND SELECTION OF REPRESENTATIVE COMPONENTS FOR ANALYSIS

Section 3 reviewed the examination history for Item Nos. B2.31, B2.32, B2.40, B3.130, C1.10, C1.20, and C1.30, including the PWR SG nozzle-to-vessel and vessel weld components evaluated in this report. In this section, representative components are selected for analysis. Selection of representative components considered the following factors:

- Whether a single PWR component could represent all plant designs types (that is, two-loop Westinghouse, three-loop Westinghouse, four-loop Westinghouse, B&W, and CE)
- Component geometry
- Component operating characteristics (loads)¹
- Component materials
- Field experience with regard to service-induced cracking
- The availability and quality of component-specific information

4.1 Steam Generators and NSSS Suppliers

All PWR plants contain SGs to convert primary-side heat into steam to generate power. As part of the primary side, all SGs have two main types of nozzles—inlet nozzles that carry hot fluid from the RPV into the SG primary side head and outlet nozzles that carry cooler fluid from the SG head to the reactor coolant pumps (RCPs). The SG secondary (shell) side takes condensate from the feedwater nozzles and produces steam, which exits through the main steam nozzles. The primary-side nozzles, primary-side head, and secondary-side shell welds are the subject of this report.

Three NSSS vendors were investigated. Westinghouse has three designs classified by the number of reactor coolant loops (two, three, or four). In Westinghouse designs, each loop contains one steam generator. CE plants have two reactor coolant loops with a total of two hot legs (each running to one SG) and four cold legs. Similar to CE plants, B&W plants also have two reactor coolant loops with a total of two hot legs (each running to one SG) and four cold legs. Both Westinghouse and CE plants use a U-tube SG design, whereas B&W plants use a once-through steam generator (OTSG) design. The schematics of Westinghouse two-loop, CE, and B&W SGs are shown in Figures 4-1, 4-2, and 4-3, respectively.

¹ General operating characteristics (loads) were considered in this section; for a detailed discussion of applicable loads, see Section 5. Similarly, only thermal and pressure transients were considered in this section with regard to degradation; for a detailed discussion of degradation mechanisms, see Section 6.

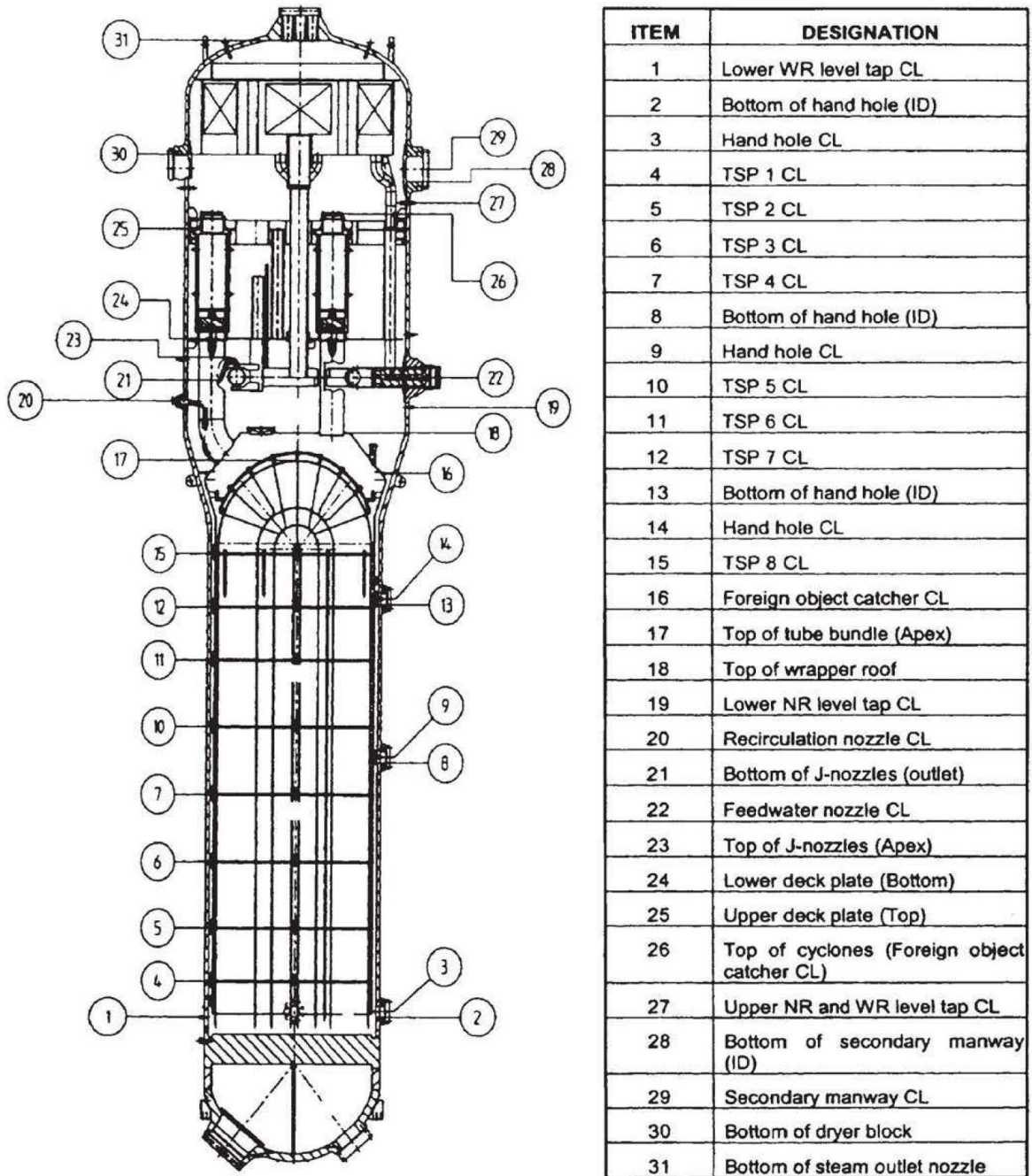


Figure 4-1
Westinghouse U-tube SG

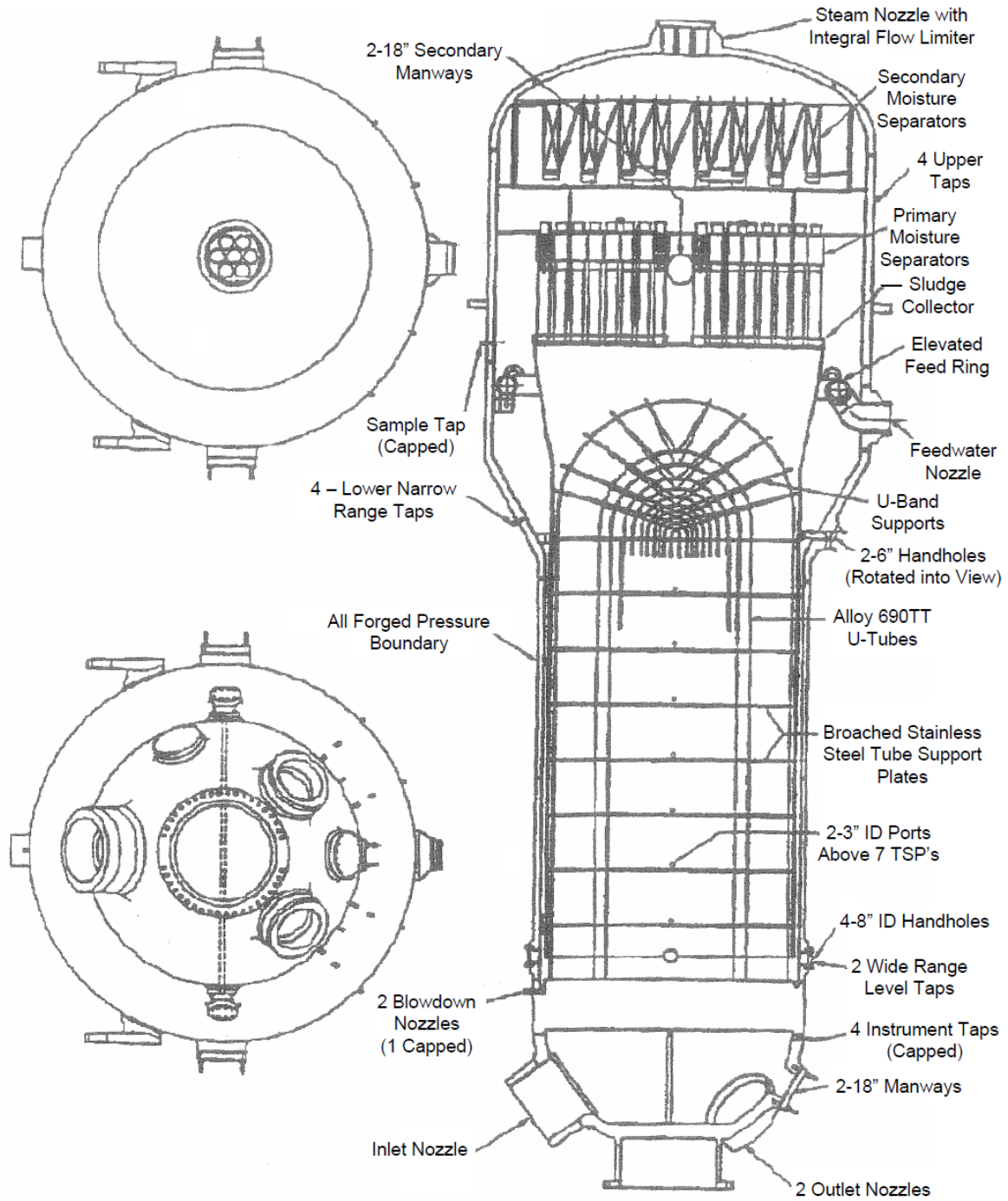


Figure 4-2
CE U-tube SG

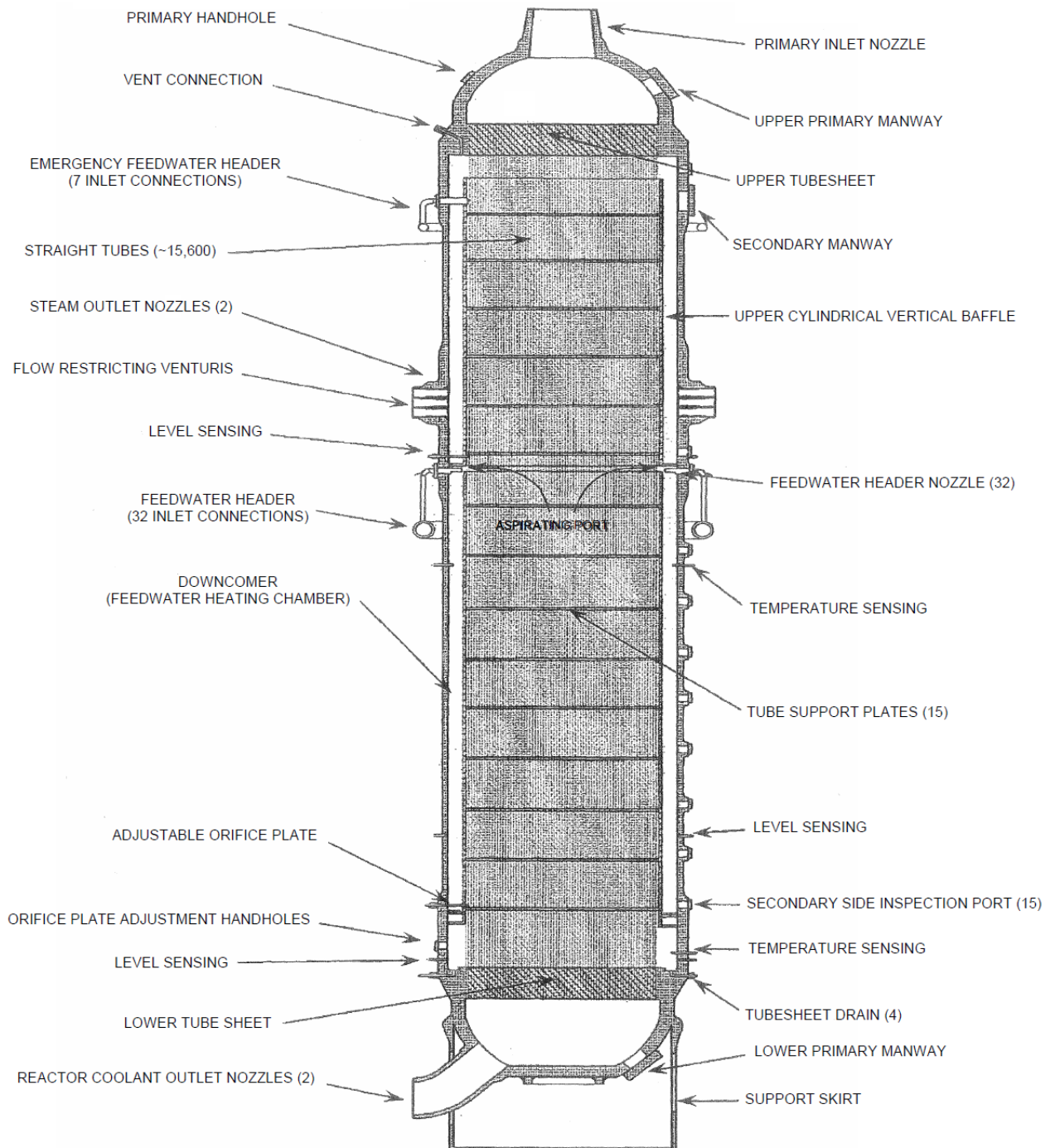


Figure 4-3
B&W OTSG

As Figures 4-1 and 4-2 show, the Westinghouse and CE SG designs are similar, though the CE design is larger. Figure 4-3 shows that the B&W OTSG design is substantially different.

4.2 SG Operating Experience

PWR SGs and their associated components have been subject to degradation throughout their operating history. The first generation of SGs had Alloy 600 tubing that was subject to stress corrosion cracking (SCC). Due to excessive cracking and the need for plugging tubes, many SGs were replaced throughout the fleet (50% as of 2004 [44]). This activity has increased as plants continue to age. Therefore, most of the information used for this report comes from RSGs. Although RSGs have not been in service for the full life of the plant, they did not substantially change the operating characteristics of the SG primary or secondary side.

SG feedwater nozzles (and connected piping) are subject to thermal fatigue and have experienced cracking incidents, mainly associated with certain design and operating characteristics [45]. By contrast, neither main steam nozzles nor the SG primary-side inlet or outlet nozzles evaluated in this report have experienced operating degradation or cracking due to thermal fatigue.

4.3 Variation Among SG Designs

As previously noted, many SGs were replaced due to plugging a large percentage of tubes. The RSGs were not always replaced by the original NSSS supplier. Because there are numerous RSG manufacturers and designers, SG designs can vary, making it challenging to identify a single bounding or representative design. To better understand the extent of the variations among SG designs, information was tabulated across the SG population using both public (for example, Final Safety Analysis Report [FSAR]) and plant-specific information. Although the tabulated information is not comprehensive, a best effort was made to compile consistent and accurate information for as many plants as possible regarding the following:

- Plant name
- NSSS vendor
- Number of reactor coolant loops
- SG manufacturer
- SG designer
- SG model designation
- Upper and lower SG shell material
- Upper and lower SG shell diameter and thickness (for U-tube designs)
- Design code
- RPV inlet nozzle material, diameter, thickness, and inner radius
- RPV outlet nozzle material, diameter, thickness, and inner radius
- Plant design/operating pressure and temperature
- Reactor coolant flow rate, steam flow rate, feedwater temperature, and steam pressure

A review of the information that was compiled showed that, despite the numerous designers and manufacturers, RSG designs are fairly consistent. This is reasonable considering constraints such as the RSG having to fit in the same space and the fact that they were designed to similar operating parameters as the original SGs. Variations are most prominent in nozzle designs. Variations in SG dimensions, design temperatures and pressures, and ASME Code design considerations are covered in Sections 4.3.1–4.3.3. Configurations where relief has been sought due to difficulties in performing ASME Code examinations are covered in Section 4.4. The selection of the main steam and feedwater nozzle components to be used in this evaluation is addressed in Section 4.5.

4.3.1 Dimensions

Based on the dimensional information compiled, the following trends were identified:

Westinghouse Designs

- The size (diameter and thickness) of the Westinghouse SG is related to the model and manufacturer rather than the number of loops. The outside diameter of the upper shell varies from 166 in. to 178 in.,² which is a variation of less than 10%. The radius-to-thickness (R/t) ratio for the upper shell varies from 24 to 30. The outside diameter of the lower head (containing the primary-side inlet and outlet nozzles) varies from 127 in. to 136 in., which is a variation of less than 10%. The R/t ratio for the lower head varies from 21 to 25.
- The SG primary-side inlet nozzle nominal pipe size (NPS) is uniformly 29 in. According to Table 3-4, a relatively small number of Westinghouse plants reported performing examinations of the SG primary-side nozzle-to-vessel weld, and there was not enough information available to develop an R/t ratio for the nozzle body. However, it is believed that the ratio would be similar to that for the SG nozzles evaluated in Reference [2] (that is, range from 2 to 3) because they are based on similar design (ASME Code Section III minimum thickness) considerations.
- The SG primary-side outlet nozzle NPS is uniformly 31 in. Per Table 3-4, a relatively small number of Westinghouse plants reported performing examinations of the SG primary-side nozzle-to-vessel weld, and there was not enough information available to develop an R/t ratio for the nozzle body. However, it is believed the ratio would be similar to that for the SG nozzles evaluated in Reference [2] (that is, range from 2 to 3) because they are based on similar design (ASME Code Section III minimum thickness) considerations.

² South Texas Units 1&2 (199.4 in.), VC Summer (210 in.), and Callaway (239.7 in.) have upper shell SG diameters outside of this range; however, the related R/t values are consistent with the rest of the Westinghouse plants.

CE Designs

- The size (diameter and thickness) of all CE SGs is similar, with negligible variation between plants. The exception is the System 80 design, which has a significantly larger lower head diameter. In all cases, the CE SG dimensions are much larger than any of the Westinghouse designs. The outside diameter of the upper shell varies from 239 in. to 244 in., which is a variation of less than 5%. The R/t ratio for the upper shell varies from 21 to 27. The outside diameter of the lower head varies from 164 in. to 203 in., which is a variation of roughly 25% (again, the System 80 design is a significant outlier). The R/t ratio for the lower head varies from 21 to 30.
- The SG primary-side inlet nozzle NPS is uniformly 42 in. Based on the available information, the R/t ratio for the nozzle body ranges from a value of 3.0 to 3.6.
- The CE SG design features two outlet nozzles. The SG primary-side outlet nozzle NPS is uniformly 30 in. Based on the available information, the R/t ratio for the nozzle body ranges from a value of 2.8 to 3.0.

B&W Designs

- The size (diameter and thickness) of all B&W OTSGs is very similar, with negligible variation between plants. The outside diameter is uniform along the length of the SG at approximately 149 in. The R/t ratios between plants using the B&W OTSG design are similar but difficult to specify due to varying thicknesses throughout the vessel. A nominal thickness can be obtained for the vessel, but nozzle locations feature increased thicknesses, and nominal thicknesses are not always provided at the same location. For this reason, a direct comparison is not feasible. However, based on the nominal dimensions, the R/t ratio is approximately 24.5.
- The SG primary-side inlet nozzle NPS is uniformly 36 in. at the nozzle inlet; the nozzle then tapers outward toward a larger diameter (identified as 45 in. based on the limited data available). Due to this tapered configuration, an average NPS of 40.5 was used when calculating R/t. Based on the available information, the R/t ratio for the nozzle body ranges from a value of 3.7 to 4.0.
- The B&W SG design features two outlet nozzles. The SG primary-side outlet nozzle NPS is uniformly 28 in. Based on the available information, the R/t ratio for the nozzle body ranges from a value of 3.0 to 3.3.

4.3.2 Design Pressures and Temperatures

Based on the information compiled from available sources, the design pressure for the primary side of the SG is essentially uniform at 2,485 psig. The design temperature for the primary side of the SG is 650°F in all cases. The design pressure for the secondary side of the SG varies from 1,000 psig to 1,285 psig. Most SGs have a design pressure of approximately 1,100 psig (the average pressure among tabulated values is approximately 1,115 psig). The design temperature for the secondary side of the SG varies from 550°F to 630°F. The majority of SGs have a secondary-side design temperature of approximately 600°F (the average temperature among tabulated values is approximately 590°F).

4.3.3 ASME Code Design Considerations

Based on the information compiled from available sources, all SGs were designed to Section III of the ASME Code, although numerous editions were used. Some SGs were designed to the 1966 edition, whereas others were designed to the 1998 edition. Despite the different ASME Code editions, the Section III stress criteria used to design the SGs have remained consistent since early versions of the ASME Code.

There are two items to consider for the SG shell and nozzles. First is the required thickness due to pressure. The general design rules for vessels is contained in ASME Code Section III, Subarticle NB-3300 [46], with the required pressure thickness (t) contained in Paragraph NB-3324 as follows:

$$t = \frac{PR_o}{S_m + 0.5P} \quad \text{Eq. 4-1}$$

where P is the design pressure, R_o is the outside radius, and S_m is the design stress intensity.

Equation 4-1 is based on the calculation of pressure stress intensity. The pressure stress intensity is dominated by the pressure hoop stress (PR/t), where R is the mean radius and t is the wall thickness. Because the SGs are all made of low-alloy steel (refer to Section 5), S_m is similar for all SGs. With the allowable stress consistent, the ratio between R and t needs to remain consistent to account for variations in the design pressure. Equation 4-1 was used to calculate the required minimum thickness, t_{\min} , of the SG shell for several plants for which data were available. In all cases, the actual thickness of the SG shell was greater than t_{\min} by 5–33%. Therefore, the component selected for analysis has a thickness closer to t_{\min} in order to be bounding because the fracture mechanics results are controlled by pressure stresses.

The second item to consider for the SG nozzles is the design requirement for openings and reinforcement. Paragraph NB-3332 [45] defines the rules for area reinforcement in vessels and formed heads. The SG primary-side inlet and outlet nozzles were designed to these requirements, which have remained consistent throughout ASME Code history. These rules define two main criteria: 1) the amount of metal required for reinforcement and 2) the distance limits for the location for reinforcement. These values are based on the size of the hole in the vessel for the nozzle, the thickness of the shell/head, and the diameter of the shell/head. For the primary-side inlet and outlet nozzles specifically, the variations in hole size have an effect on the detailed nozzle geometry and reinforcement. Because most hole sizes for these nozzles are similar, the rules in the ASME Code will cause most nozzle geometries to have a consistent reinforcement design.

Because the design parameters and materials are similar, the design rules cause consistency in the R/t ratio used to compare the relative stresses in the SGs. This is consistent with previous work, in that four of the five criteria set forth by the NRC in Reference [4] on the plant-specific applicability of the BWRVIP-108 report [3] relate to the R/t ratio. The R/t ratio also helps normalize differences between plant designs when multiple parameters are different. As noted in Section 4.3.1, R/t ratios for Westinghouse and CE SGs are reasonably consistent, even though the SG diameters for CE plants are much larger. This fact allows the CE and Westinghouse SGs to be represented by a single configuration (as will be discussed in Section 4.5). The R/t ratio controls the pressure loading because it is dependent on the geometry. Based on the data

obtained, the R/t variations are expected only to be slightly greater than 10%. Such variations are handled by sensitivity analyses in the probabilistic fracture mechanics (PFM) portion of the evaluation (see Section 8), similar to the approach used in BWRVIP-241 [5] to address the NRC plant-specific applicability criteria in Reference [4].

4.4 Configurations with Impractical or Limited Exams

The survey responses covered in Section 3 include cases where components have been the subject of a Relief Request. These Relief Requests are related to either the impracticality of performing an ISI or limited ability to obtain full inspection coverage due to plant-specific component configurations and obstructions. Table 4-1 summarizes the Relief Requests related to examinations performed on the SG nozzle-to-vessel and vessel shell welds in the scope of this evaluation. As Table 4-1 shows, only a few plants requested relief from five of the in-scope items, with no relief requested for the other two in-scope items.

Table 4-1
Units with Relief Request by Item No.

Item No.	No. of Units in Survey with This Item No.	No. of Units in Survey with Relief Requests	Reason for Relief Request(s)
B2.31	7	0	N/A
B2.32	1	0	N/A
B2.40	45	6	Less than essentially 100% coverage
B3.130	10	4	Less than 100% coverage
C1.10	67	10	Less than 100% coverage
C1.20	67	8	Less than 100% coverage
C1.30	53	7	Less than 100% coverage

4.5 Selection of Components for Evaluation

The review in Section 4.3 was performed to determine what type of geometric variations could be expected between different PWR SG designs. The main conclusion was that, where geometric variations exist, they are not considered significant and can be addressed by sensitivity analyses. Therefore, instead of determining (or defining) bounding component geometries, representative component geometries were selected based on their availability through the EPRI survey results, the factors described in Section 4.3, and a set of related criteria.

4.5.1 SG Primary-Side Nozzles

Item No. B3.130 (Class 1 Full Penetration Steam Generator Nozzle-to-Vessel Welds) is applicable to the SG primary side inlet and outlet nozzles. The inlet and outlet nozzles and the SG lower head are fabricated of the same materials and subjected to essentially the same loads and transients across all PWR design types. Thermal events during normal plant operation are benign for these locations, so the main contributor to crack growth is startup and shutdown temperature and pressure variations. Based on a review of the survey results, the total population

of these components is limited; this is likely due to SG replacements where RSGs have integrally forged nozzles in both the upper shell and lower head, thereby eliminating the subject welds. SGs differ in that the nozzle-to-vessel weld might be located on either the nozzle side or shell side of the nozzle forging; therefore, both of these possible locations were considered in the fracture mechanics evaluation.

As covered previously, the Westinghouse and CE SG designs are similar, except that the CE vessel is larger and has two primary outlet nozzles, whereas Westinghouse designs have one primary outlet nozzle. Because a larger SG size will result in larger pressure stresses in the head (where the primary inlet and outlet nozzles are located), the inlet nozzle for a CE plant was considered representative for both the Westinghouse and CE SG designs. Because the B&W OTSG design is substantially different, the inlet nozzle for a B&W plant was also modeled. The relevant geometries for the CE and B&W steam generator inlet nozzles assumed in this study are shown in Figures 4-4 and 4-5, respectively.

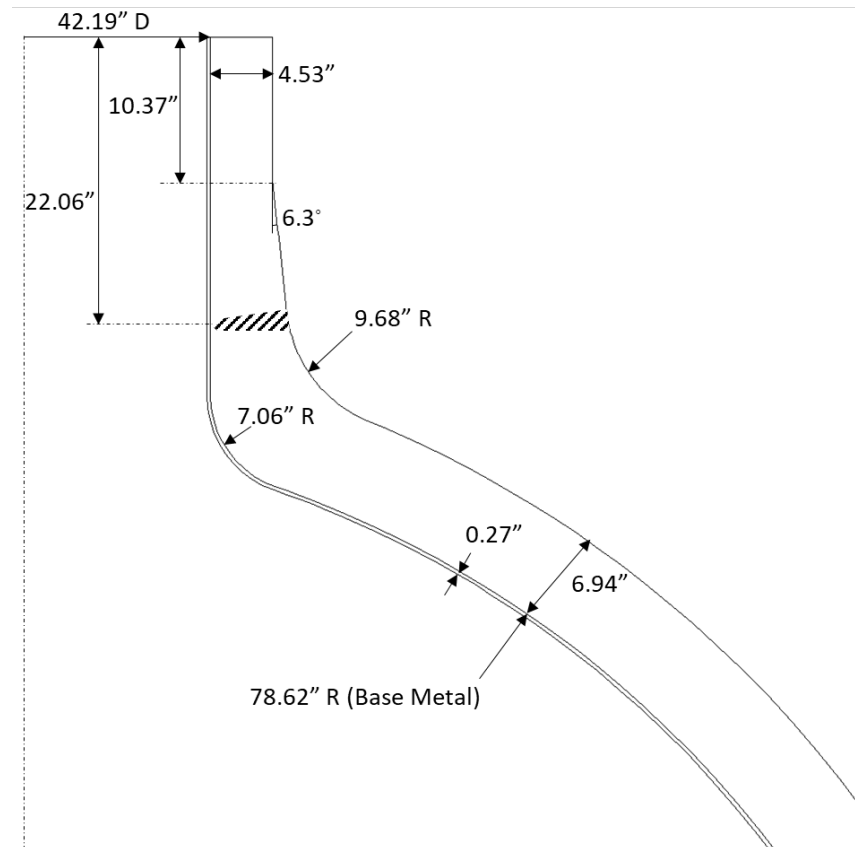


Figure 4-4
CE SG (primary side) inlet nozzle-to-vessel (Item No. B3.130) weld geometry selected for evaluation

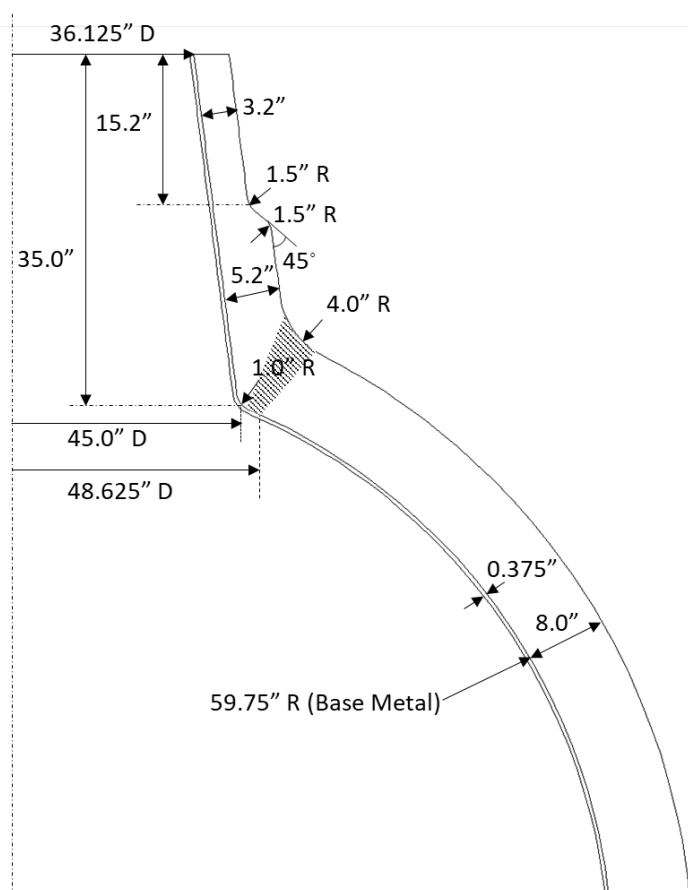


Figure 4-5
B&W SG (primary side) inlet nozzle-to-vessel (Item No. B3.130) weld geometry selected for evaluation

4.5.2 SG Primary-Side Head

4.5.2.1 Item No. B2.31: Steam Generator (Primary Side) Head Circumferential Welds

Based on the survey results, this item is present in the SGs of only three PWR design types. The dimensions of these components vary across the fleet because the SG sizes vary for each plant design. The SG shell and head are fabricated of the same materials and subjected to essentially the same loads and transients across all PWR design types due to similar operating characteristics of the plant main loop. The thermal transients are relatively benign for this item because the main loop does not have any significant temperature differences; therefore, pressure is the dominant factor for the growth of any defects. The SG with the largest diameter will result in the largest pressure stress in the head; therefore, a component from the largest-diameter SG (the CE design) was considered representative and bounding. The ratio of t_{min} to the actual thickness of this component is 95%; the component is therefore considered bounding from this perspective. Relevant SG geometry is provided in Table 4-2.

Table 4-2
Relevant dimensions of SG components selected for evaluation

SG Component	Item Nos.	Shell Diameter (in.)	Shell/Clad Thickness (in.)	Head Radius (in)	Head/Clad Thickness (in.)
SG primary side	B2.31, B2.32, B2.40	169.75 ⁽¹⁾	6.94 / 0.27	82.56	6.94 / 0.27
SG secondary side ⁽²⁾	C1.10, C1.20, C1.30	169.75 170.07 240.69	3.65 / NA 4.31 / NA 4.91 / NA	Not applicable	Not applicable

Notes:

- (1) This is the SG tubesheet diameter dimension that attaches to the head.
- (2) For the SG secondary side, the shell diameters and thicknesses of the lower shell, intermediate shell, and upper shell, respectively, are listed.

4.5.2.2 Item No. B2.32: Steam Generator (Primary Side) Head Meridional Welds

Based on the survey results, this item is present in the SG of only one PWR plant. The SG selected in Section 4.5.2.1 is considered representative for evaluation of this item. The SG heads are not perfectly spherical; therefore, the geometry evaluated is a simplification of the actual head geometry. The relevant SG geometry is provided in Table 4-2.

4.5.2.3 Item No. B2.40: Steam Generator (Primary Side) Tubesheet-to-Head Welds

Based on the survey results, this item is present in the SGs of all PWR designs. The dimensions of these components vary across the fleet because the SG sizes vary for each plant design. The SG selected in Section 4.5.2.1 was also considered representative for evaluation of this item. The relevant SG geometry is provided in Table 4-2. The tubesheet-to-head weld configuration for the selected geometry has approximately the same thickness at the weld locations as the nominal shell thickness; therefore, it results in conservative stresses for these welds compared to SG designs with thicker tubesheet-to-head welds.

4.5.3 SG Secondary-Side Shell

4.5.3.1 Item No. C1.10: Class 2 Vessel Shell Circumferential Welds

Based on the survey results, this item is present in the SGs of all PWR designs. The SG selected in Section 4.5.2.1 was also considered representative for evaluation of this item because it is the SG with the largest diameter. For the secondary side, the largest part of the SG is at the top, and the diameter and thickness at this location were used for the evaluation. The relevant SG geometry is provided in Table 4-2.

4.5.3.2 Item No. C1.20: Class 2 Vessel Head Circumferential Welds

Based on the survey results, this item is present in the SGs of all PWR designs. The SG selected in Section 4.5.2.1 was also considered representative for evaluation of this item because it is the SG with the largest diameter. The relevant SG geometry is provided in Table 4-2.

4.5.3.3 Item No. C1.30: Class 2 Vessel Tubesheet-to-Shell Welds

Based on the survey results, this item is present in the SGs of all PWR designs. The SG selected in Section 4.5.2.1 was also considered representative for evaluation of this item. The relevant SG geometry is provided in Table 4-2. The tubesheet-to-shell weld configuration for the selected geometry has approximately the same thickness at the weld locations as the nominal shell thickness; therefore, it results in conservative stresses for these welds compared to SG designs with thicker tubesheet-to-shell welds.

4.6 Conclusions

PWR SG designs and operating experience were reviewed. Information was also reviewed regarding variability among SG designs in terms of dimensions, design pressures and temperatures, and ASME Code design considerations. Geometrical variations among SG designs are shown in Tables 4-3 and 4-4.

Table 4-3
Summary of SG geometrical parameters for the various SG designs

Component	Parameter	Westinghouse	CE	B&W
SG lower head	Diameter (in.)	127–136	164–203	149
	R/t ratio	23–25	21–30	24.5
SG upper shell	Diameter (in.)	166–178	239–244	149
	R/t ratio	24–26	21–27	24.5
SG primary-side inlet nozzle	NPS (in.)	29	42	40.5 (average)
	R/t ratio	Note 1	3.0–3.6	3.7–4.0
SG primary-side outlet nozzle	NPS (in.)	31	30 (two nozzles)	28 (two nozzles)
	R/t ratio	Note 1	2.8–3.0	3.0–3.3

Note: There was not sufficient information available to develop an R/t ratio for the nozzle body.

Table 4-4
Variation of R/t ratios for various SG designs

Component	Westinghouse	CE	B&W	Range	Variation
SG lower head	23–25	21–30	24.5	21–30	30.0%
SG upper shell	24–26	21–27	24.5	21–27	12.5%
SG primary-side inlet nozzle	Note 1	3.0–3.6	3.7–4.0	3.0–4.0	33.3%
SG primary-side outlet nozzle	Note 1	2.8–3.0	3.0–3.3	2.8–3.3	17.9%

Note: There was not sufficient information available to develop an R/t ratio for the nozzle body.

The most important parameter from an ASME Section III design viewpoint is the R/t ratio. Table 4-4 shows the variations in this parameter, with the maximum variation (33.3%) associated with the primary inlet nozzle. This variation can be addressed in the flaw tolerance evaluations by performing sensitivity studies, as covered in Section 8. Therefore, instead of defining bounding component geometries, representative component geometries were selected based on the plants that responded to the EPRI survey, the factors discussed in Section 4.3, and a set of related criteria.

The selected components are representative for CE, Westinghouse, and B&W steam generator designs (with the exceptions noted previously). Section 9 covers the parameters that need to be verified to determine whether a specific plant is covered by the evaluation performed in this report.

5

MATERIALS PROPERTIES, OPERATING LOADS, AND TRANSIENTS

5.1 Materials Selection and Properties

The topic of this section is the materials selections and related properties that will be used in the stress analyses for the components selected in Section 4. Materials properties related to fracture mechanics evaluations, such as toughness and crack growth parameters, are addressed in later sections.

According to Section 4.5, two SG primary-side nozzle designs and one SG (primary- and secondary-side) vessel design were selected for evaluation. As discussed in Section 4.3, available SG data were tabulated to evaluate variation among SG designs. One item tabulated was the material of the SG head, shell, and nozzles. The tabulated materials show that many materials are the same. For all SG designs, the primary side inlet and outlet nozzles are fabricated from a forging material. This forging material specification is typically a low-alloy steel such as SA-508, Class 2. The head is also fabricated from a low-alloy steel material, but the specifications vary based on the selected fabrication practices. If the head were forged, the material specification is a low-alloy steel such as SA-508, Class 2. If the head were formed from a plate, it is made from a low-alloy steel such as like SA-533, Grade B Class 1. SG shells are typically made of a carbon steel such as SA-516, Grade 70. SG tubesheets are typically made of a low-alloy steel material such as SA-508, Class 2, and the tubesheet-to-vessel weld material will be comparable.

The exact material specification used will be based on the fabrication practices used for the SG selected for analysis. For instance, an SG shell section can be forged from a solid ingot, or a plate can be rolled and then seam-welded. Similarly, a SG head can be manufactured from a forging or a formed plate (or multiple formed plates). Regardless of the material specification used, the specifications all call for a low-alloy steel material. The weld materials used to join the nozzle to the head are a compatible low-alloy steel filler metal. The actual weld specification used was determined based on the specific welding process used. For instance, large components fabricated using rotating gimbals used submerged arc welding methods. If manual welding processes were employed, shielded metal arc welding material specifications were used. The exact process and specification are not important for this evaluation. The weld material properties are assumed to be those of a similar material to match the nozzle and head/shell.

Based on the tabulated data, the materials used in the stress analysis for this study are provided in Table 5-1. Temperature-dependent materials properties were obtained from the relevant tables in the 2013 edition of ASME Code, Section II, Part D [47] and are provided in Tables 5-2 through 5-5. A typical stainless steel (SA-204, Type 304) was assumed for all cladding material.

Table 5-1
Materials used in stress analysis

Item No.	Component	Material
B2.31, B2.32, B2.40	PWR Steam Generator (Primary Side) Head ⁽¹⁾ PWR Steam Generator (Primary Side) Tubesheet ⁽¹⁾ PWR Steam Generator (Primary Side) Tubesheet-to-Head Weld	SA-533 Grade B Class 1 SA-508 Class 2 and corresponding weld metal
B3.130	PWR Steam Generator Inlet Nozzle ^(1, 2) PWR Steam Generator Primary Head ^(1, 2) PWR Steam Generator Inlet Nozzle-to-Head Weld ⁽²⁾	SA-533 Grade B Class 1 SA-508 Class 2 and corresponding weld metal
C1.10, C1.20, C1.30	PWR Steam Generator (Secondary Side) Head and Shell PWR Steam Generator Tubesheet PWR Steam Generator (Secondary Side) Tubesheet-to-Shell Welds	SA-516 Grade 70 SA-508 Class 2 and corresponding weld metal

Notes:

- (1) Cladding is applied on the inside surface of this component. Properties for typical stainless steel (SA-204, Type 304) are assumed.
- (2) For simplicity, SA-508 Class 2 material is used for the PWR steam generator inlet nozzle and primary head in the stress analyses.

Table 5-2
Materials properties for SA-533 Gr. B Cl. 1 (low-alloy steel, identical to SA-533 Gr. A Cl. 2)
[47]

Temperature (°F)	Modulus of Elasticity, E (10 ⁶ psi)	Coefficient of Thermal Expansion, α (10 ⁻⁶ in/in/°F)	Thermal Conductivity, K (10 ⁻⁴ BTU/in-s-°F)	Specific Heat, C ^(2,3,4) (BTU/lb-°F)
70	29.0	7.0	5.49	0.107
100	28.9 ⁽¹⁾	7.1	5.46	0.108
150	28.7 ⁽¹⁾	7.2	5.44	0.111
200	28.5	7.3	5.44	0.115
250	28.3 ⁽¹⁾	7.3	5.42	0.117
300	28.0	7.4	5.42	0.121
350	27.8 ⁽¹⁾	7.5	5.39	0.123
400	27.6	7.6	5.35	0.126
450	27.3 ⁽¹⁾	7.6	5.32	0.129
500	27.0	7.7	5.25	0.131
550	26.7 ⁽¹⁾	7.8	5.21	0.134

Table 5-2 (continued)
Materials properties for SA-533 Gr. B Cl. 1 (low-alloy steel, identical to SA-533 Gr. A Cl. 2)
[47]

Temperature (°F)	Modulus of Elasticity, E (10 ⁶ psi)	Coefficient of Thermal Expansion, α (10 ⁻⁶ in/in/°F)	Thermal Conductivity, K (10 ⁻⁴ BTU/in-s-°F)	Specific Heat, C ^(2,3,4) (BTU/lb-°F)
600	26.3	7.8	5.14	0.137
650	25.8 ⁽¹⁾	7.9	5.07	0.139
700	25.3	7.9	5.00	0.142

Notes:

- (1) Linearly interpolated value based on adjacent values.
- (2) Density (ρ) = 0.280 lb/in.³, assumed temperature-independent.
- (3) Poisson's ratio (ν) = 0.3, assumed temperature-independent.
- (4) Calculated per Note 1 of Table TCD in Reference [47].

Table 5-3
Materials properties for SA-508 Cl. 2 (low-alloy steel, identical to SA-508 Gr. 2 Cl. 1) [47]

Temperature (°F)	Modulus of Elasticity, E (10 ⁶ psi)	Coefficient of Thermal Expansion, α (10 ⁻⁶ in/in/°F)	Thermal Conductivity, K (10 ⁻⁴ BTU/in-s-°F)	Specific Heat, C ⁽⁴⁾ (BTU/lb-°F)
70	27.8	6.4	5.49	0.107
100	27.6 ⁽¹⁾	6.5	5.46	0.108
150	27.4 ⁽¹⁾	6.6	5.44	0.111
200	27.1	6.7	5.44	0.115
250	26.9 ⁽¹⁾	6.8	5.42	0.117
300	26.7	6.9	5.42	0.121
350	26.5 ⁽¹⁾	7.0	5.39	0.123
400	26.2	7.1	5.35	0.126
450	26.0 ⁽¹⁾	7.2	5.32	0.129
500	25.7	7.3	5.25	0.131
550	25.4 ⁽¹⁾	7.3	5.21	0.134
600	25.1	7.4	5.14	0.137
650	24.9 ⁽¹⁾	7.5	5.07	0.139
700	24.6	7.6	5.00	0.142

Notes:

- (1) Linearly interpolated value based on adjacent values.
- (2) Density (ρ) = 0.280 lb/in.³, assumed temperature-independent.
- (3) Poisson's ratio (ν) = 0.3, assumed temperature-independent.
- (4) Calculated per Note 1 of Table TCD in Reference [47].

Table 5-4
Materials properties for SA-516 Gr. 70 (carbon steel) [47]

Temperature (°F)	Modulus of Elasticity, E (10 ⁶ psi)	Coefficient of Thermal Expansion, α (10 ⁻⁶ in/in/°F)	Thermal Conductivity, K (10 ⁻⁴ BTU/in-s-°F)	Specific Heat, C ^(2,3,4) (BTU/lb-°F)
70	29.2	6.4	8.08	0.103
100	29.1 ⁽¹⁾	6.5	8.03	0.106
150	28.8 ⁽¹⁾	6.6	7.92	0.110
200	28.6	6.7	7.80	0.114
250	28.4 ⁽¹⁾	6.8	7.64	0.117
300	28.1	6.9	7.48	0.119
350	27.9 ⁽¹⁾	7.0	7.31	0.122
400	27.7	7.1	7.15	0.124
450	27.4 ⁽¹⁾	7.2	6.97	0.126
500	27.1	7.3	6.81	0.128
550	26.8 ⁽¹⁾	7.3	6.64	0.131
600	26.4	7.4	6.48	0.134
650	25.9 ⁽¹⁾	7.5	6.32	0.136
700	25.3	7.6	6.16	0.140

Notes:

- (1) Linearly interpolated value based on adjacent values.
- (2) Density (ρ) = 0.280 lb/in.³, assumed temperature-independent.
- (3) Poisson's Ratio (ν) = 0.3, assumed temperature-independent.
- (4) Calculated per Note 1 of Table TCD in Reference [47].

Table 5-5
Material properties for SA-240 Type 304 (stainless steel) [47]

Temperature (°F)	Modulus of Elasticity, E (10 ⁶ psi)	Coefficient of Thermal Expansion, α (10 ⁻⁶ in/in/°F)	Thermal Conductivity, K (10 ⁻⁴ BTU/in-s-°F)	Specific Heat, C ⁽⁴⁾ (BTU/lb-°F)
70	28.3	8.5	1.99	0.114
100	28.1 ⁽¹⁾	8.6	2.01	0.114
150	27.8 ⁽¹⁾	8.8	2.08	0.117
200	27.5	8.9	2.15	0.119
250	27.3 ⁽¹⁾	9.1	2.22	0.121
300	27.0	9.2	2.27	0.122
350	26.7 ⁽¹⁾	9.4	2.34	0.124
400	26.4	9.5	2.41	0.126
450	26.2 ⁽¹⁾	9.6	2.45	0.127
500	25.9	9.7	2.52	0.129
550	25.6 ⁽¹⁾	9.8	2.57	0.129
600	25.3	9.9	2.62	0.130
650	25.1 ⁽¹⁾	9.9	2.69	0.131
700	24.8	10.0	2.73	0.132

Notes:

- (1) Linearly interpolated value based on adjacent values.
- (2) Density (ρ) = 0.290 lb/in.³, assumed temperature-independent.
- (3) Poisson's ratio (ν) = 0.31, assumed temperature-independent.
- (4) Calculated per Note 1 of Table TCD in Reference [47].

5.2 Operating Loads and Transients

The operating loads and transients used in the stress analysis for the components selected in Section 4 are covered in this section. The loads considered for these components are those due to thermal and pressure transients. As with other RCS components, the SG was designed to Section III of the ASME Code and considered all service levels—Design, Normal (A), Upset (B), Emergency (C), Faulted (D), and Test Conditions. ASME Code Section XI requires that the component be able to withstand these conditions during operation. For the fracture mechanics evaluation of failure (where the applied stress intensity factor, K , is compared to the fracture toughness, K_{IC}), the maximum load on the component from normal, upset, emergency, and faulted conditions needs to be considered. Because the plant is not expected to operate under emergency or faulted conditions, crack growth will be considered only for normal and upset events. Test conditions beyond a system leak test are not considered. The original hydrostatic test was performed during initial SG fabrication. Subsubarticle IWA-4540 requires a hydrostatic or system leakage test in accordance with Article IWA-5000. Paragraph IWA-5212 points to

Article IWC-5000 for hydrostatic and leakage tests of Class 2 components. Subsubarticle IWC-5220 requires the leakage test to be performed at the system pressure during normal service. Because any pressure tests will be performed at the operating pressure, no separate test conditions were included in the evaluation.

Attached piping loads are not considered in this evaluation. The piping system design required that the piping loads not exceed the criteria in ASME Code Section III, Paragraph NB-3652, which states that the combined pressure plus bending stress is required to be less than 1.5 times the design stress intensity ($1.5S_m$). Because the nozzle section is much thicker than the piping, any stresses due to bending are much smaller in the nozzle compared to those calculated in the piping attached to the nozzle. Therefore, the stresses due to loads from the attached piping were not included in the analysis because they are overwhelmed by the pressure and thermal stresses. Rather, they are addressed by sensitivity studies on stress, as described in Section 8.

Thermal and pressure transients for each of the three NSSS vendors were considered in the evaluation. The thermal and pressure transients were developed by using plant data and information from system descriptions, process and instrumentation diagrams, other plant documents, and relevant industry literature. The data tabulated to evaluate SG design variability (discussed in Section 4.3) included available operating temperatures and pressures of both the SG primary and secondary sides. As expected, there are some variations in the operating characteristics of the various SG designs. Such variations are expected, and the transients defined for evaluation were modified to ensure that they are bounding (in terms of temperature rates and changes) for all investigated plant design types. Transient modifications included increasing temperature ramp rates, increasing the magnitude of temperature and pressure changes, and/or increasing the number of design transient cycles.

During normal PWR SG operation, the primary coolant enters the inlet nozzle (primary side), flows through the SG tubes, and leaves through the outlet nozzles (primary side). Feedwater enters the SG through the feedwater nozzle (secondary side), where it is distributed through the feedwater distribution ring and mixes with the recirculation flow. The fixed recirculation flow descends through the annular downcomer, which is an annular passage formed by the inner surface of the SG shell and the cylindrical shell wrapper. At the bottom of the downcomer, the secondary water is directed upward past the vertical tubes, where heat transfer from the primary side produces a water-steam mixture. After the water-steam mixture passes through separators and dryers, a dry steam exits the SG through the main steam nozzle (secondary side). As noted in Section 4, the U-tube steam generators for the Westinghouse and CE plants are different from the OTSG design for the B&W plants. One difference is that the OTSG design allows for superheating of the steam in the SG. However, as noted in the discussion of the operating temperatures and pressures, the B&W plants still operate in nominal temperature and pressure ranges when compared to the PWR fleet as a whole. Therefore, no B&W-specific modifications to transients were needed for this study, and the modified transients (previously covered) provide sufficient margin to bound most operating PWRs.

For the primary side, the SG outlet normal power operating temperature ranges from approximately 514°F to 560°F, with an average value of approximately 537°F. The SG inlet normal power operating temperature ranges from approximately 583°F to 625°F, with an average value of approximately 604°F.

For the secondary side, the SG steam normal power operating temperature ranges from approximately 510°F to 570°F, with an average value of approximately 530°F. The normal operating pressure has a larger variation, from 735 psig to 1,042 psig, with an average of approximately 870 psig. Normal power feedwater temperatures have a narrower range, from 430°F to 470°F, with an average value of approximately 445°F.

FSARs often contain a summary of reactor coolant system design transients. As an example, Table 5-6 shows a summary of the normal, upset, emergency, and faulted transients and associated design cycles for Arkansas Nuclear One, Unit 1 (ANO-1) (B&W design) [48]. (Note: Design cycles are not necessarily indicative of how a plant actually operates.) EPRI previously performed a compilation of PWR fleet transients in MRP-393 [49]. Table 5-6 compares the design cycles from the ANO-1 Final Safety Analysis Report and MRP-393 projected cycles based on data collected from transient monitoring systems.

Table 5-6

Summary of reactor coolant system design transients for ANO-1 [48] compared to MRP-393 [49] cycles

Transient	Classification	ANO-1 40-Year Design Cycles [47]	MRP-393 60-yr Projections [49]
Heatup	Normal	240	200
Cooldown	Normal	240	200
Plant loading	Normal	18000	<1,000
Plant unloading	Normal	18000	<1,000
Step load increase	Normal	8000	Not typical
Step load decrease	Normal	8000	Not typical
Large step load decrease	Normal	—	20
Loss of load	Upset	—	Not typical
Loss of power ⁽¹⁾	Upset	40	Not typical
Loss of flow	Upset	20	Not typical
Reactor trip	Upset	400	~200
Inadvertent auxiliary spray	Upset	—	Not typical
Pipe break	Faulted	—	N/A

- (1) The loss-of-power event is infrequent and assumes that all outside electric power is lost and the emergency diesel generators do not activate. This event assumes that the reactor trips on loss of power, the reactor coolant flow decreases to natural circulation conditions, the main feedwater flow stops, and the auxiliary feedwater system is initiated. Realistic occurrences are expected to produce relatively benign thermal loading on the SG vessel. In a postulated rare instance, unheated auxiliary feedwater may be introduced into a hot SG that has been boiled dry following blackout, with the potential to thermally shock a portion of the SG vessel. However, this postulated case was not considered in this evaluation due to its rarity. In the event that such a significant thermal event occurs, its impact on the K_{IC} value may require more frequent examinations outside the scope of this report's guidance.

For 60 years of plant life, PWRs are not expected to have more than 200 heatup and cooldown cycles. Because many plants do not load-follow, many events related to loading and unloading do not occur at the frequency stipulated in FSARs. Rather than approximately 20,000 cycles over the plant lifetime, these loading and unloading cycles are projected to be less than 1,000 for 60 years of operation. Other events, like loss of load, loss of power, and loss of flow, are rare and have occurred infrequently (if at all) at most operating plants. These transients are noted as “not typical” for their frequency. This means that their number is very small, and representative transients for these conditions were not captured by fatigue monitoring systems. As such, these transients would have a negligible impact on fatigue crack growth of postulated flaws. Other events, such as reactor trips, have occurred and are projected to occur at about half of the design limit, or 200 cycles per 60 years of operation. Because many design events have not occurred, bounding cycle limits were selected based on the projected number of cycles for typical PWRs.

Because the SGs are made of ferritic steels, the failure mode was assumed as brittle fracture ($K > K_{IC}$). Therefore, for the fracture mechanics evaluation, transients (pressure and thermal) that significantly contribute to fatigue crack growth were considered. Additionally, the maximum stress state due to all applied loads was evaluated for failure. For fatigue crack growth of postulated flaws, any cycle will contribute to the growth, but small changes in temperature and pressure are expected to have an insignificant effect on the growth because the changes in stress intensity factor are small. On the other hand, heatup and cooldown events have large temperature and pressure changes associated with them because they cycle between ambient and full-power operating conditions. Therefore, the heatup and cooldown transients were assessed because they have the largest contributions to postulated crack growth.

5.2.1 Operating Conditions for PWR SG Vessel (Primary Side) Welds (Item Nos. B2.31, B2.32, and B2.40)

This section describes the operating conditions that were used for the stress analyses for the PWR SG (primary side) head circumferential welds (Item No. B2.31), SG (primary side) head meridional welds (Item No. B2.32), and SG (primary side) tubesheet-to-head welds (Item No. B2.40). Typical transients encountered in PWRs are described in Reference [49], which forms the basis for the following discussion (according to Reference [49], transients that rarely occur or are expected to be minor pressure/temperature excursions were not considered in this evaluation):

- **Heatup and cooldown (normal).** Heatup occurs from cold shutdown to rated temperature and pressure conditions, whereas cooldown occurs from the rated temperature and pressure conditions to cold shutdown. Typical rated temperature and pressure conditions for the SG primary side are 545°F and 2,235 psig. Based on plant Technical Specification limits, most heatup and cooldown events are restricted to a ramp rate of 100°F per hour or less; however, in order to bound the variation expected among various plant design types, an assumed bounding rate of 200°F per hour was used. Therefore, heatup begins at an ambient temperature of 70°F, and the temperature increases to 545°F at a rate of 200°F per hour while the pressure increases from 0 psig to 2,235 psig. Similarly, cooldown begins at 545°F, and the temperature decreases to 70°F at a rate of 200°F per hour while the pressure decreases from 2,235 psig to 0 psig. Typical design cycles for heatups and cooldowns are

200 cycles over 40 years, which most PWR plants demonstrated to remain adequate for 60 years of operation. This evaluation conservatively considered 300 heatup and cooldown cycles over a 60-year period (or 5 cycles per year).

- **Plant loading (normal).** This transient initiates at 15% power and increases to 100% power at a rate of 5% per minute. Typical 15% power temperatures are 550°F at the SG primary side inlet and 545°F at the outlet at a typical pressure of 2,300 psig. Typical 100% power temperatures are 610°F at the inlet and 550°F at the outlet at a typical pressure of 2,300 psig. Plants are typically designed to accommodate 15,000 cycles of this transient over 40 years, which most PWR plants demonstrated to remain adequate for 60 years of operation. Many U.S. plant do not load-follow and, therefore, will experience far fewer cycles in practice. However, for conservatism, this evaluation considered 5,000 cycles over a 60-year period (or 83.3 cycles per year).
- **Plant unloading (normal).** This transient initiates at 100% power and decreases to 15% power at a rate of 5% per minute. Typical temperatures and pressures and the number of events were assumed to be the same as those for the plant loading transient.
- **Reactor trip (upset).** This transient initiates at 100% power and can be caused by various conditions, such as a scrammed control rod or loss of main feedwater supply. It is assumed that the SG primary side inlet temperature increases by 5°F (starting at 610°F in 8 seconds and then decreases by 85°F in 92 seconds. The outlet temperature increases by 10°F (starting at 550°F) in 15 seconds and then decreases by 35°F in 85 seconds. The pressure increases by 200 psi (starting at 2,235 psig) in 10 seconds and decreases by 735 psi in 90 seconds. After a decrease of pressure, the pressure gradually increases back to 2,235 psig in 2,900 seconds. Plants are typically designed to accommodate 400 cycles of this transient over 40 years, which most PWR plants demonstrated to remain adequate for 60 years of operation. This evaluation conservatively considered 360 cycles over a 60-year period (or 6 cycles per year).

Design transients for faulted conditions are also defined for the SG primary side. However, these transients do not have significant stress variation because any faulted transient in the RCS will lead to depressurization and a decrease in stresses in the RCS. Therefore, the design transients for the faulted condition were assumed to be bounded by the transients previously listed.

Table 5-7 lists the thermal transients for the SG primary-side head welds that were used in the stress analysis.

Table 5-7
Thermal transients for stress analysis of the PWR SG primary-side head welds

Transient	Max. T_{HOT} , °F	Min. T_{HOT} , °F	Max. T_{COLD} , °F	Min. T_{COLD} , °F	Max. Press., psig	Min. Press., psig	60-Year Cycles
Heatup and cooldown	545	70	545	70	2,235	0	300
Plant loading	610	550	550	545	2,300	2,300	5,000
Plant unloading	610	550	550	545	2,300	2,300	5,000
Reactor trip	615	530	565	530	2,435	1,700	360

Notes: T_{HOT} = hot leg temperature; T_{COLD} = cold leg temperature

5.2.2 Operating Conditions for SG Inlet Nozzle-to-Vessel Welds (Item No. B3.130)

This section documents the operating conditions that were used for the stress analysis for the PWR SG (primary side) inlet nozzle-to-vessel welds (Item No. B3.130). Typical transients encountered in PWRs are described in Reference [49], which forms the basis for the following discussion. In accordance with Reference [49], the transients that rarely occur or are expected to be minor pressure/temperature excursions were not considered in this evaluation.

As covered in Section 4.5.1, two PWR SG inlet nozzles were selected for evaluation—a CE design and a B&W design. The thermal transients applied to the CE primary-side nozzle-to-vessel welds are the same as those described in Section 5.2.1 and listed in Table 5-7. The transients applied to the B&W primary-side nozzle-to-vessel welds are described as follows:

- **Heatup and cooldown (normal).** Heatup occurs from cold shutdown to rated temperature and pressure conditions, whereas cooldown occurs from the rated temperature and pressure conditions to cold shutdown. Typical rated temperature and pressure conditions for the SG primary side are 560°F and 2,235 psig. Based on plant Technical Specification limits, most heatup and cooldown events are restricted to a ramp rate of 100°F per hour or less; however, in order to bound the variation expected among plant design types, an assumed bounding rate of 200°F per hour was used. Heatup begins at an ambient temperature of 70°F, and the temperature increases to 560°F at a rate of 200°F per hour while the pressure increases from 0 psig to 2,235 psig. Similarly, cooldown begins at 560°F, and the temperature decreases to 70°F at a rate of 200°F per hour while the pressure decreases from 2,235 psig to 0 psig. Typical design cycles for heatups and cooldowns are 200 cycles over 40 years, which most PWR plants demonstrated to remain adequate for 60 years of operation. This evaluation conservatively considered 300 heatup and cooldown cycles over a 60-year period (or 5 cycles per year).
- **Plant loading (normal).** This transient initiates at 15% power and increases to 100% power at a rate of 5% per minute. Typical 15% power temperature and pressure are 560°F and 2,235 psig, respectively. Typical 100% power temperature and pressure are 620°F and 2,235 psig, respectively. Plants are typically designed to accommodate 18,000 cycles for this transient over 40 years, which most PWR plants demonstrated to remain adequate for 60 years of operation. Many U.S. plant do not load-follow and, therefore, will experience far fewer cycles in practice. However, for conservatism, this evaluation considered 5,000 cycles over a 60-year period (or 83.3 cycles per year).
- **Plant unloading (normal).** This transient initiates at 100% power and decreases to 15% power at a rate of 5% per minute. Typical temperatures and pressures and the number of events were assumed to be the same as those for the plant loading transient.
- **Reactor trip (upset).** This transient initiates at 100% power, and it can be caused by various reasons like a scrammed control rod or loss of main feedwater supply. It is assumed that the temperature increases by 15°F (starting at 620°F) in 10 seconds and then decreases by 75°F in 10 seconds. The pressure increases by 250 psi (starting at 2,235 psig) in 10 seconds and then decreases by 650 psi in 10 seconds. Plants are typically designed to accommodate 400 cycles of this transient over 40 years, which most PWR plants demonstrated to remain adequate for 60 years of operation. This evaluation conservatively considered 360 cycles over a 60-year period (or 6 cycles per year).

Design transients for faulted condition are also defined for the SG primary side. However, these transients do not have any significant stress variation because any faulted transient in the RCS will lead to depressurization and a decrease in stresses in the RCS. Therefore, the design transients for the faulted condition were assumed to be bounded by the transients previously listed. Table 5-8 lists the thermal transients for the B&W SG (primary side) inlet nozzle that were used in the stress analysis.

Table 5-8
Thermal transients for stress analysis of the B&W SG primary inlet nozzle

Transient	Max. T _{HOT} , °F	Min. T _{HOT} , °F	Max. Press., psig	Min. Press., psig	60-Year Cycles
Heatup and cooldown	560	70	2,235	0	300
Plant loading	620	560	2,235	2,235	5,000
Plant unloading	620	560	2,235	2,235	5,000
Reactor trip	635	560	2,485	1,835	360

Notes: T_{HOT} = hot leg temperature; 1,000 psig = 6.89 MPa

5.2.3 Operating Conditions for PWR SG Vessel (Secondary Side) Welds (Item Nos. C1.10, C1.20, and C1.30)

This section defines the operating conditions for the PWR SG (secondary side) shell circumferential welds (Item No. C1.10), SG (secondary side) head circumferential welds (Item No. C1.20), and SG (secondary side) tubesheet-to-shell welds (Item No. C1.30). The various NSSS designs use two, three, or four SGs to transfer the heat generated in the RCS to the secondary side for power generation. The primary coolant enters the inlet nozzle (primary side), flows through the SG tubes, and leaves through the outlet nozzles (primary side). Feedwater enters the SG through the feedwater nozzle (secondary side), where it is distributed through the feedwater distribution ring and mixes with recirculating flow. The fixed recirculating flow descends through the annular downcomer, which is an annular passage formed by the inner surface of the SG shell and the cylindrical shell wrapper. At the bottom of the downcomer, the secondary water is directed upward past the vertical tubes, where heat transfer from the primary side produces a water-steam mixture. After the water-steam mixture passes through separators and dryers, a dry steam exits the SG through the main steam nozzle (secondary side).

The transients applied to the SG secondary-side vessel welds are described as follows:

- **Heatup and cooldown (normal).** Heatup occurs from cold shutdown to rated temperature and pressure conditions. Cooldown occurs from the rated temperature and pressure conditions to cold shutdown. Typical rated temperature and pressure conditions for the SG secondary side are 545°F and 1,000 psig. Based on plant Technical Specification limits, most heatup and cooldown events are restricted to a ramp rate of 100°F per hour or less; however, in order to bound the variation expected among plant design types, an assumed bounding rate of 200°F per hour was used. Therefore, heatup begins at an ambient temperature of 70°F, and the temperature increases to 545°F at a rate of 200°F per hour while the pressure increases following saturated conditions from 0 psig to 1,000 psig. Similarly, cooldown begins at 545°F, and the temperature decreases to 70°F at a rate of 200°F per hour while the pressure decreases following saturated conditions from 1,000 psig to 0 psig. Typical design cycles for

heatups and cooldowns are 200 cycles over 40 years, which most PWR plants demonstrated to remain adequate for 60 years of operation. This evaluation conservatively considered 300 heatup and cooldown cycles over a 60-year period (or 5 cycles per year).

- **Plant loading (normal).** This transient initiates at 15% power and increases to 100% power at a rate of 5% per minute. Typical 15% power temperature and pressure are 545°F and 1,000 psig, respectively, for the secondary-side fluid. Typical 100% power temperature and pressure are 540°F and 1,000 psig, respectively, for the secondary-side fluid. Plants are typically designed to accommodate 15,000 cycles of this transient over 40 years, which most PWR plants demonstrated to remain adequate for 60 years of operation. This evaluation conservatively considered 5,000 cycles over a 60-year period (or 83.3 cycles per year).
- **Plant unloading (normal).** This transient initiates at 100% power and decreases to 15% power at a rate of 5% per minute. Typical temperatures and pressures and the number of events were assumed to be the same as those for the plant loading transient.
- **Reactor trip (upset).** This transient initiates at 100% power and can be caused by various reasons, such as a scrammed control rod or loss of main feedwater supply. It is assumed that the secondary-side fluid temperature increases by 15°F in 10 seconds and then decreases by 25°F in 50 seconds. The pressure increases to 1,130 psig from 1,000 psig in 10 seconds and then decreases back to 1,000 psig in 50 seconds. Plants are typically designed to accommodate 400 cycles of this transient over 40 years, which most PWR plants demonstrated to remain adequate for 60 years of operation. This evaluation conservatively considered 360 cycles over a 60-year period (or 6 cycles per year).

Design transients for faulted conditions are also defined for the SG secondary side. During these events, the Safety Injection system is postulated to activate, which will lead to depressurization of the SG primary side and an associated decrease in temperature in the RCS. It is also assumed to cause a decrease of the temperature and pressure in the SG secondary side. Two of the more significant design transients for faulted conditions in the SG secondary side are a steam line break and a feedwater line break. For a steam line break, the temperature in the SG secondary side is postulated to increase instantaneously after the rupture; however, the magnitude of the increase is assumed to be small. For a feedwater line break, the temperature in the SG secondary side is postulated to increase in the active loops, but the inactive loop temperature is assumed to decrease after the rupture; however, the magnitude of the temperature decrease is postulated to be small. Therefore, the design transients for the faulted condition were assumed to be bounded by the transients previously listed. Table 5-9 lists the thermal transients for the SG secondary-side vessel welds that were used in the stress analysis.

Table 5-9
Thermal transients for stress analysis of the PWR SG secondary-side vessel welds

Transient	Max. T _{ss} , °F	Min. T _{ss} , °F	Max. Press., psig	Min. Press., psig	60-Year Cycles
Heatup and cooldown	545	70	1,000	0	300
Plant loading	545	540	1,000	1,000	5,000
Plant unloading	545	540	1,000	1,000	5,000
Reactor trip	555	530	1,130	1,000	360

Note: T_{ss} = secondary-side temperature

6

EVALUATION OF POTENTIAL DEGRADATION MECHANISMS

This section evaluates the potential degradation mechanisms for the SG primary- and secondary-side components selected in Section 4. The materials, operating loads, and transients (including pressures and temperatures) applicable to these components were covered in Section 5. All components are assumed to experience a constant, high flow of fluid (primary water, secondary water, or steam) during normal operations, which is typical of operating PWRs. In addition, the fluids of PWRs are typically chemistry-controlled to limit the concentration of dissolved oxygen and initiating contaminants (for example, chloride, fluoride, and sulfate).

6.1 Degradation Mechanisms

Potential degradation mechanisms affecting nuclear power plant components are addressed in References [23] and [50]. The mechanisms relevant to the selected components are as follows:

- Environmentally assisted cracking:
 - Intergranular stress corrosion cracking (IGSCC)
 - Transgranular stress corrosion cracking (TGSCC)
 - External chloride stress corrosion cracking (ECSCC)
 - Primary water stress corrosion cracking (PWSCC)
 - Corrosion fatigue
- Localized corrosion:
 - Microbiologically influenced corrosion (MIC)
 - Pitting
 - Crevice corrosion
- Flow-sensitive:
 - Erosion-cavitation
 - Erosion (that is, abrasive wear)
 - Flow-accelerated corrosion (FAC)
- General corrosion
 - Corrosion/wastage
 - Galvanic corrosion

- Fatigue
 - Thermal stratification, cycling, and striping (TASCS)
 - Thermal transients
 - Mechanical fatigue (that is, vibration)

In Section 6.2, the selected components are evaluated for potential susceptibility to each of these degradation mechanisms.

6.2 Degradation Mechanism Evaluation

6.2.1 Intergranular Stress Corrosion Cracking

IGSCC results from a combination of sensitized stainless steel materials (caused by a depletion of chromium in regions adjacent to the grain boundaries in weld heat-affected zones), high stress caused by applied loads or welding residual stress, and a corrosive environment (high level of oxygen or other contaminants). For PWRs, welds and heat-affected zones in wrought austenitic steel piping exposed to high dissolved oxygen levels and stagnant flow (such as stagnant, oxygenated boric acid water systems) are susceptible to IGSCC.

The SG secondary-side components are not susceptible to IGSCC because they are fabricated from carbon steel or low-alloy steel. The SG primary-side components are fabricated from carbon steel and/or low-alloy steel, but they also have stainless steel cladding. However, all fluid is chemistry-controlled, with strict limits placed on oxygen, oxidizing species, and initiating contaminants. Therefore, no components in the scope of this evaluation are susceptible to IGSCC.

6.2.2 Transgranular Stress Corrosion Cracking

TGSCC is stress corrosion cracking that occurs through the grains of the material and usually occurs in the presence of halogens and sulfides. It is not necessarily associated with a particular metallurgical condition, such as grain boundary sensitization, but it is affected by high local residual stresses, such as caused by welding or local cold work. In PWRs, austenitic stainless steels are generally susceptible to TGSCC in the presence of chlorides and oxygen.

The SG secondary-side components are not susceptible to TGSCC because they are fabricated from carbon steel or low-alloy steel. The SG primary-side components are fabricated from carbon steel and/or low-alloy steel, but they also have stainless steel cladding. However, the fluid is chemistry-controlled, with strict limits placed on oxygen, oxidizing species, halides, and caustics. Therefore, no components in the scope of this evaluation are susceptible to TGSCC, provided that strict fluid chemistry controls are maintained at all times.

In 1982, significant cracking was observed in the upper shell-to-transition-cone girth weld of the Indian Point Unit 3 SG, which led to a through-wall leak [51, 52]. Similar cracking was observed at Surry Unit 2 in 1983 [52]. A comprehensive failure analysis performed in Reference [53] concluded that the cracking at Indian Point Unit 3 was due to TGSCC resulting from higher-than-normal oxygen levels, combined with increased copper levels in the system fluid and a massive chloride intrusion. This operating experience indicates that TGSCC is possible in SGs under off-normal chemistry conditions. However, the most recent survey

performed by EPRI in Reference [39] did not identify any evidence of such cracking, which indicates that utilities have been diligent in controlling the chemistry in their SGs in recent years to prevent TGSCC. As such, TGSCC is not considered a concern for SG components.

6.2.3 External Chloride Stress Corrosion Cracking

ECSCC is the electrochemical reaction caused by a corrosive medium on the external surfaces of a piping system. Austenitic steel piping and welds are considered susceptible to ECSCC when exposed to chloride contamination (from insulation, brackish water, or concentration of fluids containing chlorides), temperatures greater than 150°F, and tensile stress.

This mechanism is relevant only to the external surface of the SG, and therefore the tubesheet-to-vessel components and any internal cladding are not affected. All other SG primary-side and secondary-side components in the scope of this evaluation are not susceptible to ECSCC because they are fabricated from carbon steel or low-alloy steel. In addition, any nonmetallic thermal insulation would very likely be controlled for chlorides according to NRC RG 1.36, Revision 1 [54].

6.2.4 Primary Water Stress Corrosion Cracking

PWSCC occurs in PWRs when high-temperature primary water is present in combination with a susceptible material and high tensile stress. Component susceptibility is established under the plant's existing Alloy 600 program.

The SG primary- and secondary-side components in the scope of this evaluation are not susceptible to PWSCC because they are not fabricated using Alloys 82/182/600 materials.

6.2.5 Corrosion Fatigue

Corrosion fatigue (also referred to as *environmental assisted fatigue* [EAF]) is the reduction in the fatigue life of a component due to the synergistic combination of mechanical fatigue and corrosion in a corrosive environment. The reactor and SG water environments are sufficiently corrosive to promote corrosion fatigue, depending on the nature of the fluid chemistry control. The presence of contaminants, such as sulfur/sulfates or chlorides, in combination with cyclic loading, are required for this mechanism to be active.

Even though all SG primary- and secondary-side components in the scope of this evaluation are exposed to chemistry-controlled fluid, which limits the presence of contaminants such as sulfur/sulfates and chlorides, these components might still be susceptible to corrosion fatigue (components in a steam environment, such as secondary-side welds near the main steam nozzles, are not affected). Corrosion fatigue was considered, where applicable, when performing the flaw tolerance evaluations documented in Section 8. It was addressed through the use of the ASME Code Section XI water fatigue crack growth law.

6.2.6 Microbiologically Influenced Corrosion

Microbes—primarily bacteria—can cause widespread damage to low-alloy and carbon steels, stainless steels, and other alloys. Areas considered susceptible to degradation from MIC are piping components with fluids containing organic material or with organic material deposits. The most vulnerable components are raw water systems, storage tanks, and transport systems. Systems with low to intermittent flow conditions, temperatures less than 150°F, and a pH below 10 are primary candidates.

The SG primary- and secondary-side components in the scope of this evaluation are not susceptible to MIC due to the elevated operating temperatures, constant high flow rates, and chemistry-controlled fluid.

6.2.7 Pitting

Pitting corrosion is a form of localized attack on exposed surfaces, with much greater corrosion rates at some locations than at others. High local concentrations of impurity ions, such as chlorides or sulfates, tend to concentrate in oxygen-depleted pits, giving rise to a potentially concentrated aggressive solution in this zone. All structural materials are potentially susceptible to pitting. Pitting can occur in low-flow or stagnant regions in components, or within crevices. Susceptibility to pitting is a strong function of the material and the oxygen and chloride level concentrations.

The SG primary- and secondary-side components in the scope of this evaluation are not susceptible to pitting due to the constant high flow rates and chemistry-controlled fluid, which limits the presence of oxygen, oxidizing species, and initiating contaminants.

6.2.8 Crevice Corrosion

Crevice corrosion is the electrochemical process caused by differences in anodic and cathodic reactions that are produced by geometric crevices in an oxygenated medium within a piping system. Regions containing crevices (narrow gaps), such as those caused by the presence of thermal sleeves, that can result in oxygen depletion and, subsequently, a relatively high concentration of chloride ions, or other impurities are considered susceptible to crevice corrosion. Crevices produced by other geometric effects (such as at backing rings) can also provide sites for crevice corrosion.

The SG primary- and secondary-side components in the scope of this evaluation are not susceptible to crevice corrosion because no components are covered by thermal sleeves or have backing rings.

6.2.9 Erosion-Cavitation

This degradation mechanism represents degradation caused by turbulent flow conditions, which might erode the pipe wall by cavitation. Cavitation damage is the result of the formation and instantaneous collapse of small voids within a fluid subjected to rapid pressure and velocity changes as it passes through a region where the flow is restricted (such as a valve, pump, or orifice).

The SG primary- and secondary-side components in the scope of this evaluation are not susceptible to erosion-cavitation because there are no cavitation sources immediately upstream of the components.

6.2.10 Erosion

This degradation mechanism is applicable to all metals and alloys, and it can occur when the operating fluid contains particulates (more severe at higher concentrations). For each environment-material combination, there is a threshold velocity above which impacting objects may produce metal loss.

The SG primary- and secondary-side components in the scope of this evaluation are not susceptible to erosion because they are all exposed to chemistry-controlled water (or steam), which eliminates particulates.

6.2.11 Flow-Accelerated Corrosion

FAC is a complex phenomenon that generally occurs in plain carbon steels and exhibits attributes of erosion and corrosion under both single-phase (water) and two-phase (water/steam) conditions. Factors that influence FAC include the following:

- Flow path geometry and velocity (FAC rates are highest in the vicinity of sharp discontinuities, such as branch connections, elbows, and in areas of shop and field welds, particularly at locations where backing rings were used and/or weld repairs were performed)
- pH and dissolved oxygen (results have shown that FAC rates decrease as pH and dissolved oxygen are increased)
- Moisture content of steam (higher moisture content results in higher rates of FAC)
- Temperature (FAC is most severe at a temperature of approximately 180°C)
- Material chromium content (FAC rates are highest in plain carbon steels; small amounts of alloying elements, such as chromium, can provide excellent resistance to FAC)

Component susceptibility is typically established under the plant's existing FAC program.

The SG primary- and secondary-side components in the scope of this evaluation are not susceptible to FAC because they are not included in the plant FAC program.

6.2.12 Corrosion/Wastage

General corrosion is characterized by an electrochemical reaction that occurs relatively uniformly over the entire surface area that is exposed to a corrosive environment. For carbon and alloy steels, normal reactor water can serve as that corrosive environment, depending on the nature of the fluid chemistry control. In contrast, austenitic stainless steels are not susceptible to general corrosion in the reactor environment. As required by ASME Code, Section III [45], corrosion is considered in component design, and appropriate allowances are provided.

The SG secondary-side components are carbon steel or low-alloy steel in a reactor fluid environment; however, they are exposed to fluids subjected to strict chemistry control and are therefore not susceptible to general corrosion/wastage. The SG primary-side components are carbon steel and/or low-alloy steel, but they also have stainless steel cladding, which is not susceptible to general corrosion in the reactor fluid environment. Therefore, no components in the scope of this evaluation are susceptible to corrosion/wastage.

6.2.13 Galvanic Corrosion

Galvanic corrosion results when two electrochemically dissimilar materials are in contact with one another in the presence of an electrolyte. In the light water reactor environment, reactor water and other fluid sources can serve as an electrolyte. More corrosion-resistant alloys will not suffer from galvanic corrosion, but they may affect the galvanic corrosion of other materials.

No SG primary- or secondary-side components feature two electrochemically dissimilar metals in contact with one another in the presence of an electrolyte. Therefore, no components in the scope of this evaluation are susceptible to galvanic corrosion.

6.2.14 Thermal Stratification, Cycling, and Striping

Areas where there can be leakage past valves separating hot and cold fluids and regions where there might be intermittent mixing of hot and cold fluids caused by fluid injection are susceptible to TASCs. Alternating stresses caused by thermal cycling of a component result in accumulated fatigue usage and can lead to crack initiation and growth.

The SG primary- and secondary-side components in the scope of this evaluation are not susceptible to TASCs because there is no high-cycle hot/cold fluid mixing occurring at any component locations.

6.2.15 Thermal Transients

Areas considered susceptible to thermal transients include components where there are significant pressure and/or thermal excursions. In piping, significant temperature excursions consist of a relatively rapid cold water injection that results in a temperature change that is greater than 150°F for carbon steel piping or 200°F for austenitic steel piping. When these temperature changes are exceeded, additional evaluations are required to determine whether the temperature change is greater than the allowed temperature change.

The thermal transients associated with the SG primary- and secondary-side components in the scope of this evaluation are identified in Tables 5-7, 5-8, and 5-9 and were considered, where applicable, when performing the fracture mechanics analyses in Section 8.

6.2.16 Mechanical Fatigue

Mechanical fatigue (vibration) can occur in locations subjected to high-frequency reversible loads, such as pressure fluctuations caused by pumps. Therefore, mechanical fatigue potentially affects all SG primary- and secondary-side components in the scope of this evaluation.

Mechanical fatigue was considered, where applicable, when performing the fracture mechanics analyses in Section 8.

6.3 Conclusions

All SG primary- and secondary-side components in the scope of this evaluation were evaluated for their susceptibility to the degradation mechanisms listed in Section 6.1. The results conclude that all components investigated in this study are susceptible to corrosion fatigue, mechanical fatigue, and thermal fatigue. (**Note:** components in a steam environment, such as secondary-side welds near the main steam nozzles, are not affected by corrosion fatigue.) Therefore, only these fatigue-related mechanisms will be considered when performing the probabilistic and deterministic fracture mechanics evaluations in Section 8.

7

COMPONENT STRESS ANALYSIS

This section covers the stress analyses for the SG primary- and secondary-side components selected in Section 4 as well as some alternate configurations to assess geometric differences. Due to the complex behavior of the stress distribution near the welds, finite-element analyses (FEAs) were performed for all components. The materials properties, operating loads, and transients listed in Section 5 were used as inputs for the stress analyses. Finite-element models (FEMs) were developed for the components using the ANSYS³ finite-element analysis software package [55]. Two-dimensional (2-D) axisymmetric or three-dimensional (3-D) models were used for the components, as appropriate.

Stress analyses were performed for thermal transients and internal pressure. For loads due to thermal transients, thermal analyses were performed to determine the temperature distribution histories for each transient. The temperature distribution history was then used as input to perform a stress analysis for each transient. For internal pressure, arbitrary unit internal pressure was applied to the FEMs. The stress results from the unit pressure were scaled to correspond to the actual transient pressure values. The stress results were used in fracture mechanics evaluations conducted in Sections 8.

In performing the analyses, the following assumptions were made during development of the FEMs and thermal/mechanical stress evaluations:

- The welds were not specifically modeled. The materials properties between the base metals and the weld materials are similar enough that the effect of this assumption is assumed to be minimal.
- Representative heat transfer coefficients during thermal transients were conservatively assumed for each component.
- All thermal transients were assumed to start and end at a steady-state, uniform temperature.
- The stress-free reference temperature for thermal stress calculations was assumed to be an ambient temperature of 70°F, which was also used for thermal strain calculations.
- All outside surfaces were assumed to be fully insulated, and the insulation itself was treated as perfect, with zero heat transfer capability. This assumption is typical for stress analyses in similar components.

³ ANSYS is a registered trademark of ANSYS, Inc.

- Pressure stresses were calculated at a stress-free temperature of 70°F and do not include any thermal stress effects.
- For all thermal heat transfer analyses, 3,600 seconds was added to the end of each transient time to ensure that any lagging peak stresses were captured, followed by a steady-state load step (at an arbitrary 400 seconds after the 3,600 seconds of additional time).

7.1 Stress Analysis for PWR SG Inlet Nozzle-to-Vessel Welds (Item No. B3.130)

7.1.1 Finite-Element Model

FEMs of the two SG primary inlet nozzle designs (CE and B&W) were developed using the ANSYS finite-element analysis software package [50], using the dimensions shown in Figures 4-4 and 4-5. Because of the axisymmetric nature of this configuration, 2-D models were used in the development of the FEMs. The 2-D axisymmetric models were generated using 2-D structural solid, PLANE42, elements. The thermal equivalent element for the thermal transient analyses is PLANE55. The FEMs for the CE and B&W inlet nozzle designs are shown in Figures 7-1 and 7-2, respectively, and include a local portion of the SG primary head and cladding as well as the primary inlet nozzle and cladding. The designation of the materials involved in the model and associated materials properties are covered in Section 5.1.

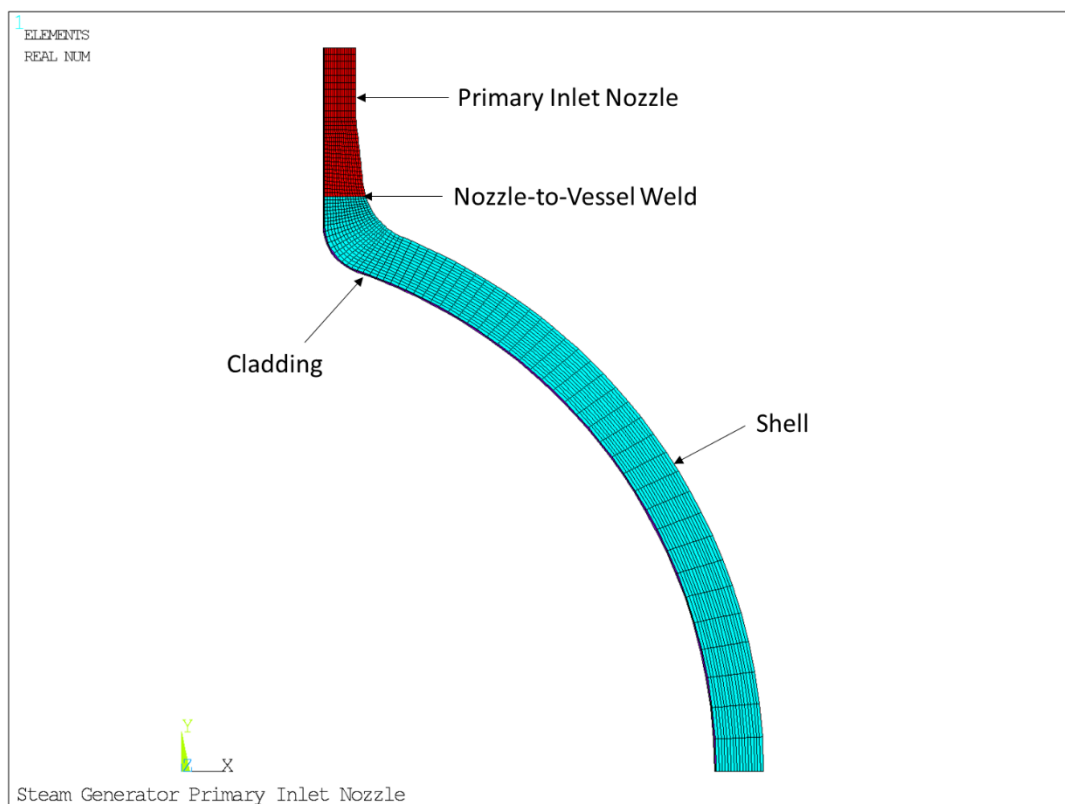


Figure 7-1
2-D finite-element model and mesh for PWR SG inlet nozzle (CE design)

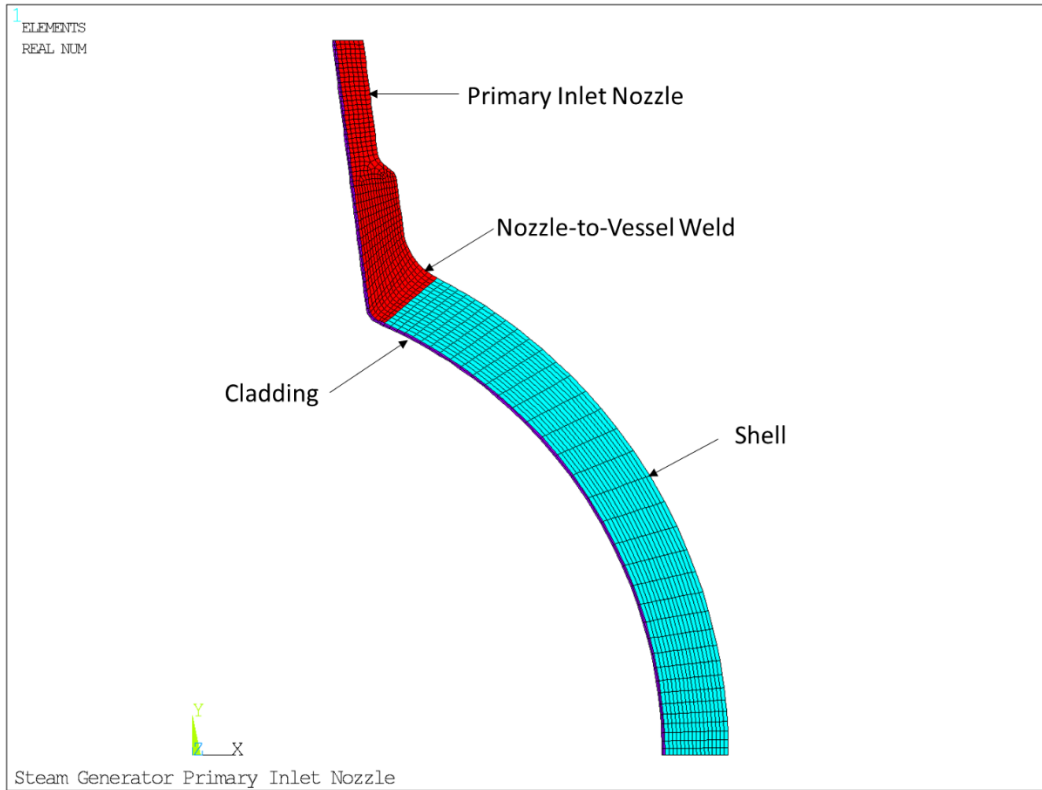


Figure 7-2
2-D finite-element model and mesh for PWR SG inlet nozzle (B&W design)

7.1.2 Pressure/Thermal Stress Analysis

7.1.2.1 Internal Pressure Loading Analysis

A unit internal pressure of 1,000 psi was applied to the interior surfaces of each model. The resulting stresses were scaled to the appropriate pressures for the fracture mechanics evaluations. An induced end-cap load was applied to the free end of the primary inlet nozzle in the form of tensile axial pressures calculated using Equation 7-1.

$$P_{\text{end-cap}} = \frac{P \cdot ID^2}{OD^2 - ID^2} \quad \text{Eq. 7-1}$$

where,

$P_{\text{end-cap}}$ = end-cap pressure on nozzle free end (psi)

P = internal pressure (psi)

ID = inside diameter of nozzle free end (in.)

OD = outside diameter of nozzle free end (in.)

Symmetric boundary conditions were applied to one axial free end of the SG head, and axial displacement couples were applied on the free end of the nozzle. The representative applied pressure load and boundary conditions for this case are shown in Figure 7-3 and Figure 7-4 for the CE and B&W design primary inlet nozzles, respectively.

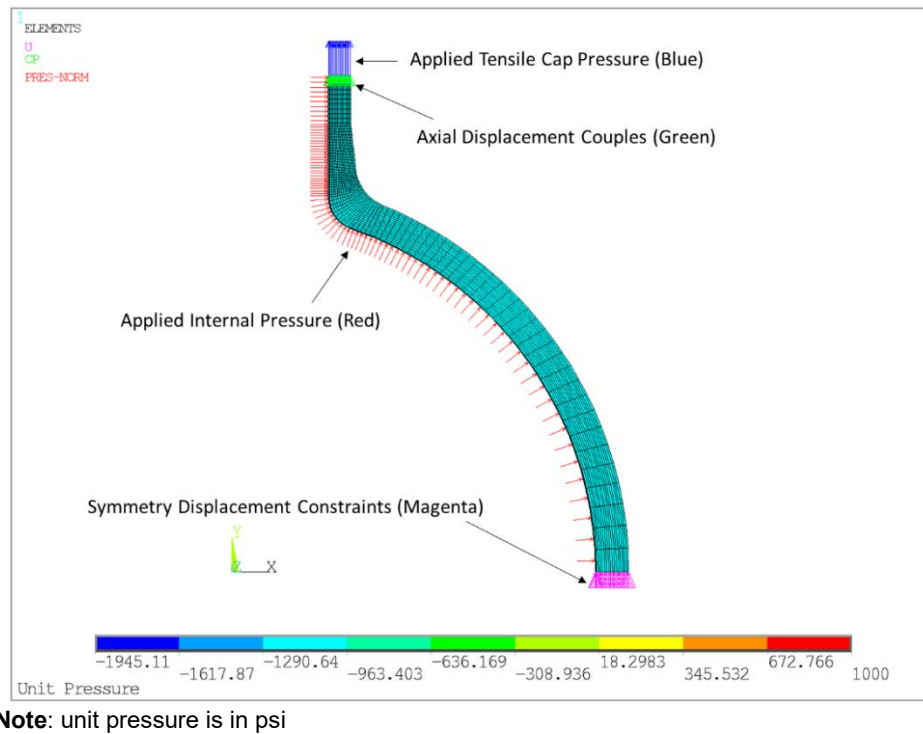


Figure 7-3
Applied boundary conditions and unit internal pressure for PWR SG inlet nozzle (CE design)

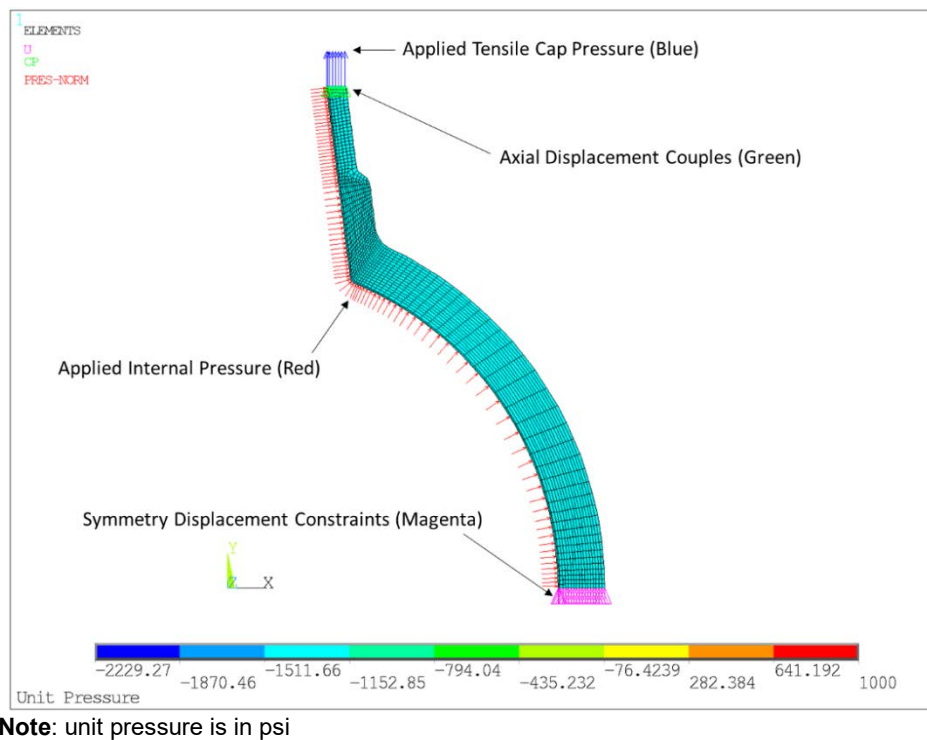
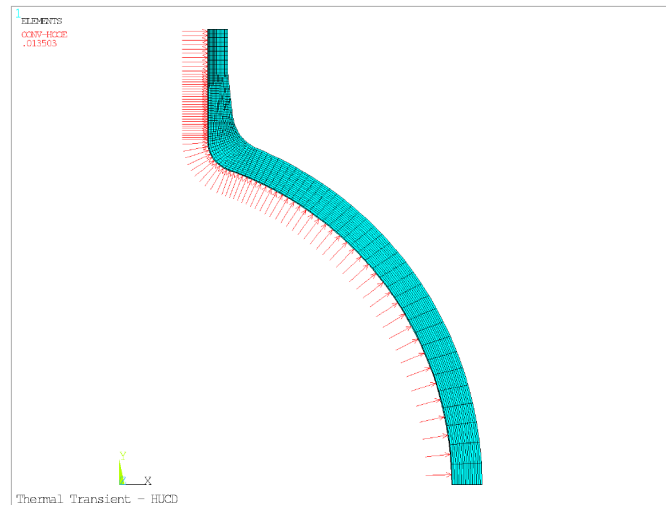


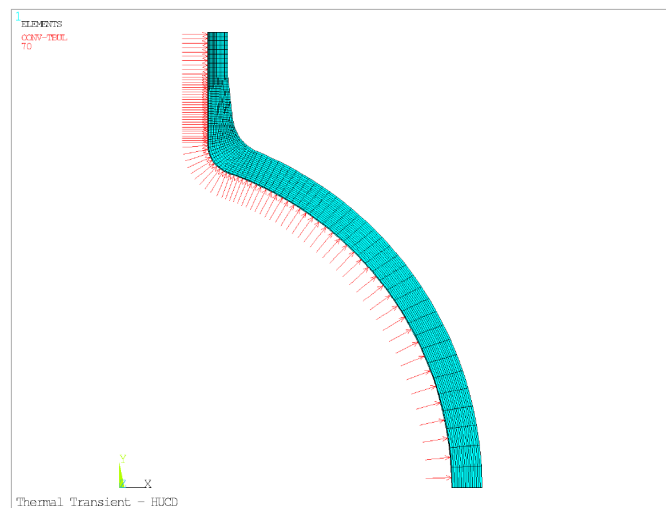
Figure 7-4
Applied boundary conditions and unit internal pressure for PWR SG inlet nozzle (B&W design)

7.1.2.2 Thermal Heat Transfer Analyses

The thermal transients identified in Table 5-7 (CE design) and Table 5-8 (B&W design) were applied to the interior surface nodes of the nozzle and shell in each FEM. Nominal heat transfer coefficients of 7,000 BTU/hr-ft²-°F (39,746 W/hr-m²-°C) for the CE design and 10,000 BTU/hr-ft²-°F (56,780 W/hr-m²-°C) for the B&W design were applied to the inside surfaces of the nozzle and shell for all evaluated transients. The applied heat transfer coefficients were determined based on the normal operating temperature, the flow rate in the primary inlet nozzle, and the nozzle dimensions. Neither heat transfer coefficients nor temperatures were applied to the insulated outside surfaces. Figure 7-5 and Figure 7-6 show representative plots of the thermal loads for the combined heatup/cooldown transient applied to the SG primary inlet nozzle of the CE and B&W designs, respectively. Note that the heatup and cooldown transients were evaluated as a single, combined transient (heatup followed by cooldown). Therefore, discussion in this section and others refers to the single composite transient as *heatup/cooldown*.



Heat Transfer Coefficient



Bulk Temperature

Notes:

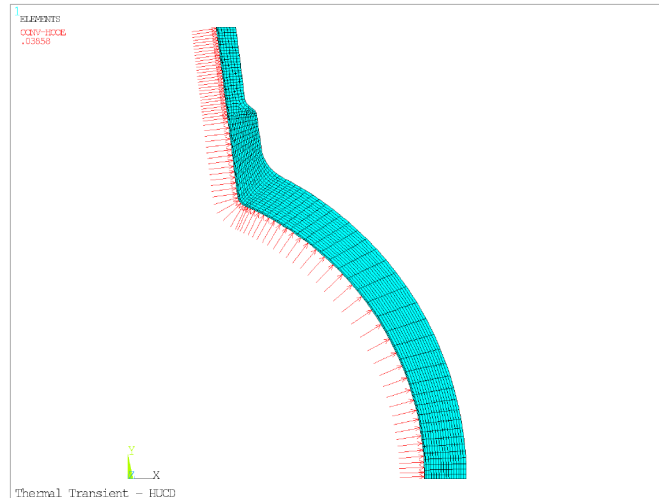
Heatup/cooldown transient shown.

Loads applied at time = 45,900 seconds.

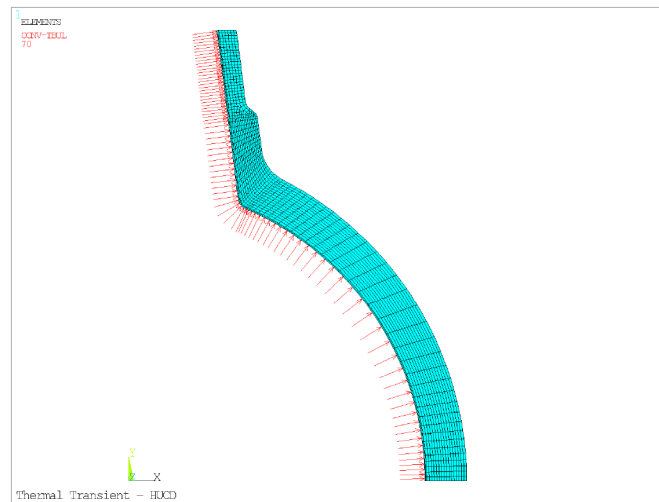
Units for heat transfer coefficient are BTU/sec-in²-°F; 1
BTU/hr-ft²-°F = 5.678 W/hr-m²-°C.

Units for bulk temperature are °F; °C= (°F-32) x 5/9.

Figure 7-5
Applied thermal boundary conditions for thermal transient analyses for PWR SG inlet nozzle (CE design)



Heat Transfer Coefficient



Bulk Temperature

Notes:

Heatup/cooldown transient shown.

Loads applied at time = 46,440 seconds.

Units for heat transfer coefficient are BTU/sec-in²-°F;

1 BTU/hr-ft²-°F = 5.678 W/hr-m²-°C.

Units for bulk temperature are °F; °C= (°F-32) x 5/9.

Figure 7-6

Applied thermal boundary conditions for thermal transient analyses for PWR SG inlet nozzle (B&W design)

7.1.2.3 Thermal Stress Analyses

Symmetric boundary conditions were applied to the free end of the head, and axial displacement couples were applied on the free end of the nozzle. The reference temperature for the thermal strain calculation was assumed to be 70°F. Figure 7-7 and Figure 7-8 show representative plots of the boundary conditions applied for the thermal stress analyses of the CE and B&W designs, respectively.

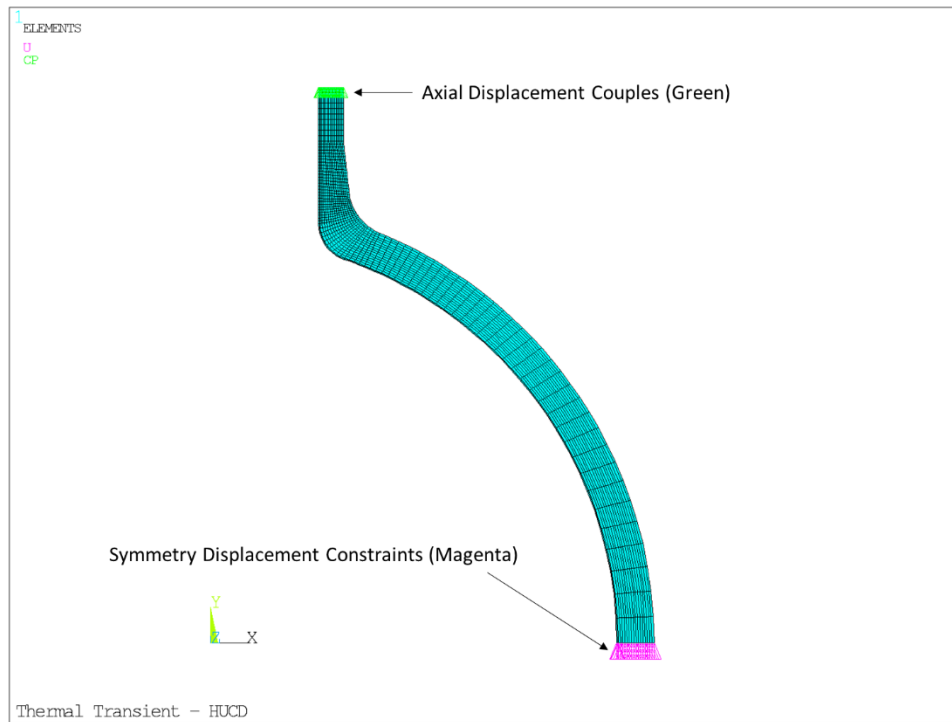


Figure 7-7
Applied mechanical boundary conditions for thermal stress analyses for PWR SG inlet nozzle (CE design)

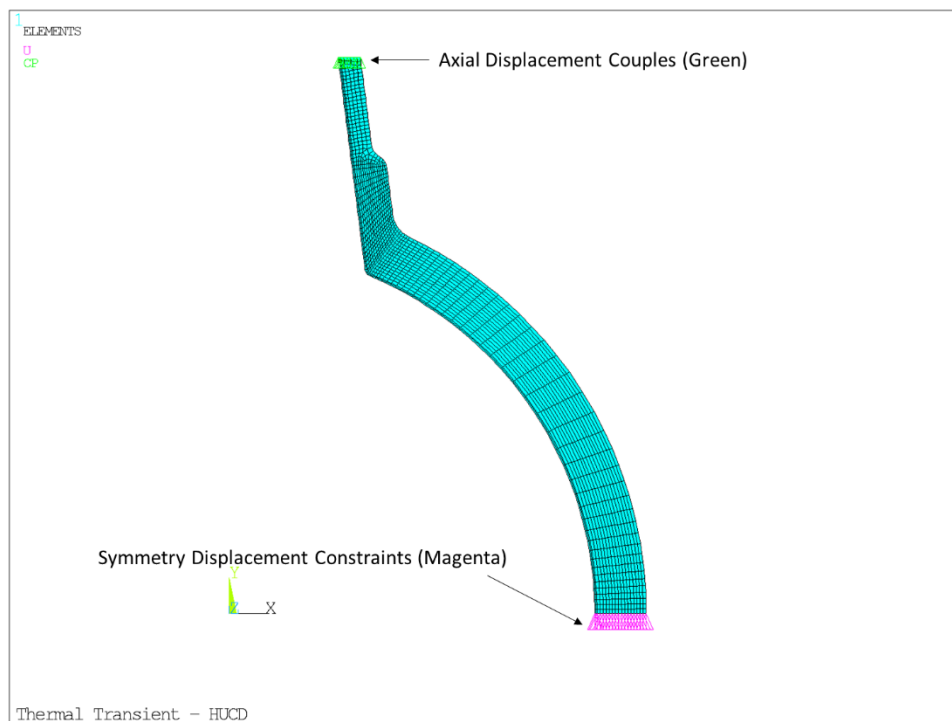
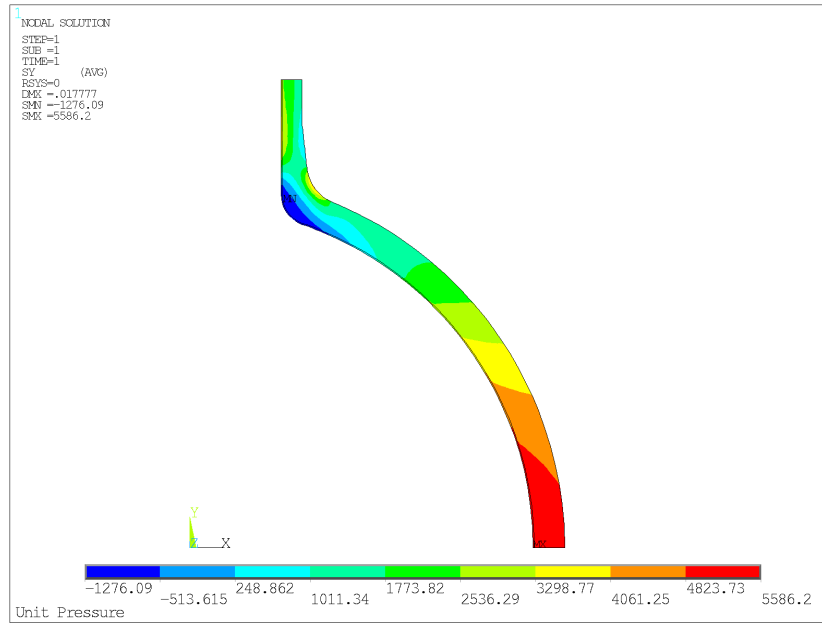


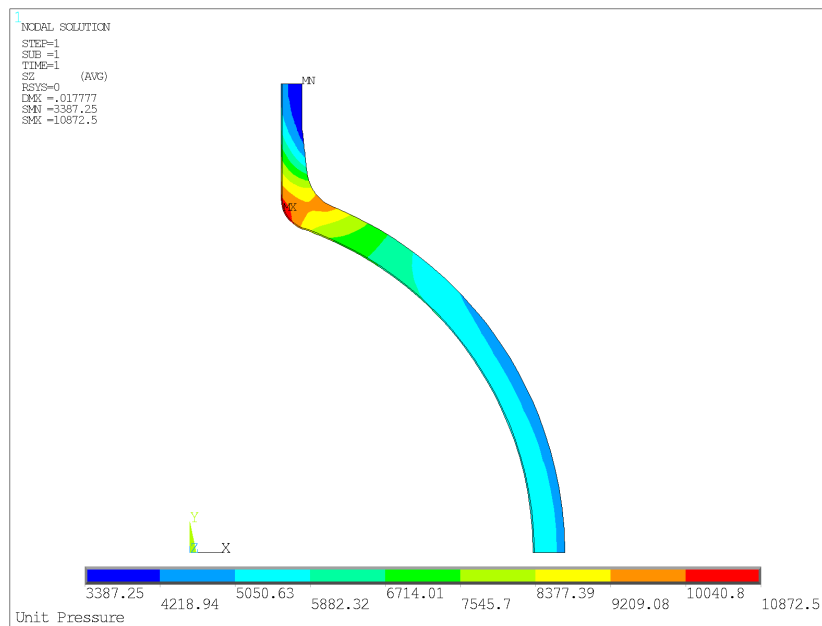
Figure 7-8
Applied mechanical boundary conditions for thermal stress analyses for PWR SG inlet nozzle (B&W design)

7.1.3 Stress Analysis Results

The component stress contour plots were plotted in the global Cartesian coordinate system, where the z-direction aligns with the nozzle hoop direction and the y-direction aligns with the nozzle axial direction. The stresses for a unit internal pressure of 1,000 psig are shown in Figure 7-9 for the CE design and Figure 7-10 for the B&W design. Representative temperature and stress contour plots for the composite heatup/cooldown transient (CE design) are shown in Figures 7-11 and 7-12, respectively. Representative temperature and stress contour plots for the composite heatup/cooldown transient (B&W design) are shown in Figures 7-13 and 7-14, respectively. The times shown in Figures 7-11 through 7-14 are when the maximum stress intensity occurs. Figures 7-15 and 7-16 show the path locations where stresses were extracted for use in the fracture mechanics evaluations. Paths P1(N) and P2(N) were chosen as representative of the nozzle-to-vessel weld in each nozzle design. As shown in Figures 1-3, 1-4, and 1-5, this weld can be located on either the nozzle side or the shell side of the nozzle forging. Therefore, stresses were also extracted from Paths P1(S) and P2(S) on the shell side, which are also shown in Figures 7-15 and 7-16. Due to the alignment of the weld with the global Cartesian coordinate system, stresses for the CE design (Path P1) were extracted in a global Cartesian coordinate system, which is the same coordinate triad shown in Figure 7-9. Stresses for the B&W design (Path P2) were extracted in a local coordinate system along Path P2 because the weld does not align with the global Cartesian coordinate system. The local X-direction is from the inside node to the outside node of the path, the local Y-direction is perpendicular to the path (axial for the nozzle-to-vessel weld), and the local Z-direction is the same as the global Z-direction (hoop for nozzle-to-vessel weld). Typical through-wall stress distributions for Paths P1(N) and P2(N) are shown in Figures 7-17 and 7-18. In these figures, thermal stresses are shown at the times when the maximum total inside stress intensity occurs for each transient.



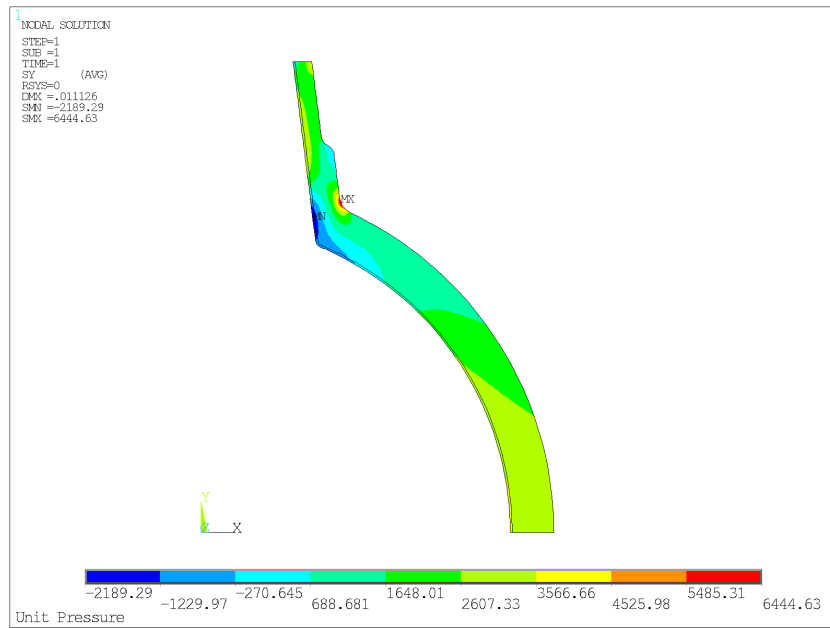
Axial Stress (to the Nozzle)



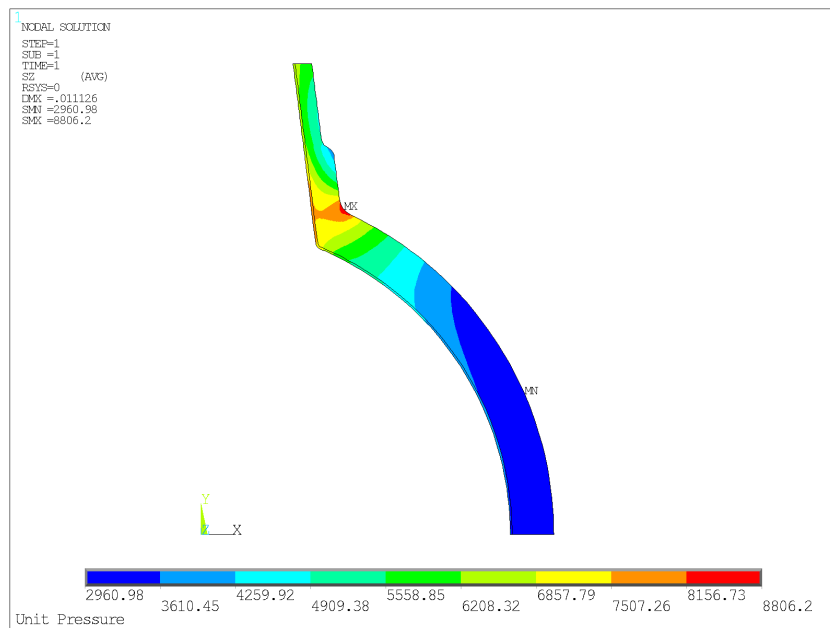
Hoop Stress (to the Nozzle)

Note: units for stress are psi

Figure 7-9
Stress contours due to unit internal pressure for PWR SG inlet nozzle (CE design)



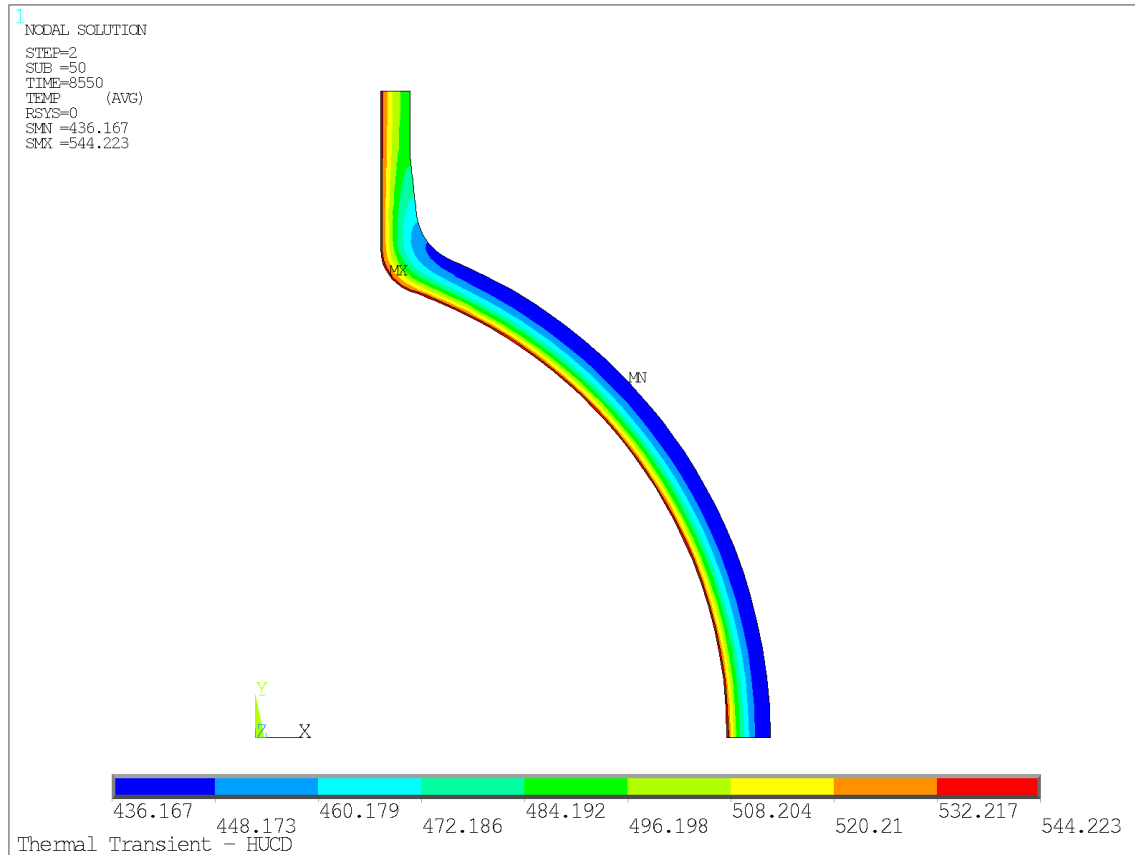
Axial Stress (to the Nozzle)



Hoop Stress (to the Nozzle)

Note: units for stress are psi

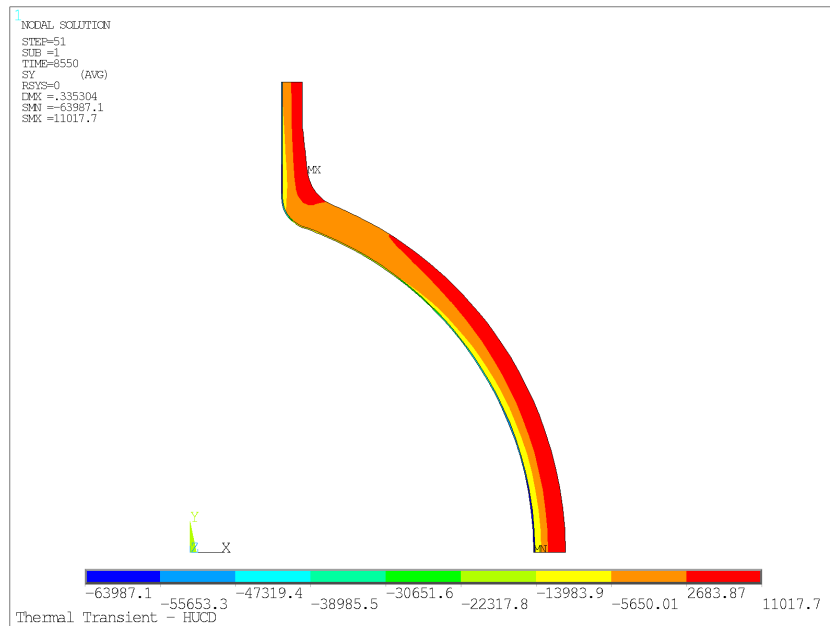
Figure 7-10
Stress contours due to unit internal pressure for PWR SG inlet nozzle (B&W design)



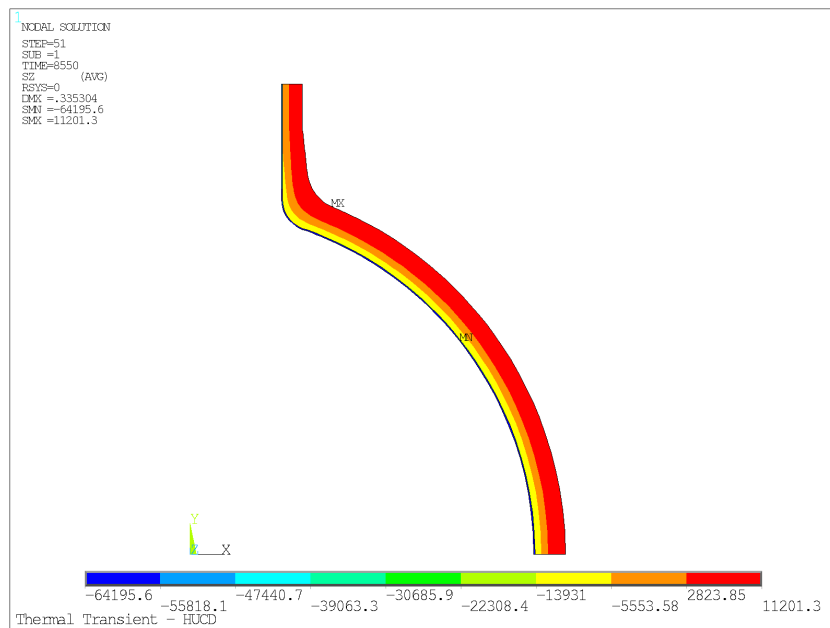
Note: units for temperature are °F

Figure 7-11

Temperature contour for heatup/cooldown transient (time = 8,550 seconds, end of heatup) for PWR SG inlet nozzle (CE design)



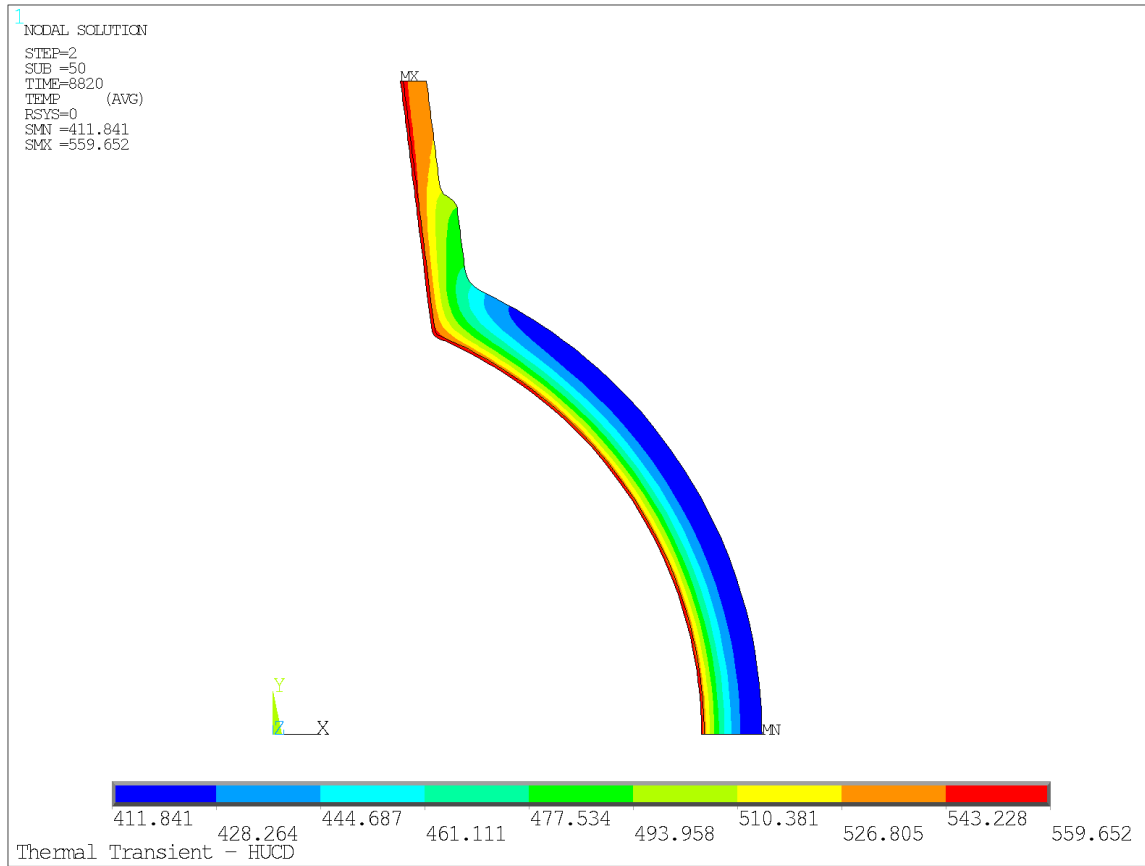
Axial Stress (to the Nozzle)



Hoop Stress (to the Nozzle)

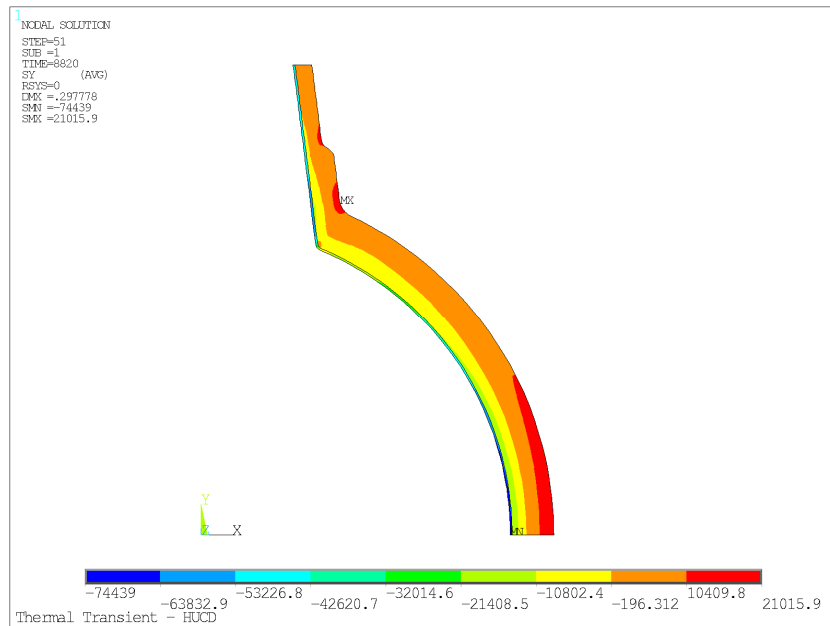
Note: units for stress are psi

Figure 7-12
Stress contours for heatup/cooldown transient (time = 8,550 seconds, end of heatup) for PWR SG inlet nozzle (CE design)

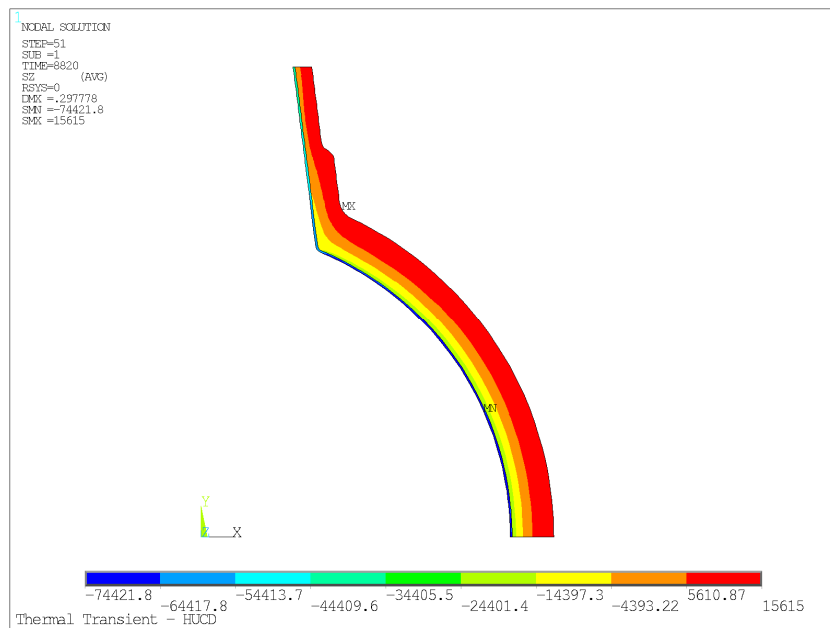


Note: units for temperature are °F

Figure 7-13
Temperature contour for heatup/cooldown transient (time = 8,820 seconds, end of heatup)
for PWR SG inlet nozzle (B&W design)



Axial Stress (to the Nozzle)



Hoop Stress (to the Nozzle)

Note: units for stress are psi

Figure 7-14
Stress contours for heatup/cooldown transient (time = 8,820 seconds, end of heatup) for PWR SG inlet nozzle (B&W design)

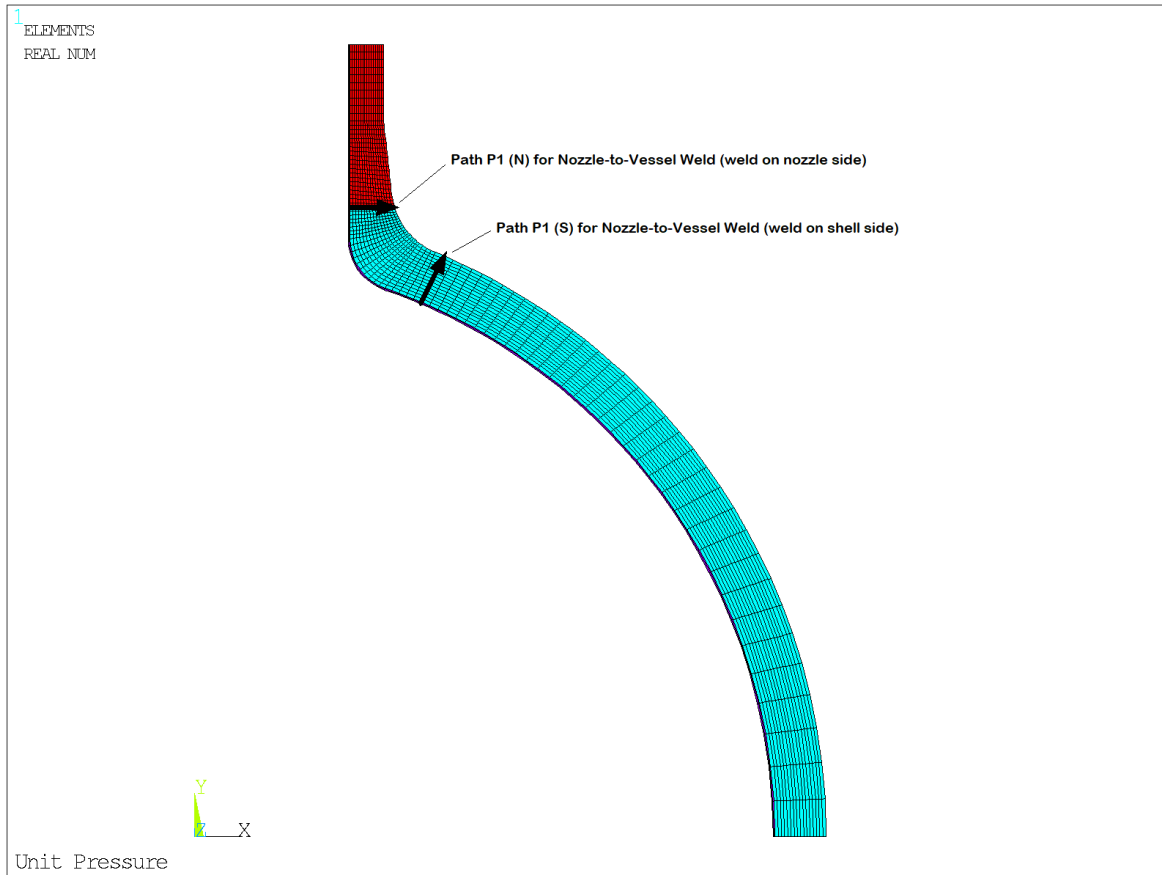


Figure 7-15
Path location for PWR SG inlet nozzle (CE design) (Path P1 will be used in this report.)

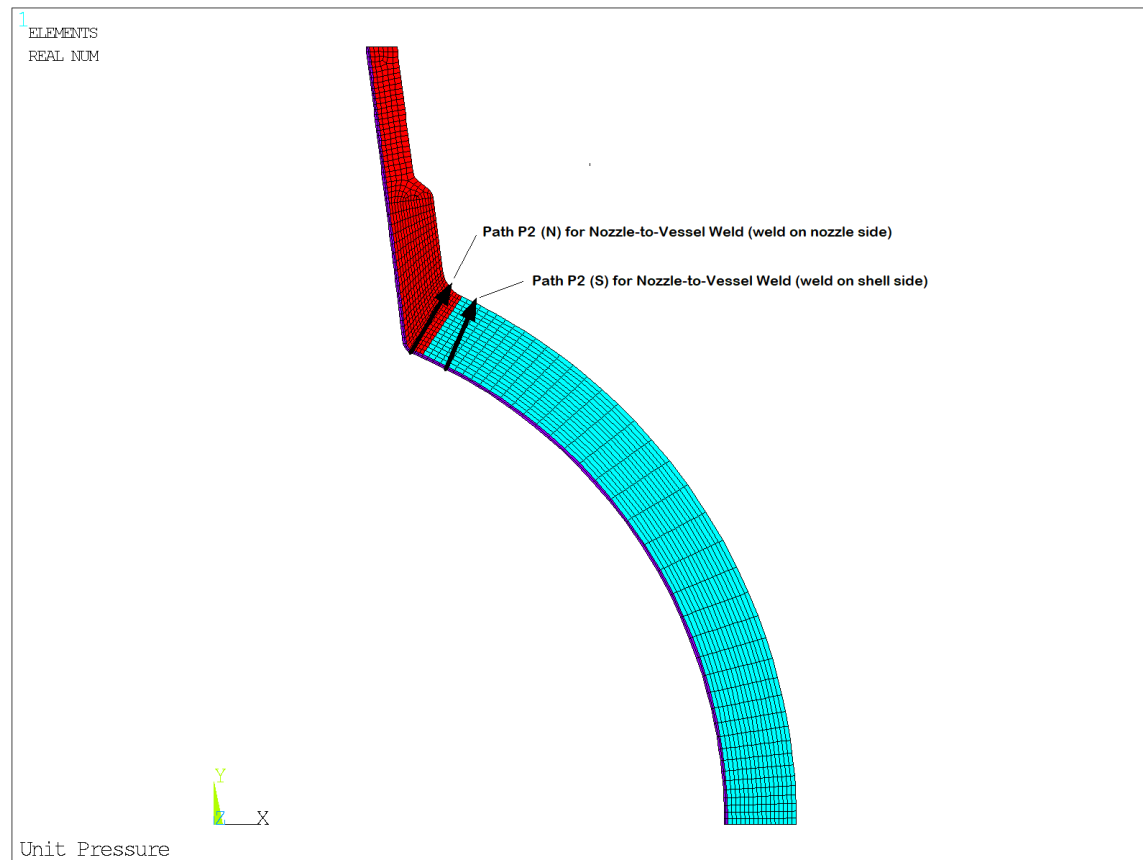


Figure 7-16
Path location for PWR SG inlet nozzle (B&W design) (Path P2 will be used in this report.)

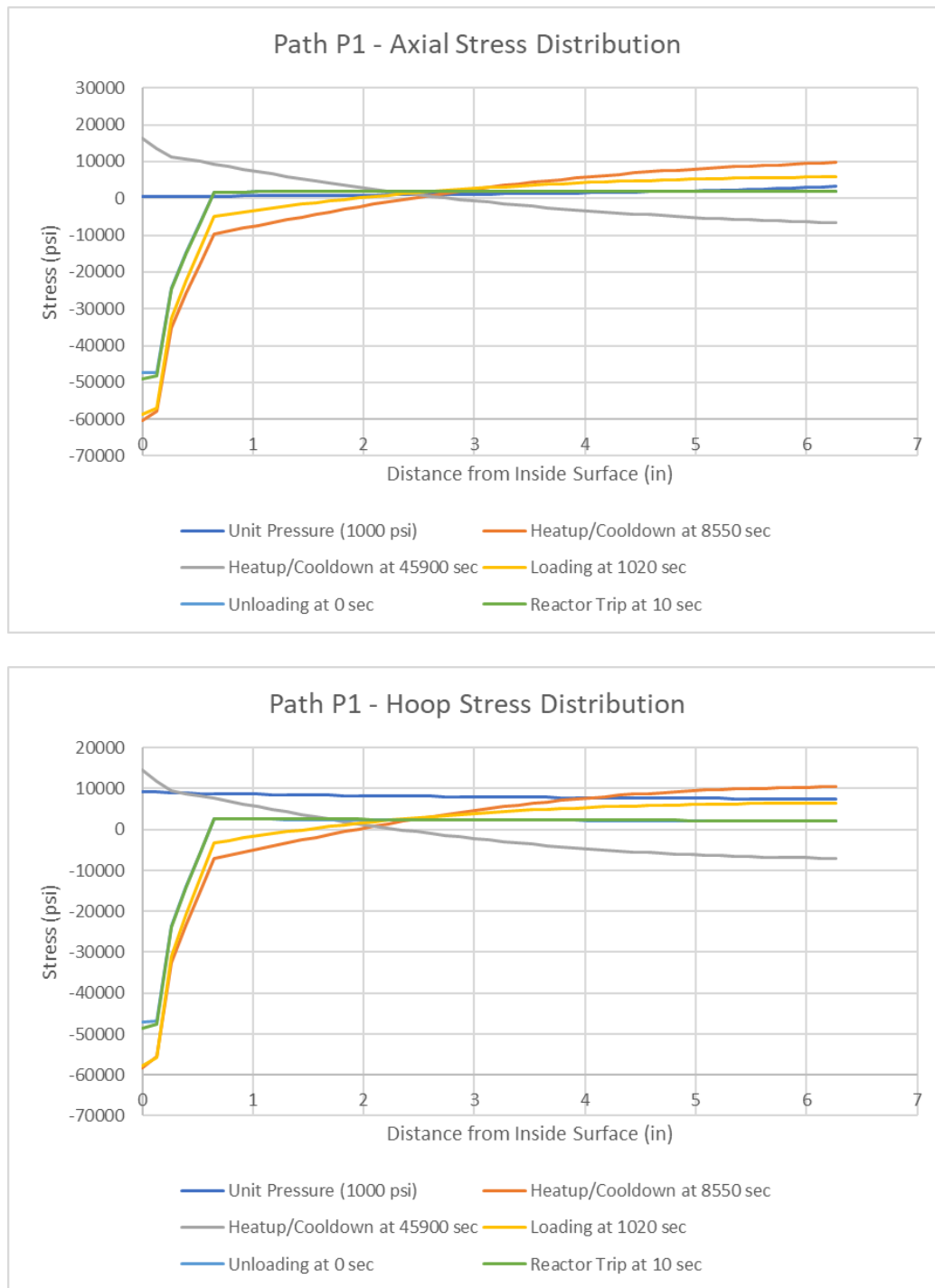


Figure 7-17
Through-wall stress distribution at Path P1(N) for PWR SG inlet nozzle (CE design)

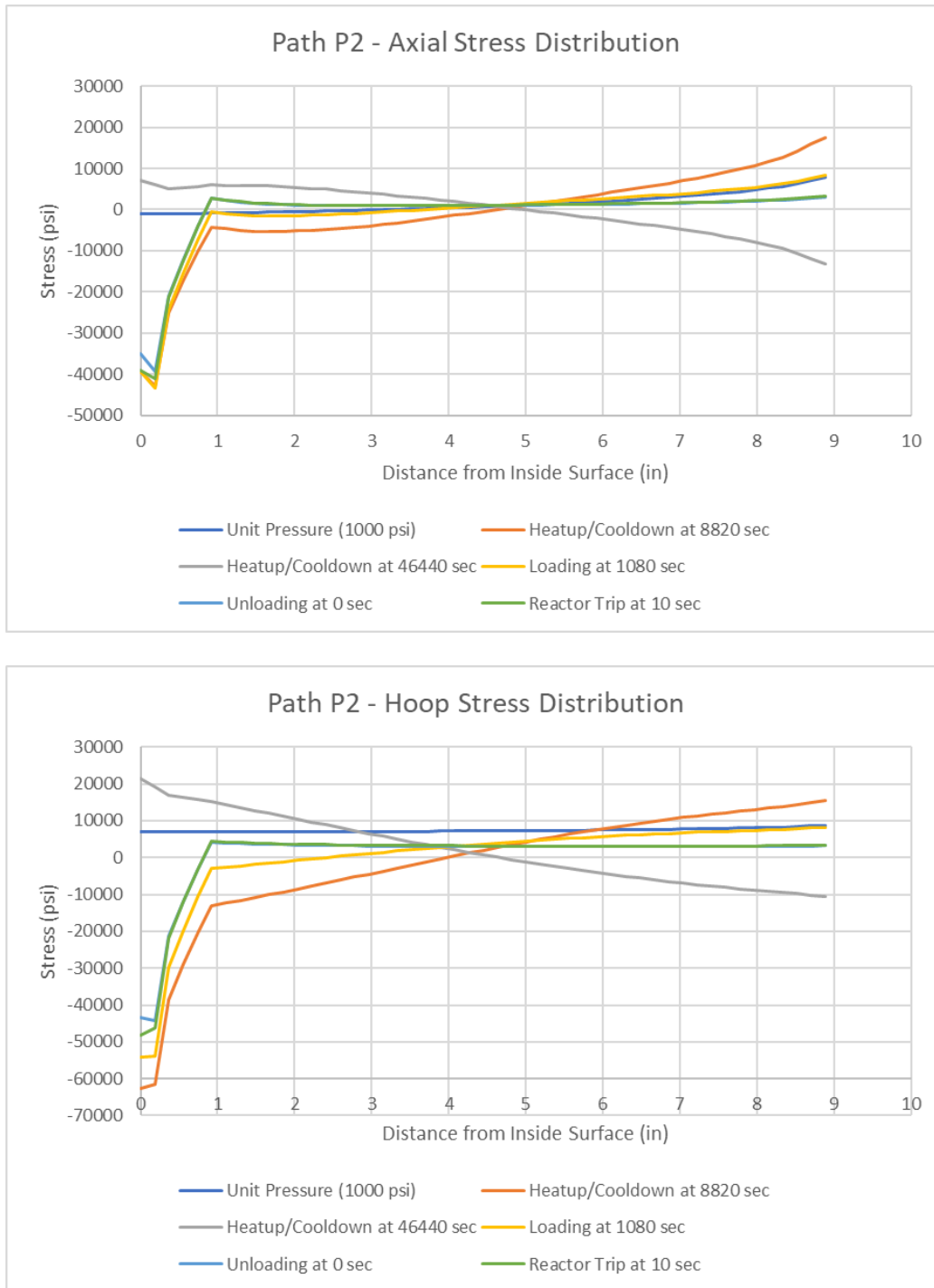


Figure 7-18
Through-wall stress distribution at Path P2(N) for PWR SG inlet nozzle (B&W design)

7.2 Stress Analysis for PWR SG Vessel Welds (Item Nos. B2.31, B2.32, B2.40, C1.10, C1.20, and C1.30)

7.2.1 Finite-Element Model

An FEM of the SG primary head, divider plate, tubesheet, and secondary shell was developed using the ANSYS finite element analysis software package [50], with dimensions shown in Table 4-2. Because of the geometric complexity in the primary head-to-divider plate weld and head-to-tubesheet weld, a 3-D half model was used in the FEA.

The 3-D half-model was constructed using eight-node structural solid, SOLID45, elements. The thermal equivalent element for the thermal transient analyses is SOLID70. The FEM is shown in Figure 7-19 and includes the SG primary head and cladding, tubesheet and cladding (primary side), secondary shell and head, and primary divider plate. The SG vessel penetrations (such as primary inlet/outlet nozzles, manways, snubber lugs, and support skirt) were not modeled, nor were any internal components (such as U-tubes, tube support plates, and feed rings), other than the tubesheet and primary divider plate; this is because they do not significantly affect the temperature distributions of the welds under consideration.

Note that neither the welds nor the perforated region of the tubesheet were specifically modeled. For the region of the perforated tubesheet, the equivalent materials properties (that is, modulus of elasticity and Poisson's ratio) were applied. The equivalent modulus of elasticity, E , and Poisson's ratio values, ν , were obtained from Reference [56] using the ligament efficiency for the tubesheet. The designation of the materials involved in the model and the associated materials properties are covered in Section 5.1.

7.2.2 Pressure/Thermal Stress Analysis

7.2.2.1 Internal Pressure Loading Analysis

For internal pressure, appropriate internal pressures for each transient were interpolated for each time step and applied to the stress analysis for each transient (see Section 7.2.2.3).

7.2.2.2 Thermal Heat Transfer Analyses

The thermal transients covered in Sections 5.2.1 and 5.2.3 were applied to the interior surface nodes of the tubesheet and to primary and secondary shells. A heat transfer coefficient of 10,000 BTU/hr-ft²-°F (56,780 W/hr-m²-°C) was applied to the inside surfaces of the primary side and the water phase portion of the secondary side, and a heat transfer coefficient of 5,000 BTU/hr-ft²-°F (28,390 W/hr-m²-°C) was applied to the inside surfaces of the steam phase portion of the secondary side. The elevation of the normal water level was used for the boundary of the water-steam interface of the secondary side.

Figure 7-20 shows representative plots of the thermal loads for the plant loading transient applied to the PWR SG model.

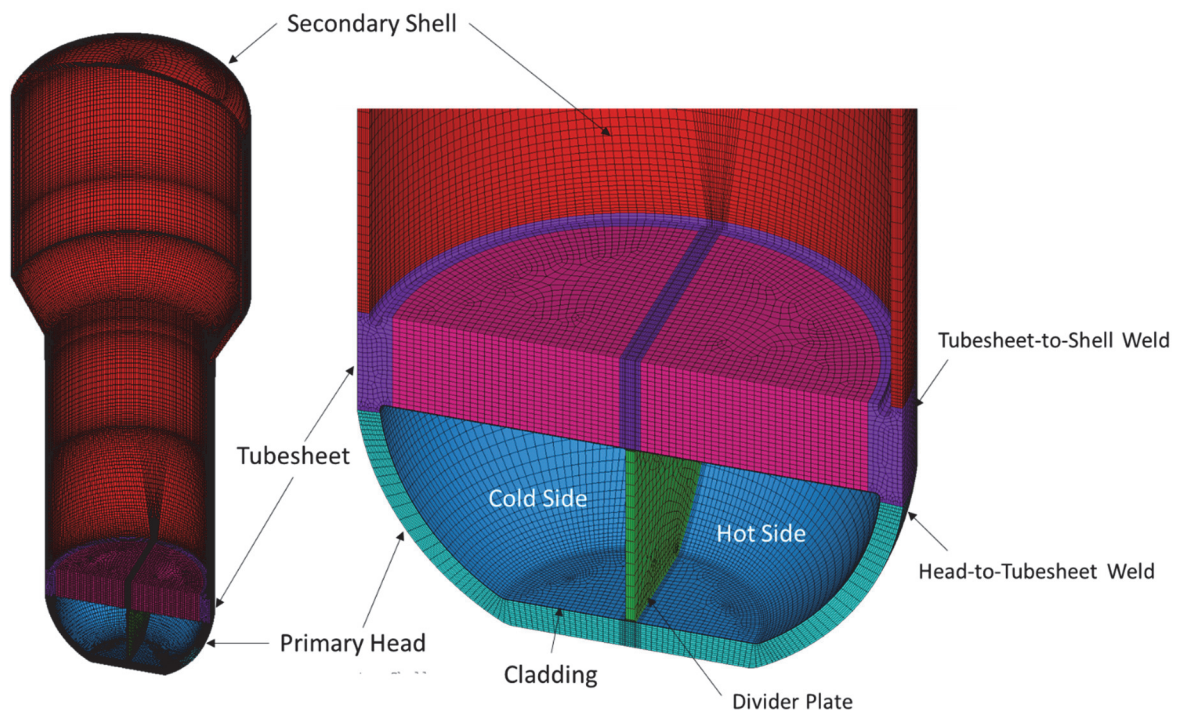
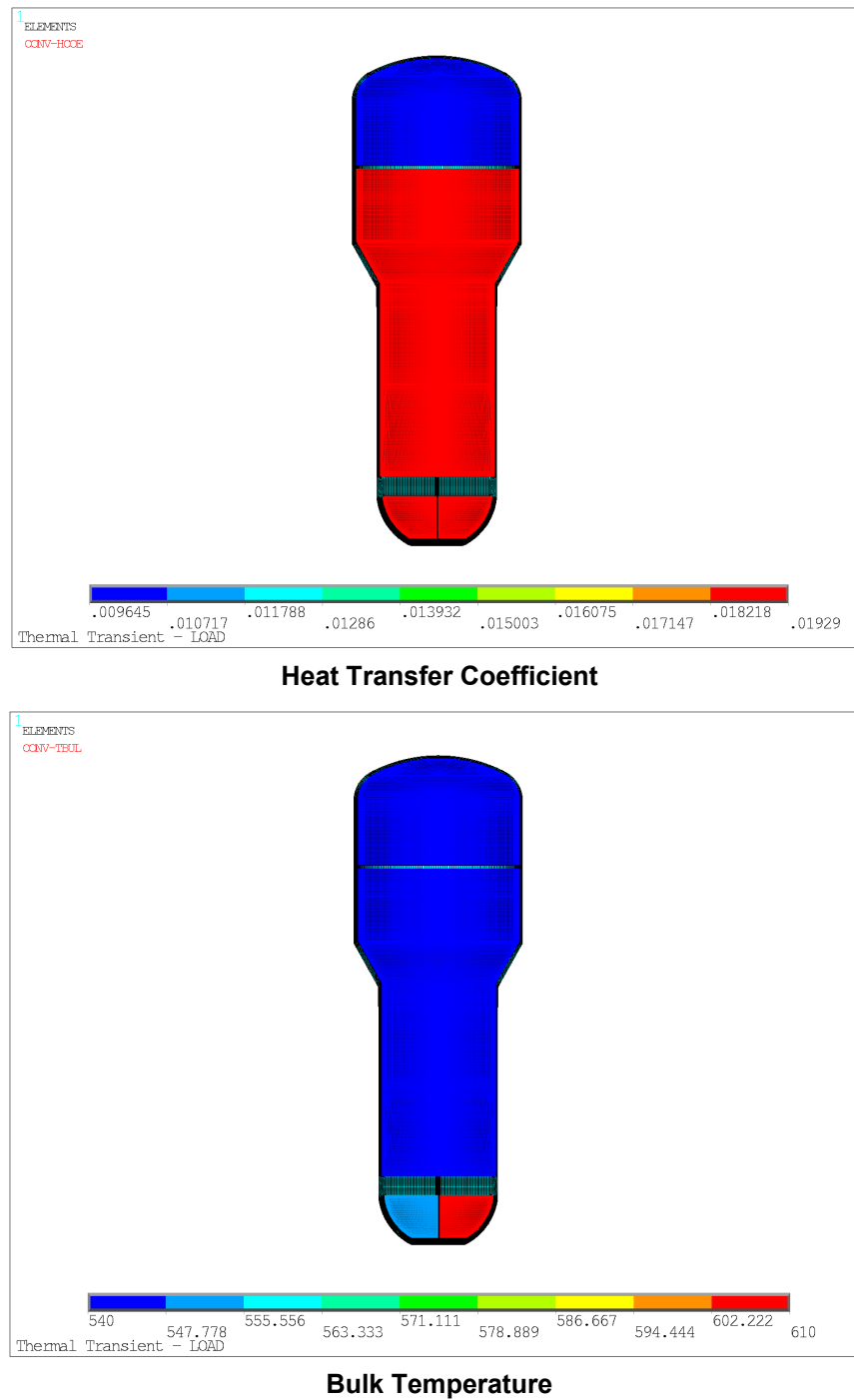


Figure 7-19
3-D finite-element model and mesh for the PWR SG



Notes:

Plant loading transient shown.

Loads applied at time = 1,800 seconds.

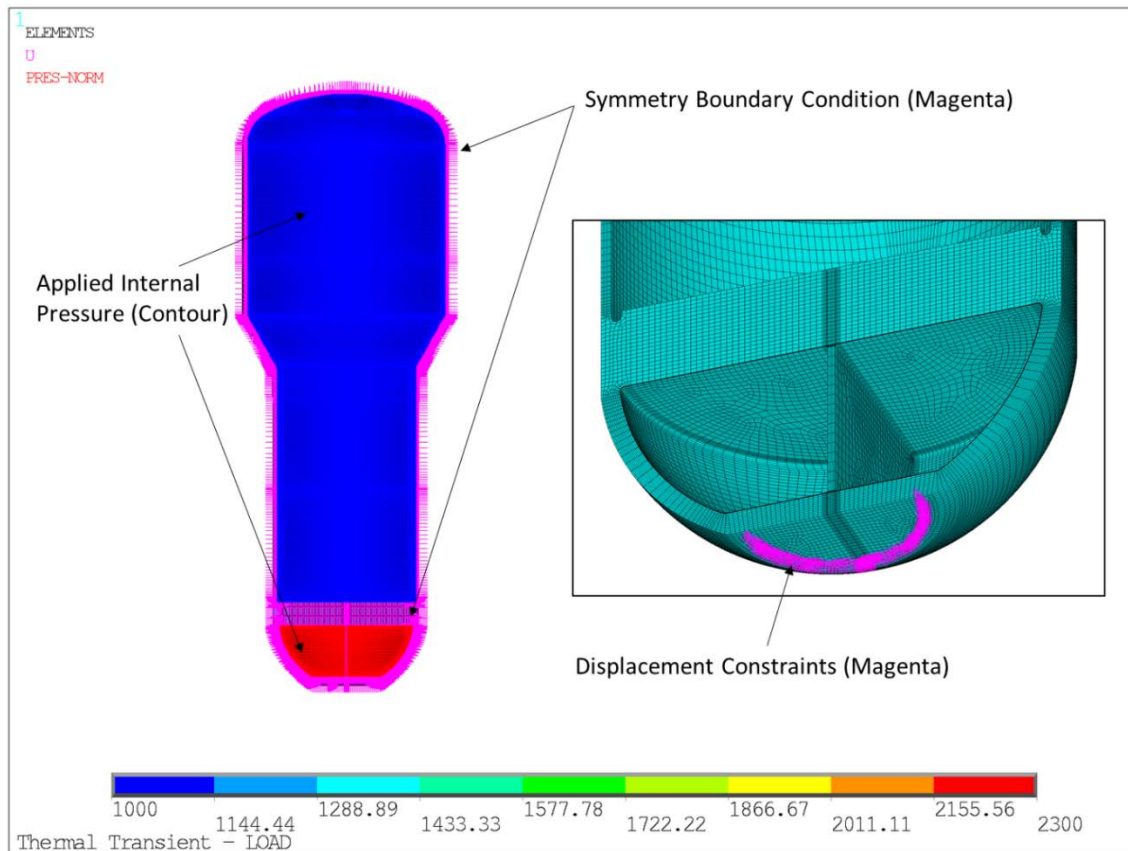
Units for heat transfer coefficient are BTU/sec-in²-°F; 1 BTU/hr-ft²-°F = 5.678 W/hr-m²-°C.

Figure 7-20

Applied thermal boundary conditions for thermal transient analyses for the PWR SG

7.2.2.3 Thermal Stress Analyses

Symmetric boundary conditions were applied to the symmetry planes of the FEM. The outside surface on nodes located where the support skirt is attached at the bottom of the SG were circumferentially and vertically restrained to account for the presence of the support skirt. Appropriate internal pressure for each transient was also applied to the interior surfaces of the model. The reference temperature for the thermal strain calculation was assumed to be 70°F. Figure 7-21 shows an example plot of the pressure load and boundary conditions applied for the plant loading transient thermal stress analyses.



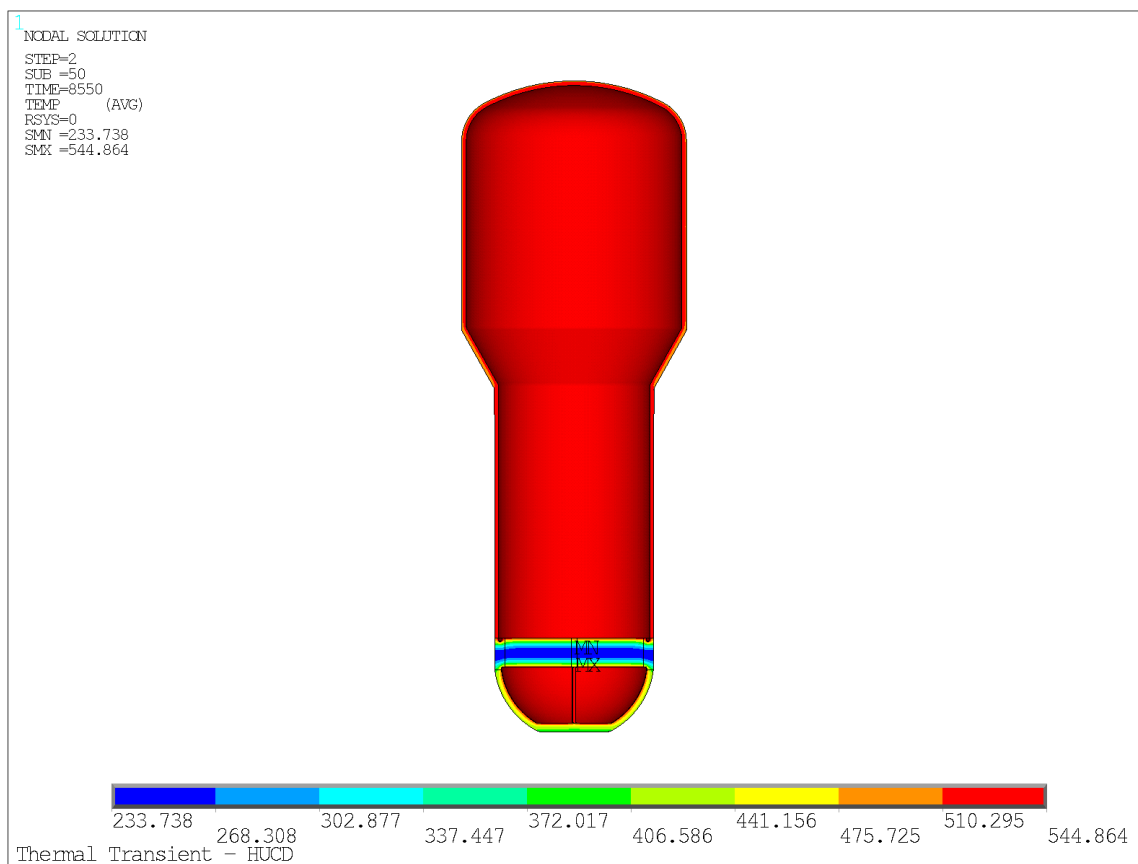
Notes:
 Plant loading transient shown.
 Loads applied at time = 1,800 seconds.
 Units for stress are psi.

Figure 7-21
 Applied mechanical boundary conditions and pressure for thermal stress analyses for the PWR SG

7.2.3 Stress Analysis Results

Representative temperature contour and stress contour plots for the combined heatup/cool-down transient are shown in Figure 7-22 and Figure 7-23, respectively. The time shown in Figure 7-22 and Figure 7-23 is when the maximum total stress intensity occurs. Figure 7-24 shows the path locations where stresses were extracted. Paths P3–P6 were chosen for the tubesheet-to-head/divider plate welds, Paths P7–P9 were chosen for the vessel circumferential welds,

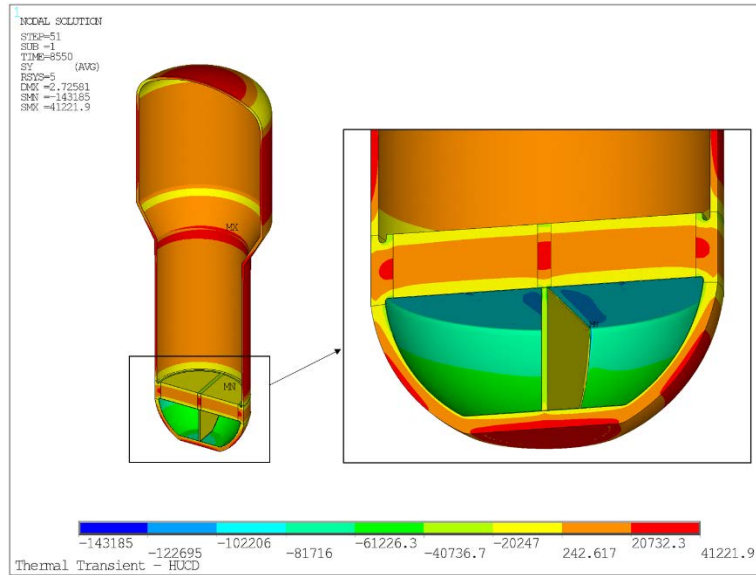
Paths P10 and P11 were chosen for the head circumferential welds, and Paths P12–P14 were chosen for the tubesheet-to-shell welds. All stresses are extracted in a cylindrical coordinate system with “y” along the hoop direction of the shell and “z” along the axial direction of the shell. Because Path 11 is parallel to the global “y” direction, “x” direction stress was treated as the axial stress for Path P11. Representative through-wall stress distributions for Paths P4, P9, P11, and P12 are shown in Figures 7-25–7-28, respectively.



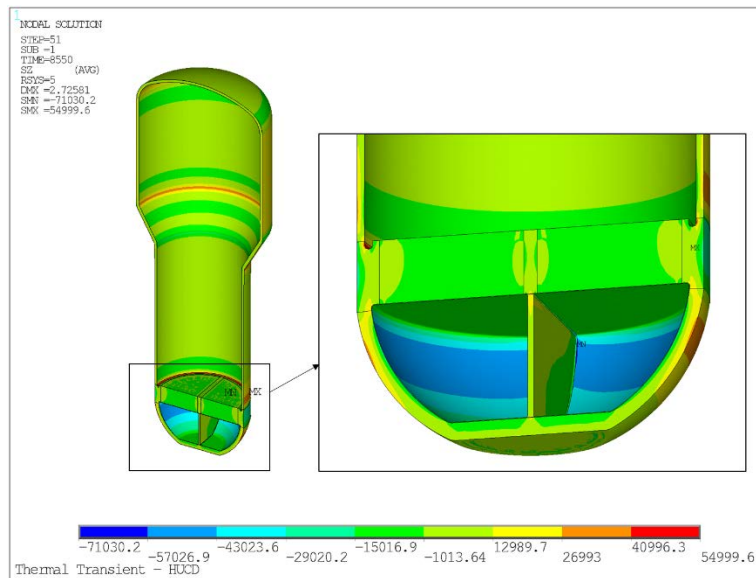
Note: units for temperature are °F

Figure 7-22

Temperature contour for the plant loading transient (time = 8,550 seconds, end of heatup) for the PWR SG



Hoop Stress (to the SG shell)



Axial Stress (to the SG shell)

Note: Units for stress are psi

Figure 7-23
Stress contours for the plant loading transient (time = 8,550 seconds, end of heatup) for the PWR SG



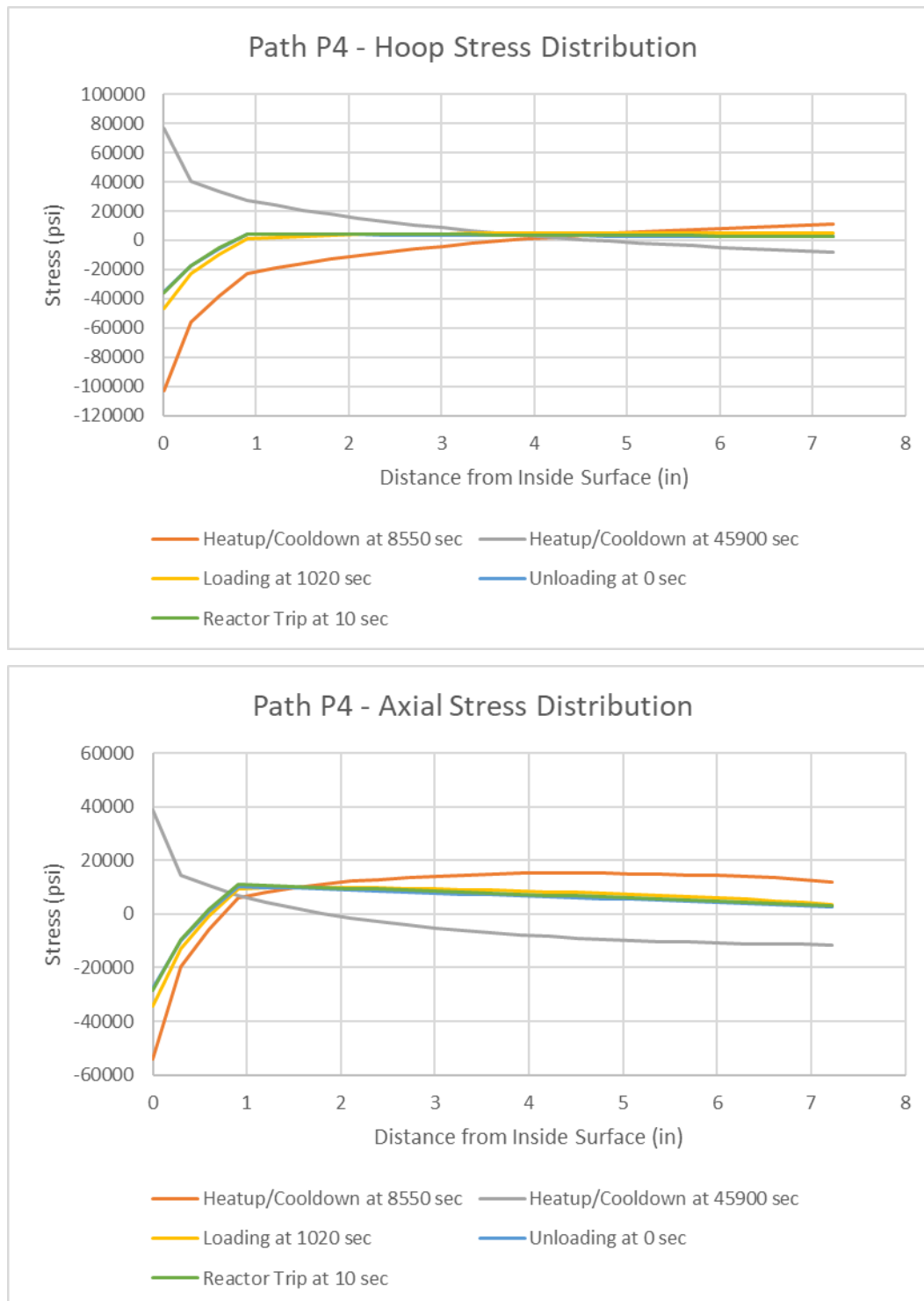


Figure 7-25
Through-wall stress distribution at Path P4 for the PWR SG

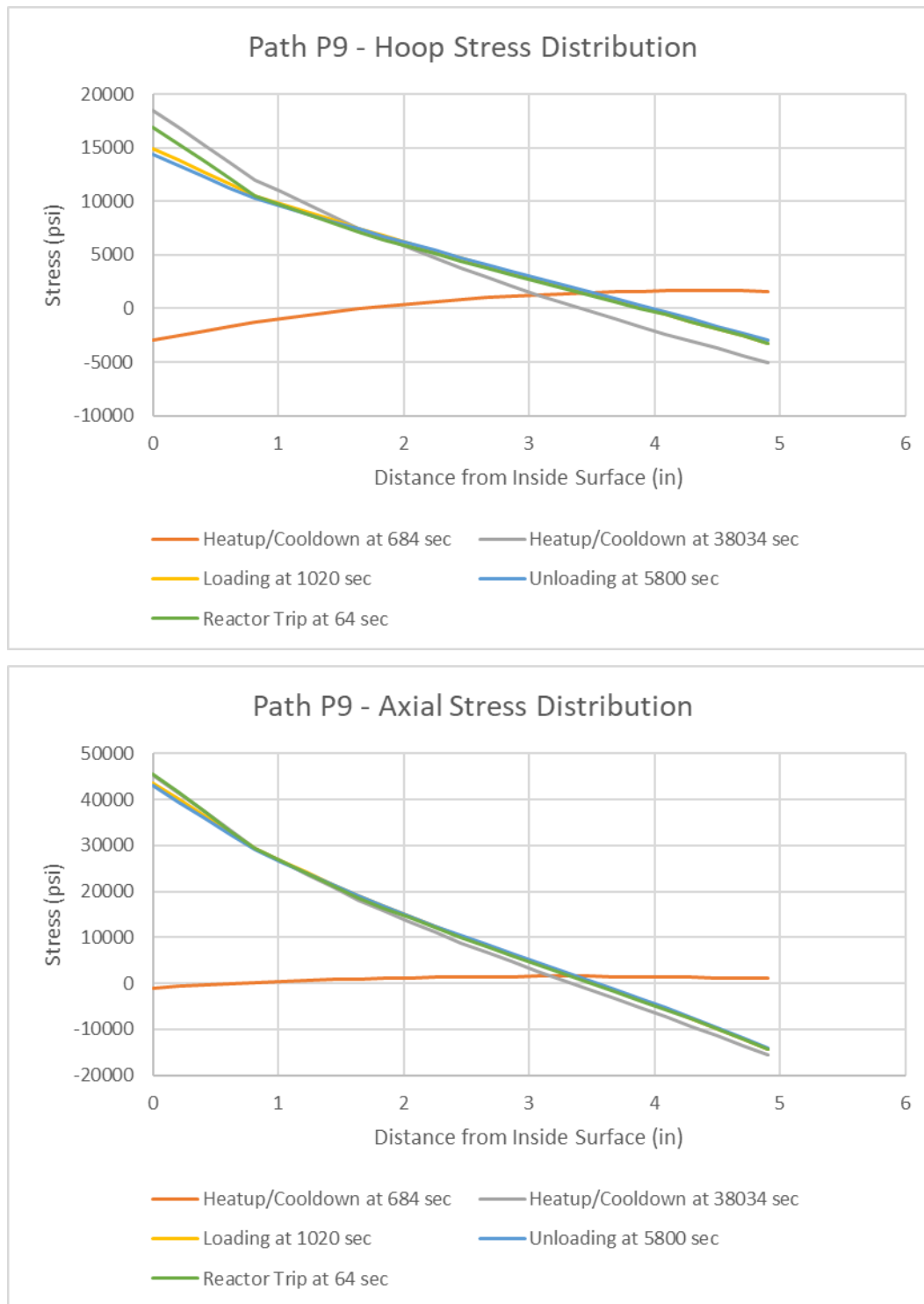


Figure 7-26
Through-wall stress distribution at Path P9 for the PWR SG

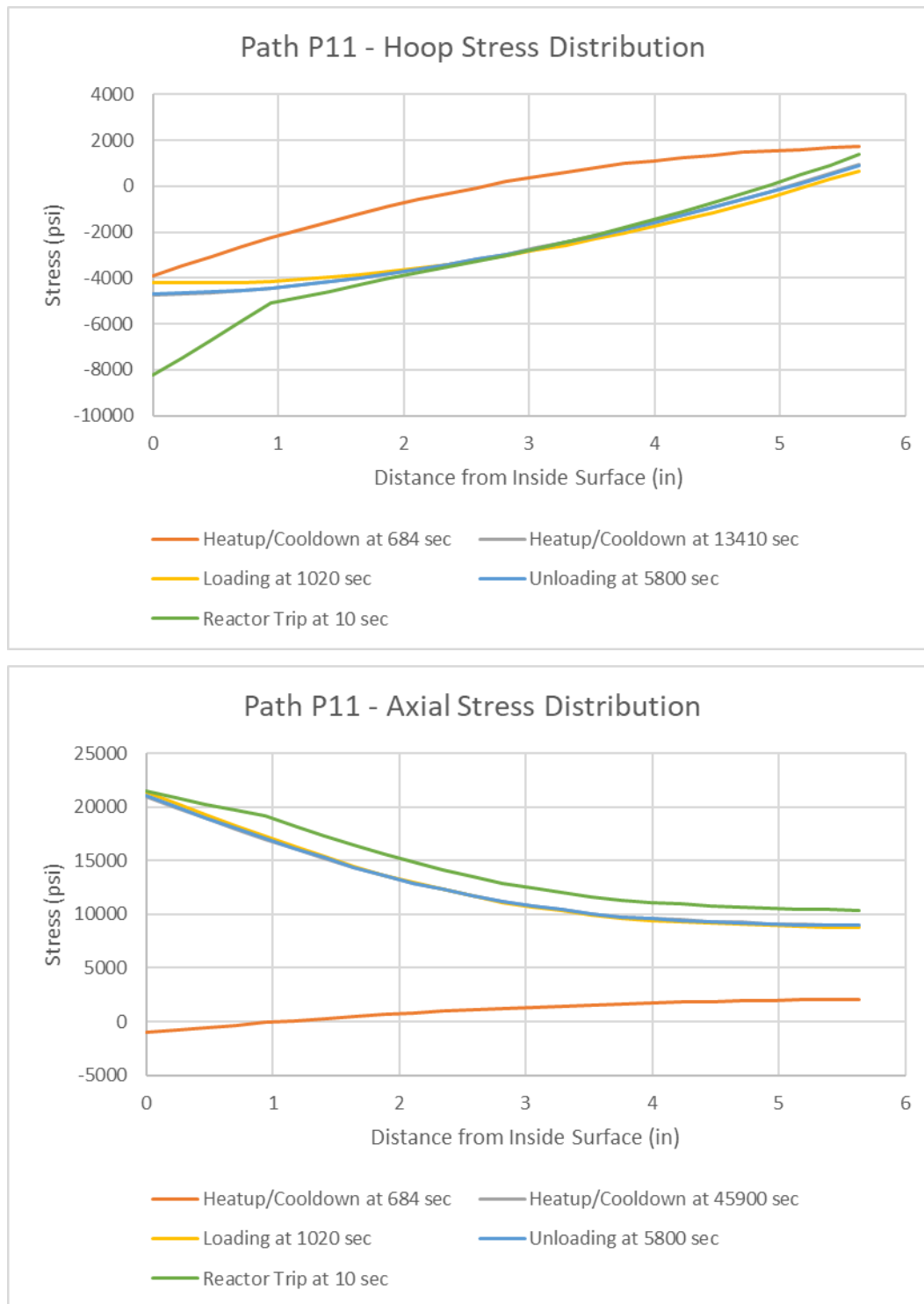


Figure 7-27
Through-wall stress distribution at Path P11 for the PWR SG

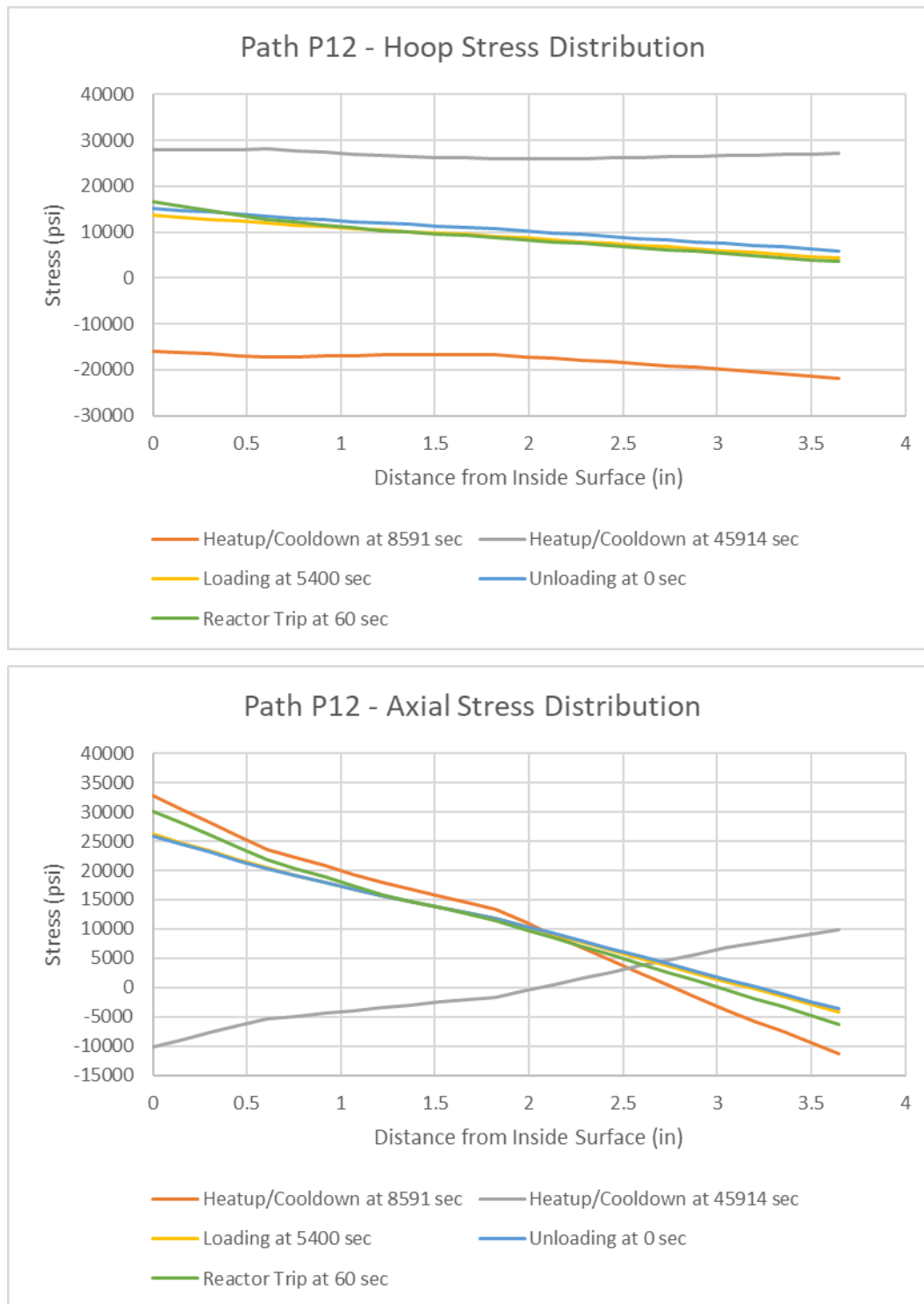


Figure 7-28
Through-wall stress distribution at Path P12 for the PWR SG

8

DETERMINISTIC AND PROBABILISTIC FRACTURE MECHANICS EVALUATION

This section describes the deterministic fracture mechanics (DFM) and PFM analyses performed on the SG items selected in Section 4.5. As covered in Section 3.4, Items Nos. B2.31, B2.32, and B.130 involve only a few plants; however, for completeness, all seven items (B3.130, B2.31, B2.32, B2.40, C1.10, C1.20, and C1.30) are evaluated in this section. The primary objective of the PFM and DFM analyses is to assess various inspection frequencies for these nozzles, including the current ASME Section XI requirements described in Section 2.

8.1 Overview of Technical Approach

The DFM evaluations were performed using average and limiting parameters to determine operability with a postulated flaw. In this case, they were also used as a screening process to determine the critical paths considered in the PFM analyses. The PFM evaluations were performed to demonstrate the reliability of the selected components assuming various inspection scenarios. Both the DFM and PFM approaches were used in previous ISI optimization projects involving examination frequency reduction, examination scope reduction, or both, as shown in Table 8-1.

Table 8-1
Previous ISI projects that evaluated inspection requirements

Document	Description	Approach		Result			Ref.	Revised Inspection Requirement
		D	P	SR	FR	CEM		
BWRVIP-05	BWR vessel welds		X	X			14	Elimination of circumferential weld inspections.
BWRVIP-108	BWR inner radius and vessel-to-shell welds	X	X	X			3	Sample size reduced from 100% to 25% of each nozzle type.
WCAP-16168-NP-A	PWR vessel and nozzle-to-shell welds		X		X		9	Inspection frequency extended from 10 years to 20 years.
SIR-94-080	RCP flywheel: CE and B&W	X			X		57	Inspection frequency extended from 3.5 years to 10 years.
WCAP-15666	Westinghouse RCP flywheel	X	X		X		58	Inspection frequency extended from 3.5 years to 10 years.
EPRI-3002007626	RPV thread in flange	X			X		32	Inspection frequency extended from 10 years to (at least) 20 years.
PVP-2001 (Bamford et al.)	RPV inner radius inspections	X	X	X			59	Elimination of these inspections.
PVP2006-ICPVT-11-93892	Regen and residual heat exchangers	X	X			X	13	Inspection method changed from volumetric to visual.
PVP2015-45194 supplemented by MRP-82 and NUREG/CR-6934	Appendix L flaw tolerance evaluation to manage fatigue in surge line	X			X		60	Justified maintaining the current 10-year inspection interval.
MRP-375	Alloy 690 RPV head nozzle penetration nozzles	X	X	X	X		61	Inspection frequency extended from 10 years to 20 years. Scope reduced using sister head concept.

D = deterministic

P = probabilistic

SR = scope reduction

FR = frequency reduction

CEM = change in examination method

All documents listed in Table 8-1 involving scope reduction have some probabilistic aspect, whereas most documents involving frequency reduction have some deterministic aspect. Therefore, to evaluate the potential for possible scope and/or frequency reductions, both deterministic and probabilistic approaches are employed in this report.

8.2 DFM Evaluation

The objective of the DFM evaluation is to determine the time that it takes for a postulated flaw to grow to the ASME Code allowable flaw size. From the results of the DFM evaluation, critical paths are then selected for use in the PFM evaluation. The DFM evaluation is performed using average parameters to supplement the PFM evaluation.

8.2.1 Technical Approach

The technical approach used in the DFM evaluation is to postulate an initial flaw size equivalent to the relevant ASME Code, Section XI acceptance standard. The ASME Code, Section XI fatigue crack growth (FCG) law, with the through-wall stress distributions from Section 7 and appropriate fracture mechanics models, is then used to determine the length of time for the postulated initial flaw to grow to a depth of 80% of the wall thickness (assumed to equate to leakage in this evaluation) or the depth at which the allowable toughness (K_{IC} reduced by a structural factor of 2) is reached, whichever is less.

8.2.2 Design Inputs

The design inputs used in the DFM evaluation are summarized in Table 8-2 and covered in Sections 8.2.2.1–8.2.2.7.

8.2.2.1 Geometry

The geometries of the components considered in the evaluation are presented in Figures 4-4 and 4-5 for the CE and B&W steam generator primary-side inlet nozzle, respectively, for Item B3.130. Table 4-2 provides the SG geometry used for evaluation of Items B2.31, B2.32, B2.40, C1.10, C1.20, and C1.30.

8.2.2.2 Initial Crack Size and Shape

For all components, an initial crack size of 5.2% of the wall thickness (which corresponds to the most conservative ASME Code Section XI flaw acceptance standard for these components from Tables IWB-3510-1 and IWC-3510-1 of ASME Code Section XI) was used in the DFM evaluation. This initial crack depth is the maximum value from these two tables with an associated crack aspect ratio (half crack length-to-crack depth) of 1.0. This crack shape results in the most conservative initial stress intensity factor (K) at the deepest point of the crack. As indicated earlier, the aspect ratio is then subsequently allowed to vary during the crack growth process.

8.2.2.3 Applied Stresses

8.2.2.3.1 Operating Transient Stresses

The applied stresses consist of through-wall stresses due to pressure and the thermal transients described in Section 7. Typical through-wall stress distributions for stress paths used in the evaluation are shown in Figures 7-17, 7-18, 7-25, 7-26, 7-27, and 7-28.

8.2.2.3.2 Weld Residual Stresses

Pressure vessel welds typically receive post-weld heat treatment (PWHT) to reduce the effects of weld residual stresses. In this evaluation, weld residual stresses remaining after PWHT were characterized in the form of a cosine distribution with a peak stress of 8 ksi [62], as shown in Figure 8-1. This value was previously used in the fracture mechanics evaluations of a BWR nozzle-to-shell weld in BWRVIP-108 [3] and BWR shell welds in BWRVIP-05 [14] and was found acceptable by the NRC.

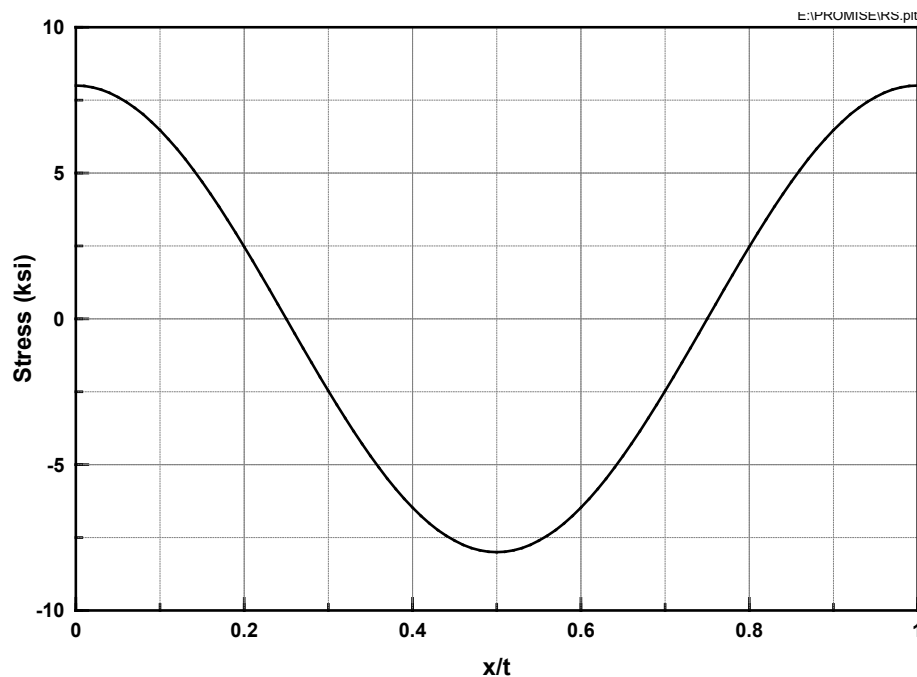


Figure 8-1
Weld residual stress distribution

8.2.2.4 Fracture Mechanics Models

In this evaluation, all pre-existing flaws were conservatively assumed to be surface flaws. Two different fracture mechanics models were used for axial and circumferential flaws. For the axial flaw, the stress intensity factor (K) solution for an internal, semi-elliptical crack from API-579/ASME-FFS-1 [63] was used. This model is shown in Figure 8-2. The aspect ratio (a/c) was allowed to vary during crack growth.

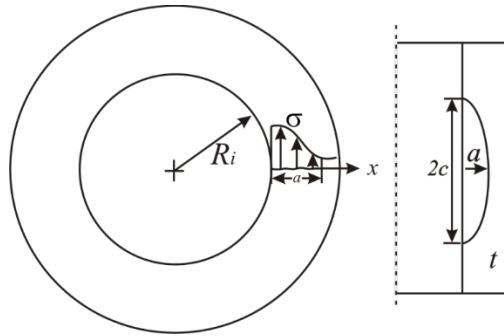


Figure 8-2
Semielliptical axial crack in a cylinder model

Similarly, for a circumferential flaw, the K solution for an internal, semielliptical crack from API-579/ASME-FFS-1 [62] was used. This model is shown in Figure 8-3. The aspect ratio (a/c) was allowed to vary during crack growth.

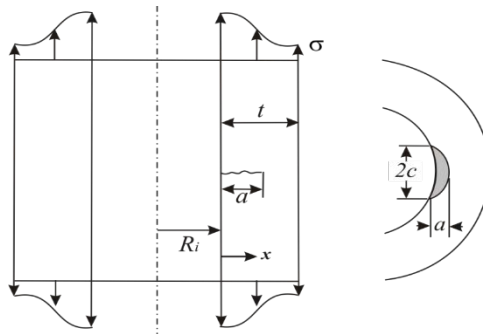


Figure 8-3
Semielliptical circumferential crack in a cylinder model

These fracture mechanics models were incorporated into TIFFANY [64], software developed by Structural Integrity Associates, that determines the K distribution due to through-wall stress profiles for both circumferential and axial cracks. The outputs of TIFFANY are the maximum and minimum K distributions as well as the ΔK distribution for each transient.

8.2.2.5 Fracture Toughness

The materials under consideration are all ferritic steels; therefore, the fracture toughness curve provided in ASME Code, Section XI, Appendix A (Figure A-4200-1) [1] was used for this evaluation. From Section 5.2, the minimum temperature experienced across all transients corresponds to the heatup/cooldown case. Figures 7-11, 7-13, and 7-22 provide plots of the temperature during this transient for the SG inlet nozzle (CE design), SG inlet nozzle (B&W design), and SG vessel evaluated in this report. The minimum temperature across all components during this transient corresponds to Figure 7-22 and is always above 200°F. The maximum RT_{NDT} for either the SA-533 SG shell material or the SA-508 Class 2 SG nozzle material allowed by Branch Technical Position 5-3 [65] is 60°F. Because the temperature of the transients and components analyzed is always above 200°F, the minimum possible temperature to use when entering the ASME Code, Section XI, Figure A-4200-1 is (200°F - 60°F) = 140°F. This temperature is greater than the temperature of the end of the K_{IC} curve shown in Figure A-4200-1, so an upper shelf fracture toughness of at least 200 $\text{ksi}\sqrt{\text{in.}}$ was used.

Figure 8-4 [66, 67] shows the fracture toughness of vessel steels as a function of temperature and shows that the ASME Code, Section XI fracture toughness is a reasonable lower bound.

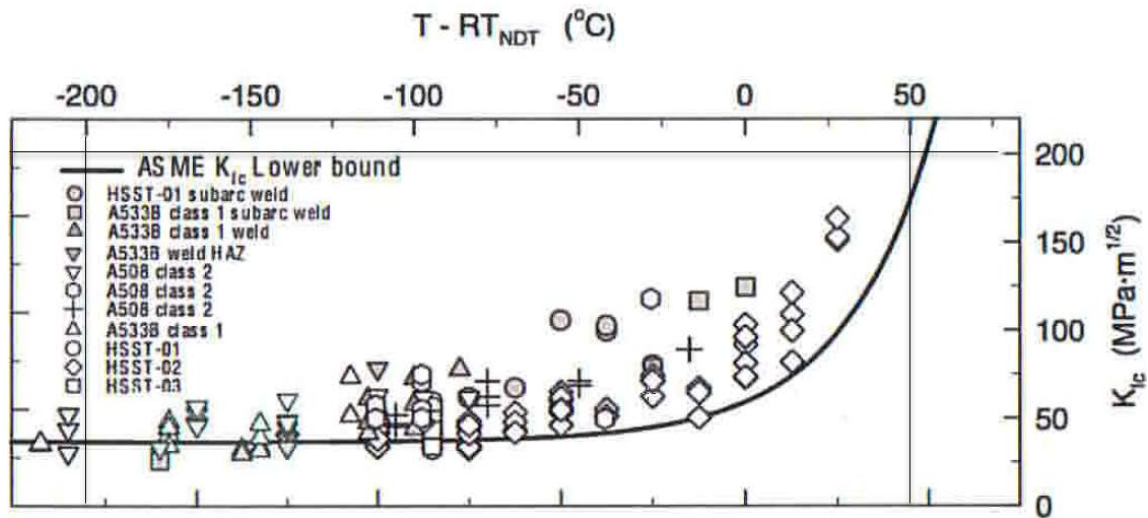


Figure 8-4
ASME Section XI fracture toughness curve for vessels versus experimental data points [66, 67]

8.2.2.6 Fatigue Crack Growth Law

From the degradation mechanism evaluation performed in Section 6, the only potential degradation mechanism identified for the in-scope SG components is fatigue (such as corrosion fatigue, mechanical fatigue, and/or thermal fatigue). The FCG law for ferritic steels, as defined in ASME Code, Section XI, Appendix A, Paragraph A-4300 [1], was used in the evaluation.

8.2.2.7 Summary of Design Inputs

The design inputs covered in the preceding are summarized in Table 8-2 and were used to perform the DFM evaluation.

Table 8-2
Summary of DFM design inputs

Input	Value
Geometry	From Section 4
Initial crack size	5.2% of the thickness, $c/a = 1$
Fracture toughness	200 ksi√in.
Fatigue crack growth law	ASME Code, Section XI Appendix A, Paragraph A-4300
Operating transient stresses	From Section 7
Residual stresses	Cosine curve with 8-ksi peak (see Figure 8-1)

8.2.3 Results of DFM Evaluation

The results of the DFM evaluation are summarized in Table 8-3. Table 8-3 shows that the periods required for hypothetical postulated flaws to leak are very long, which indicates that all of the evaluated components are very flaw-tolerant. Because the DFM evaluation considered hypothetical postulated flaws, structural factors of 2.0 on primary loads and 1.0 on secondary loads (consistent with ASME Code, Section XI, Appendix G) were applied. Also, because the most dominant load is pressure, which results in a primary stress, the structural factor of 2.0 was conservatively applied to the fracture toughness of 200 ksi√in. This results in an allowable fracture toughness of 100 ksi√in. Table 8-3 shows that the maximum K values for all locations are below this allowable fracture toughness after 80 years.

One axial crack path and one circumferential crack path were selected for each component for further PFM evaluation based on the minimum number of years to leak from the DFM evaluation. These selected paths are identified with red bold text in Table 8-3. It should be noted that for Item B3.130 (CE design), the selected stress path with the weld on the nozzle side is not limiting; however, this does not change the conclusion of the fracture mechanics analyses because another path is controlling.

Table 8-3
Results of the DFM evaluation

Item No.	Component Description	Case Identification (Note 1)	Years to Leak	Max. K at 80 Years (ksi√in.)
B3.130 (CE)	SG (primary side), nozzle-to-vessel welds (CE design)	SGPNV-P1A-(N)	1082	34.00
		SGPNV-P1C-(N)	3796	19.69
		SGPNV-P1A-(S)	848	38.50
		SGPNV-P1C-(S)	2085	23.75
B3.130 (B&W)	SG (primary side), nozzle-to-vessel welds (B&W design)	SGPNV-P2A-(N)	771	42.30
		SGPNV-P2C-(N)	9235	12.50
		SGPNV-P2A-(S)	940	42.9
		SGPNV-P2C-(S)	3167	26.3
B2.31 B2.32 B2.40	SG (primary side), head welds, circumferential SG (primary side) tubesheet-to-head welds SG (primary side), head welds, meridional	SGPTH-P3A	798	44.00
		SGPTH-P3C	1223	23.00
		SGPTH-P4A	641	77.58
		SGPTH-P4C	2319	33.09
		SGPTH-P5A	725	75.69
		SGPTH-P5C	3527	33.07
		SGPTH-P6A	1045	43.41
		SGPTH-P6C	5156	22.00

Table 8-3 (continued)
Results of the DFM evaluation

Item No.	Component Description	Case Identification (Note 1)	Years to Leak	Max. K at 80 Years (ksi√in.)
C1.10	SG shell (secondary side) circumferential welds	SGSSC-P7A	8077	18.00
		SGSSC-P7C	4.08E+04	12.30
		SGSSC-P8A	4138	22.89
		SGSSC-P8C	3.97E+04	8.60
		SGSSC-P9A	1.63E+04	17.90
		SGSSC-P9C	3533	33.90
C1.20	SG head (secondary side) circumferential welds	SGSHC-P10A	3.51E+04	14.10
		SGSHC-P10C	6.05E+04	12.50
		SGSHC-P11A	5.98E+04	8.90
		SGSHC-P11C	1.05E+04	19.80
C1.30	SG (secondary side) tubesheet-to-shell welds	SGSTS-P12A	1940	20.97
		SGSTS-P12C	3154	23.93
		SGSTS-P13A	2100	20.56
		SGSTS-P13C	4023	22.70
		SGSTS-P14A	1950	20.97
		SGSTS-P14C	3208	23.93

Note 1:

The Case Identification terminology is as follows: SG for steam generator, PNV for primary nozzle-to-vessel, PTH for primary tubesheet-to-head, SSC for secondary-side circumferential, SHC for shell head circumferential, and STS for secondary tubesheet-to-shell; (N) indicates that the weld is on the nozzle side, and (S) indicates that the weld is on the shell side; P1–P14 represent the crack paths (see Figures 7-15, 7-16, and 7-24); C is circumferential part-through-wall crack; and A is axial part-through-wall crack.

Note: Limiting stress paths considered in PFM analyses are displayed in **red bold** text.

8.3 PFM Evaluation

8.3.1 Technical Approach

Monte Carlo probabilistic analysis techniques were used in the PFM analyses to determine the effect of various inspection scenarios on the probability of failure of the components evaluated. The overall technical approach is illustrated in Figure 8-5. An analysis of the sensitivity of the PFM evaluation to various input parameters was also performed to determine the key parameters that influence the results.

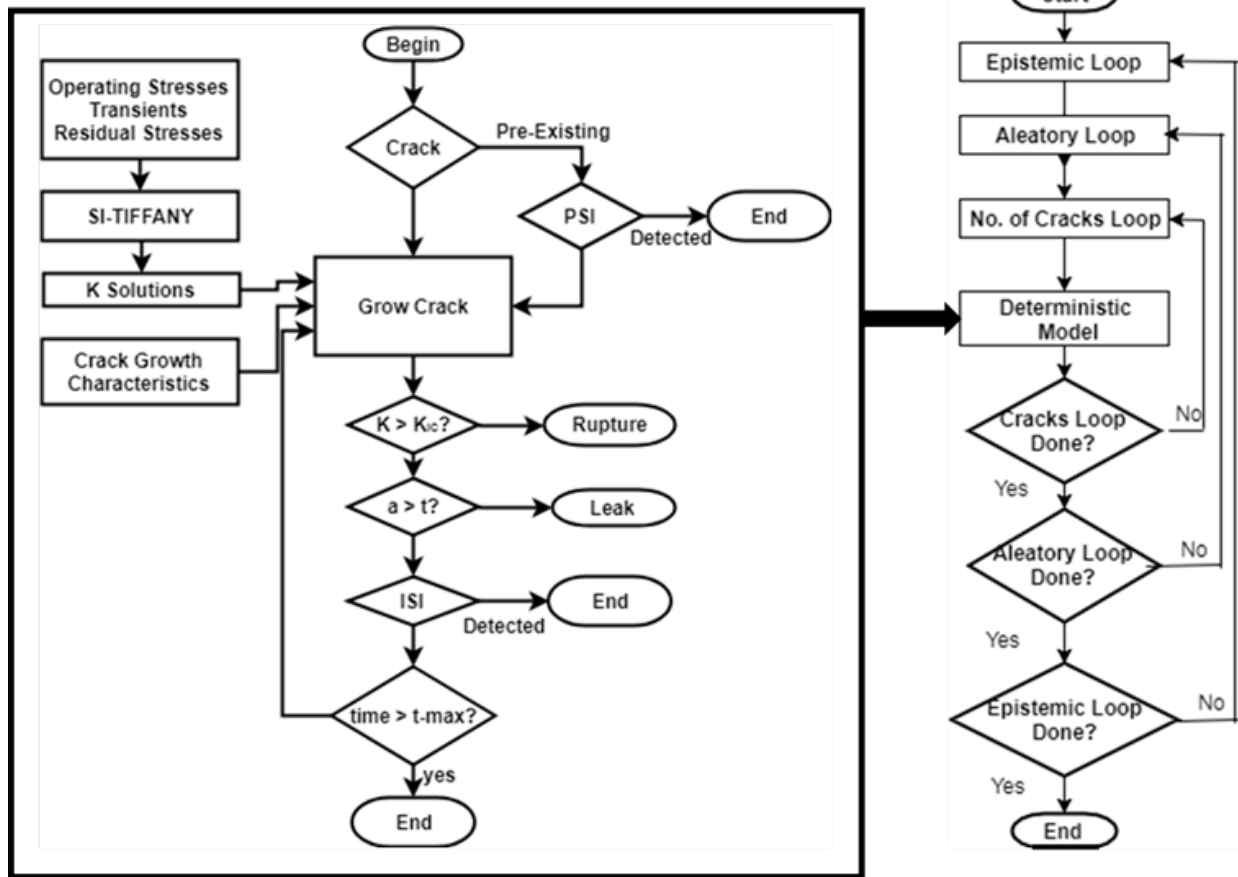


Figure 8-5
PFM overall technical approach

8.3.1.1 Treatment of Uncertainties

Separation of sources of uncertainty was considered in the PFM evaluation because characterization of the contribution of uncertainty is one of the primary reasons for performing the analyses. There are two contributors to uncertainty in PFM analyses [68].

One contributor is inherent scatter (or random scatter), which is termed *aleatory* uncertainty. In this case, the probability of obtaining each outcome can be measured or estimated, but the precise outcome in any particular instance is not known in advance. Unlike a scenario such as rolling dice, obtaining additional data will not help reduce the variability.

A second contributor to uncertainty is caused by lack of knowledge, which is termed *epistemic* uncertainty. Unlike aleatory uncertainty, gathering more data can be helpful in reducing epistemic uncertainty. Both aleatory and epistemic uncertainties were considered in the PFM evaluation, as shown on the right side of Figure 8-5.

8.3.1.2 Sampling Method

Monte Carlo simulation was used for computing failure probabilities. A random number generator with a repeat cycle beyond 10^{15} was employed, with a provision for user input of the random number seed used in the analysis. All random variables were user-selected as either

normal, log-normal, Weibull, exponential, uniform, or logistic; alternatively, the cumulative distribution can be defined by a tabular input. Provisions are made to perform a deterministic calculation of lifetime, in which case calculations are performed using specified values of the input variables. A user selection for deterministic analysis is provided. Provisions are made to consider variances in inputs due to inherent scatter (aleatory) and due to lack of knowledge (epistemic). This entails two loops in the calculations, as illustrated in Figure 8-5. This means that instead of a single line for probability of failure as a function of time, there will be a band of lines.

8.3.2 Details of Analysis Methodology and Inputs

8.3.2.1 Component Geometry

The geometries of the components considered in the evaluation are the same as those used in the DFM analyses and presented in Figures 4-4 and 4-5 for the CE and B&W SG primary-side inlet nozzles, respectively, for Item B3.130. Table 4-2 provides the SG geometry used for evaluation of Item Nos. B2.31, B2.32, B2.40, C1.10, C1.20, and C1.30.

8.3.2.2 Initial Flaw Distribution and Number of Flaws per Weld

The initial flaw size (depth) distribution used in the evaluation was previously derived by the NRC during its review of the BWRVIP-05 project in Reference [69], based on flaw data from the Pressure Vessel Research User's Facility (PVRUF) vessel. This distribution was subsequently used in BWRVIP-05 [19] in lieu of the Marshall flaw distribution [70], which was initially used in the ISI optimization of BWR RPV welds. The PVRUF distribution was also used in the ISI optimization of the RPV nozzle-to-shell welds in BWRVIP-108 [3]. The PVRUF flaw distribution was found to be slightly more conservative than the Marshall flaw distribution in Reference [69]. Even though the PVRUF data were based on an RPV, they can be applied to a steam generator vessel because both are large-diameter vessels fabricated from similar plate and forging processes and from the same materials (SA-533 and SA-508 Class 2). As such, the fabrication processes should be similar and the PVRUF data are judged to be reasonably representative for this evaluation. The PVRUF flaw distribution derived by the NRC is represented in the cumulative distribution form by Equation 8-1:

$$P(a \leq 0.0787) = 0.9054$$

$$P(a > 0.0787) = 1 - 0.1616e^{-6.94a} - 0.0139e^{-4.06a} \quad \text{Eq. 8-1}$$

The PVRUF flaw data are provided in Reference [71]. Previous evaluations used a constant aspect ratio [3, 14], and, as such, once the flaw depth is known, the flaw length can be calculated. In this evaluation, the distribution of crack length was derived from data in NUREG/CR-6817 [72]. This results in a log-normal distribution for the crack length with the following parameters:

- $\mu = 0.74$
- median $(\ell - a)/d = 2.08$

The evaluation procedures for the length distribution are detailed in Reference [73].

In the present work, for the PWR SG primary-side inlet nozzle-to-vessel weld, the number of fabrication flaws was assumed to be 1.0 per nozzle. This value is consistent with those approved by the NRC during the optimization of the BWR RPV nozzle-to-shell welds in Reference [4].

8.3.2.3 Probability of Detection Curve

The probability of detection (POD) curve used in this evaluation was based on the Performance Demonstration Initiative (PDI) on full-scale vessel mockups containing realistic defects; the same as used for the optimization of the BWR RPV nozzle-to-shell welds in Reference [3]. Separate POD curves were derived in Reference [3] for automated weld techniques, manual weld techniques, and a combination of the two. The final POD curve used in Reference [3] was the combined curve, which was also used in this evaluation. The combined POD curve is presented in Figure 8-6. This POD curve is more conservative than that used in the development of ASME Code, Section XI, Appendix L, for carbon steel pipe sections [74], which is presented in Figure 8-7. As shown in Figure 8-7, the POD curve used for Appendix L shows a very high probability of detecting a crack (approximately 95%), regardless of flaw depth.

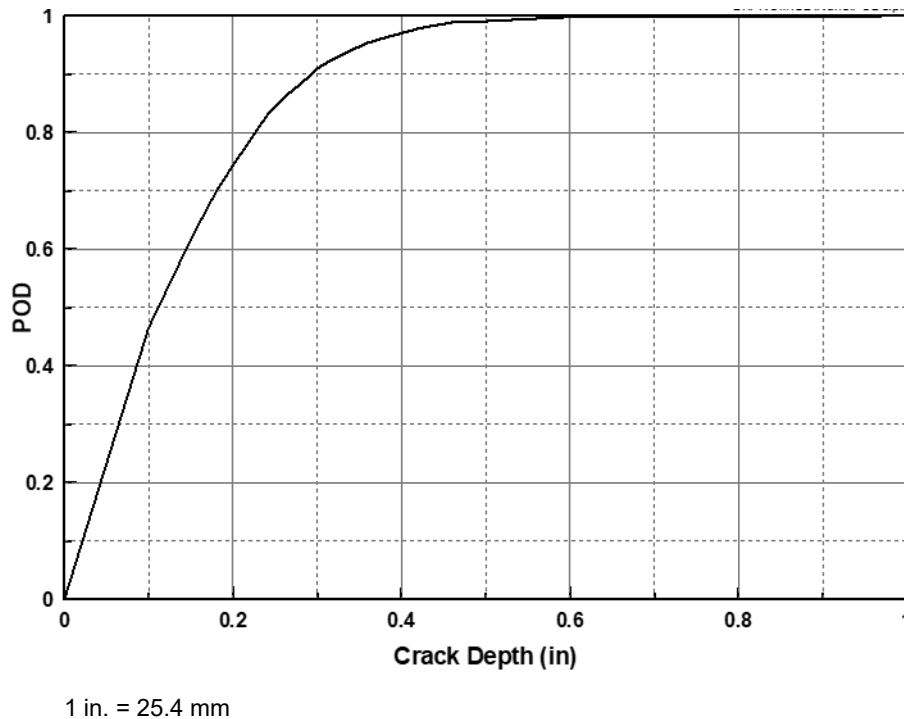


Figure 8-6
POD curve for vessels from BWRVIP-108 [3]

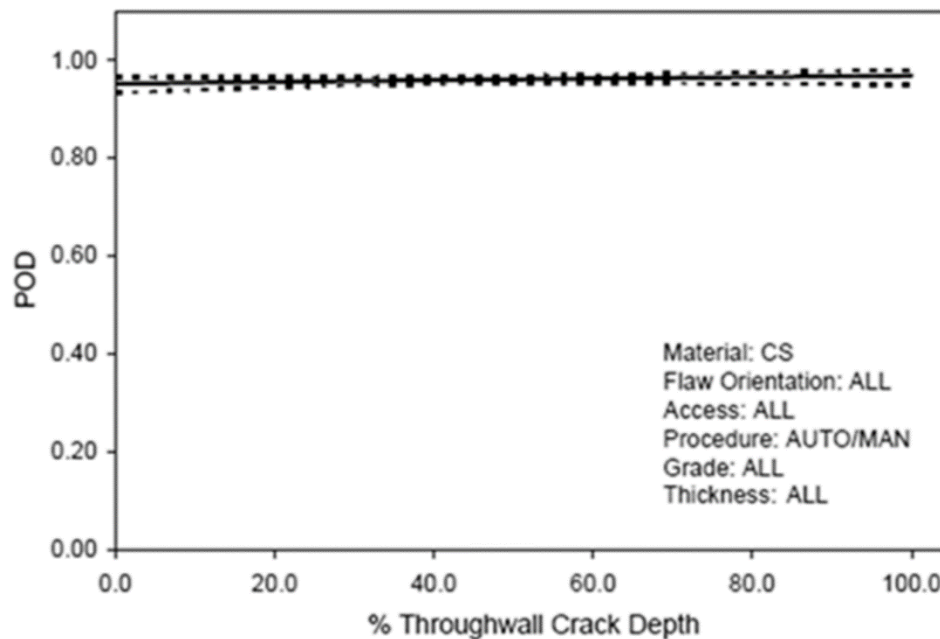


Figure 8-7
Carbon steel POD curve for all pipe section thicknesses used to develop Section XI
Appendix L [74]

8.3.2.4 Applied Stresses

The applied stresses consist of through-wall stresses due to pressure and the thermal transients, as covered in Section 8.2.2.3.1. The vessel weld residual stress distribution covered in Section 8.2.2.3.2 was also considered in the PFM analyses as a constant value (non-random distribution).

8.3.2.5 Fracture Mechanics Models

The semielliptical axial crack in a cylinder model and a circumferential semielliptical crack in a cylinder used in the DFM evaluation and shown in Figures 8-2 and 8-3 were also used in the PFM evaluations.

8.3.2.6 Fatigue Crack Growth

The ASME Code, Section XI, Appendix A, Paragraph A-4300 [1] fracture crack growth law used in the DFM evaluation was also used in the PFM evaluations. In the PFM evaluations, the calculated crack growth rate was considered log-normally distributed, consistent with the distribution used in the Extremely Low Probability of Rupture (xLPR) project [75]. The calculated value of the crack growth based on Paragraph A-4300 was considered as the median value of the log-normal distribution with a second parameter of 0.467 from Reference [75], which was derived from FCG in ferritic materials in a PWR environment and was considered applicable for this evaluation. The FCG threshold was also assumed to be log-normally distributed as described in Reference [75].

8.3.2.7 Fracture Toughness

The fracture toughness curve provided in ASME Code, Section XI, Appendix A (Figure A-4200-1) [1] that was used in the DFM evaluation was also used for the PFM evaluation. Although the ASME Code, Section XI fracture toughness curve is considered to be a lower bound, significant conservatism was incorporated into the PFM evaluation. The ASME Code Section XI fracture toughness curve shown in Figure 8-4 was assumed to be normally distributed with a median value of 200 ksi $\sqrt{\text{in.}}$ and a standard deviation of 5 ksi $\sqrt{\text{in.}}$ to be consistent with that used in BWRVIP-108 [3] and accepted by the NRC.

8.3.2.8 Inspection Schedule Scenarios

The inspection schedule scenarios considered in the evaluation are shown in Table 8-4. For all scenarios, it was assumed that pre-service inspection (PSI) was performed. ISI is then performed with the current ASME Code, Section XI schedule of a 10-year inspection interval up to 30 years, followed by subsequent 20- or 30-year inspection intervals. This sequence was repeated with a 20- or 30-year inspection interval from the time of the last 10-year inspection. The objective is to determine whether an increased inspection interval can be justified regardless of how long an SG has operated with the current ASME Code, Section XI inspection schedule.

Table 8-4
Inspection schedule scenarios

Inspection Schedule	0	10	20	30	40	50	60	70	80
PSI only	X								
PSI + 10	X	X							
PSI + 10 + 20	X	X	X						
PSI + 10 + 20 + 30	X	X	X	X					
PSI, 20-year interval	X		X		X		X		
PSI + 10, 20-year interval	X	X		X		X		X	
PSI + 10 + 20, 20-year interval	X	X	X		X		X		
PSI + 10 + 20 + 30, 20-year interval	X	X	X	X		X		X	
PSI, 30-year interval	X			X			X		
PSI + 10, 30-year interval	X	X			X			X	
PSI + 10 + 20, 30-year interval	X	X	X			X			
PSI + 10 + 20 + 30, 30-year interval	X	X	X	X			X		

8.3.2.9 Acceptance Criterion

The acceptance criterion used for the probabilistic fracture mechanics evaluation was that failure frequencies must be less than the NRC's safety goal of 10^{-6} failures per year, consistent with that used for the optimization of the BWR RPV shell welds in BWRVIP-05 [14] and the optimization of the BWR RPV nozzle-to-shell weld in BWRVIP-108 [3]. This failure criterion was used in the development of alternative fracture toughness requirements for protection against pressurized thermal shock events [76] and has been adopted for use in the xLPR project [77].

Failure was defined to occur either by rupture or by leak. Rupture was assumed to occur in the probabilistic simulation when, for a given iteration, the applied K exceeded the materials fracture toughness (K_{IC}), that is, $K > K_{IC}$. A leak was assumed to occur when, for a given iteration, the crack depth exceeded 80% of the wall thickness ($a > 0.80t$). Due to the limitation in the fracture mechanics models used in this evaluation, it was conservatively assumed that a leak occurs when the crack depth reaches 80% of the component wall thickness.

8.3.2.10 Limitations and Assumptions

Two assumptions were made in the PFM evaluation. First, consistent with the discussion in Section 6, SCC was not considered because all materials are ferritic steels in a PWR environment. It was further assumed that no Alloy 82/182 welds are present.

Second, cracks in the welds were all characterized as either axial or circumferential cracks in a cylinder. The assumed axial and circumferential flaws ensured that a limiting flaw case was evaluated.

8.3.3 Computer Software Application

8.3.3.1 Software Development

The PFM methodology illustrated in Figure 8-5 and all inputs described in Section 8.3.2 were implemented in PROMISE (PRObabilistic OptiMization of InSpEction), Version 2.0, a software code developed by Structural Integrity Associates. PROMISE provides a probabilistic model of initiation and growth of cracks due to SCC and fatigue. (**Note:** The crack initiation and SCC modules were not used in the present work.) The growth and final instability of cracks are treated using linear elastic fracture mechanics. Monte Carlo simulation is used to generate numerical results, which include the probability of the crack depth exceeding 80% of the wall thickness ($a/t > 0.8$) and the probability of the applied stress intensity factor exceeding the allowed fracture toughness ($K > K_{IC}$). PROMISE consists of the following modules:

- Crack growth
- Stress intensity factor solutions (calculated by TIFFANY)
- Loads
- Inspection

PROMISE uses the following random variables:

- Initial crack size (depth and length)
- Loads (transient stresses)
- Weld residual stresses
- Fracture toughness
- Crack detection
- Number of cracks per weld or nozzle
- Inspection frequency
- Crack growth rate

Table 8-5 summarizes the various random variable distributions selected in PROMISE for this evaluation.

Table 8-5
Random variables and their associated distributions

Variable	Distribution
Crack depth	Tabular (PVRUF or NUREG-6817)
Crack length	Log-normal
Transient stresses	Constant
Fracture toughness	Normal
Fatigue crack growth rate	Log-normal
Fatigue crack growth threshold	Log-normal
Crack detection	Tabular (POD curve)
Number of cracks per weld	Poisson or constant
Weld residual stresses	Constant
Outside diameter, thickness	Constant

8.3.3.2 Software Verification and Validation

The verification and validation (V&V) of the PROMISE software involved two phases. In the first phase, a software project plan was developed [78]. The software project plan includes the requirements specification, functional specification, and software V&V plan. The second phase involved comparisons to benchmark problems against existing software codes.

8.3.3.2.1 Software Testing

The PROMISE software was tested extensively according to the software V&V plan to ensure that it produced expected and realistic results. The testing of the software and the results are documented in Reference [79]. A user's manual for PROMISE was also developed [80].

8.3.3.2.2 Benchmarking

A benchmarking exercise was performed to validate the PROMISE software against the VIPERNOZ Version 1.1 software code [81]. VIPERNOZ was used for performing the PFM analyses of the BWR RPV nozzle-to-shell welds and the nozzle inner radii in BWRVIP-108 [3]. The VIPERNOZ software was chosen for the benchmarking because it was presented to the NRC in BWRVIP-108. It should be noted that this benchmarking is used only to compare methodologies, and the nozzle corner crack model used in VIPERNOZ is not directly relevant to this report. The model used in VIPERNOZ for calculating the stress intensity factors was updated in PROMISE using the weight function method [82]. However, in the benchmarking exercise, the stress distribution was chosen such that the two models provided the same stress results. In addition, the PVRUF distribution was used for the initial crack size to be consistent with BWRVIP-05 and BWRVIP-108. The BWRVIP-108 FCG equation was used along with a Weibull distribution for the coefficient of the growth law equation. The FCG threshold was assumed to be zero. A summary of the key inputs to the benchmarking exercise is provided in Table 8-6.

Table 8-6
Benchmarking inputs

Input	Value
No. of cracks per inner radius section	1, constant
Crack depth distribution	PVRUF
Fracture toughness (ksi√in.)	Normal (200, 5)
PSI	None
ISI	None
POD curve	Not applicable
Fatigue crack growth law and threshold	BWRVIP-108
Uncertainties on transients	None
Residual stresses (ksi)	None

Analyses were performed for several combinations of cyclic stress and numbers of load cycles. The cumulative probability of leakage results for the benchmarking exercise is presented in Table 8-5. As can be seen from Table 8-7, reasonably good agreement was obtained between PROMISE and VIPERNOZ, and the probability of leakage results are similar between the two software codes. Therefore, the PROMISE software yields results that are consistent with previously NRC-approved PFM software.

Table 8-7
Comparison of cumulative probability of leak between PROMISE and VIPERNOZ for benchmarking

Cyclic Stress (ksi)	Cycles/Year	PROMISE	VIPERNOZ
25	500	2.8E-2	3.1E-2
15	500	1.7E-4	3.0E-4

8.3.4 Base Case, Sensitivity Analysis, and Sensitivity Studies

The PFM analysis was performed on the SG primary- and secondary-side components considered in this report using the critical stress paths identified from the DFM analyses and presented in red boldface font in Table 8-3.

8.3.4.1 Base-Case Evaluation

Nuclear plants have been in operation for various time periods, and many units have replaced their SGs at various times during their respective plant histories. As such, their SG inspection intervals and histories are quite different. However, the one inspection that is consistent across all plants is that they all received PSI before entering service. The Section III fabrication examination required for these components was robust, as was the Section XI PSI. In this report, the term *PSI* refers to a combination of the Section III fabrication examination and Section XI PSI. A scenario with PSI-only inspection was used for the base case. This base case is more limiting than the base case considered in the Reference [2] report in that no credit is taken for any ISI, whereas in the Reference [2] report, the base case also considered ISI at 20, 40, and 60 years in addition to the PSI. Other input parameters for the base-case evaluation are covered in Section 8.3.2 and are listed in Table 8-8.

Table 8-8
PFM base-case inputs

No. of Realizations	Epistemic = 1, Aleatory = 10 million
No. of cracks per weld	1, constant
Crack depth distribution	PVRUF
Crack length distribution	NUREG/CR-6817-R1
Fracture toughness (ksi√in.)	Normal (200,5)
Inspection coverage	100%
PSI	Yes
ISI	None
POD curve	BWRVIP-108, Figure 8-6
Fatigue crack growth law and threshold	A-4300, log-normal, second parameter = 0.467
Uncertainties on transients	None
Weld residual stresses (ksi)	Cosine curve (8, 8), constant (not random)

The inputs selected for the base-case evaluation are considered the most appropriate data for the current report. The selected crack size distribution, POD curve, and weld residual stress profile were used in similar projects [3, 14]. The crack length distribution was derived from the most recent data on cracks in welds [72, 73]. The FCG curve defined in ASME Code, Section XI, Appendix A, Paragraph A-4300 [1] falls above the least square best fit to the data and was based on a 95% global confidence limit of the data [83]. In the present analysis, the FCG curve defined in Paragraph A-4300 was considered as the median curve; however, it is higher than the median curve discussed in Reference [1] and is therefore conservative. The second parameter of log-normal distribution (analogous to standard deviation) is obtained from the xLPR project [75]. As covered, the upper shelf ASME Code, Section XI fracture toughness (K_{IC}) used in this evaluation is conservative compared to the actual data. All the distributed variables were considered aleatory because they are conservative or based on large sets of data.

Unless indicated otherwise, 10 million aleatory realizations were performed for all cases investigated in this report.

The results of the base case are listed in Table 8-9 for the probabilities of rupture and leakage. As indicated in Table 8-9, the most limiting location is Path SGPTH-P4A. For all components, the probabilities of rupture and leakage are below the acceptance criterion of 10^{-6} for up to 80 years of operation. This shows that all components are very flaw-tolerant, and it implies that once the PSI examination is performed, no other follow-on ISI examinations are required for up to 80 years of operation in order to maintain plant safety.

Table 8-9
Probability of rupture (per year) and probability of leakage (per year) for base case
(PSI only)

Item No.	Path	P(Rupture) at 80 yrs.	P(Leakage) at			
			20 yrs.	40 yrs.	60 yrs.	80 yrs.
B3.130 (CE)	SGPNV-P1A(N)	1.25E-09	5.00E-09	2.50E-09	1.67E-09	1.25E-09
	SGPNV-P1C(N)	1.25E-09	5.00E-09	2.50E-09	1.67E-09	1.25E-09
B3.130 (B&W)	SGPNV-P2A(N)	1.25E-09	5.00E-09	2.50E-09	1.67E-09	1.25E-09
	SGPNV-P2C(N)	1.25E-09	5.00E-09	2.50E-09	1.67E-09	1.25E-09
B2.31	SGPTH-P4A	1.25E-09	5.00E-09	2.50E-09	1.67E-09	5.00E-09
B2.32	SGPTH-P4C	1.25E-09	5.00E-09	2.50E-09	1.67E-09	1.25E-09
B2.40						
C1.10	SGSSC-P9A	1.25E-09	5.00E-09	2.50E-09	1.67E-09	1.25E-09
	SGSSC-P9C	1.25E-09	5.00E-09	2.50E-09	1.67E-09	1.25E-09
C1.20	SGSHC-P11A	1.25E-09	5.00E-09	2.50E-09	1.67E-09	1.25E-09
	SGSHC-P11C	1.25E-09	5.00E-09	2.50E-09	1.67E-09	1.25E-09
C1.30	SGSTS-P12A	1.25E-09	5.00E-09	2.50E-09	1.67E-09	1.25E-09
	SGSTS-P12C	1.25E-09	5.00E-09	2.50E-09	1.67E-09	1.25E-09

Note: The limiting case is displayed in **red bold** text. For Paths SGPNV-P1A, SGPNV-P1C, SGPNV-P1A, and SGPNV-P2C, the results are shown for the (N)ozzle-side weld. The (S)hell-side weld results are not shown, nor are they limiting.

8.3.4.1.1 Effect of Various In-Service Inspection Scenarios

The limiting location, Path SGPTH-P4A, was chosen to determine the effects of the inspection scenarios listed in Table 8-4 on the probabilities of rupture and leakage. Table 8-10 presents the case in which PSI was performed followed by combinations of 10-year ISIs and/or 20- or 30-year ISIs.

Table 8-10
Probability of rupture (per year) and probability of leakage (per year) for 80 years for PSI
followed by combinations of 10-year ISIs and/or 20- or 30-year ISIs for Path SGPTH-P4A

ISI Scenario	Scenario No.	ISI at (Year)	Probability of Rupture (per Year)	Probability of Leakage (per Year)
PSI only	Base Case	0	1.25E-09	5.00E-09
PSI followed by 10-year inspections	1	0,10	1.25E-09	1.25E-09
	2	0,10,20	1.25E-09	1.25E-09
	3	0,10,20,30	1.25E-09	1.25E-09
PSI followed by 20-year inspections	4	0,20,40,60	1.25E-09	1.25E-09
PSI followed by 10-year inspections followed by 20-year inspections	5	0,10,30,50,70	1.25E-09	1.25E-09
	6	0,10,20,40,60	1.25E-09	1.25E-09
	7	0,10,20,30,50,70	1.25E-09	1.25E-09
PSI followed by 30-year inspections	8	0,30,60	1.25E-09	1.25E-09
PSI followed by 10-year inspections followed by 30-year inspections	9	0,10,40,70	1.25E-09	1.25E-09
	10	0,10,20,50	1.25E-09	1.25E-09
	11	0,10,20,30,60	1.25E-09	1.25E-09

As can be seen from Table 8-10, all inspection scenarios involving ISI result in improved probability of leakage values compared to the base case of PSI only. These results demonstrate the benefits of ISI.

8.3.4.2 Sensitivity Analyses

The purpose of performing sensitivity analyses is to identify the variables that have the most impact on the calculated probabilities (rupture or leakage). The Degree of Separation Method, as developed and documented in Reference [84], was used to rank the effect of input variables on output probabilities. The most limiting location, Path SGPTH-P4A, was chosen for this evaluation because it is the most limiting in terms of the probability of leakage. The inputs were the same as those used in the base case, except that the standard deviation of the fracture toughness was increased to 30 ksi√in. The results of the sensitivity analysis are provided in Table 8-11 in terms of probabilities of rupture and leakage.

Table 8-11
Results of sensitivity analysis for Path SGPTH-P4A

Variable	Importance Factor (%)	
	Probability of Leakage	Probability of Rupture
Fatigue crack growth rate coefficient	99.56	14.92
Crack depth	0.29	0.37
Crack length	0.06	0.02
Fatigue crack growth rate threshold	0.04	0.03
Fracture toughness	0.05	84.66

In this scenario, fracture toughness was the most dominant variable affecting the rupture probabilities. On the other hand, the FCG rate coefficient was the most dominant variable affecting the probability of leakage, while also having a relatively strong influence on the probability of rupture.

A sensitivity analysis was also performed in which a random multiplier was applied to stress. This scenario added six new variables to the five variables used in Table 8-11. The 11 variables and associated results of this sensitivity analysis are shown in Table 8-12.

Table 8-12
Results of sensitivity analysis with random stress multiplier for Path SGPTH-P4A

Variable	Importance Factor (%) for Probability of Leakage
FCG rate coefficient	84.23
Crack length	0.31
Crack depth	0.28
FCG rate threshold	0.01
Fracture toughness	2.32
Crack face pressure	0.5
Residual stress	2.52
Heatup/cooldown	5.57
Load increase (5%)	0.04
Load decrease (5%)	3.51
Trip	0.7

In this scenario, the FCG rate coefficient was the most dominant variable affecting the probability of leakage.

8.3.4.3 Sensitivity Studies

The sensitivity analyses identified only a few parameters that have significant influence on the probabilities of rupture and leakage; however, additional parameters were included for completeness. Sensitivity studies were performed on the following parameters:

- Fracture toughness (rupture and leakage)
- Stress (rupture and leakage)
- Initial crack depth (rupture and leakage)
- Number of flaws (rupture and leakage)
- Flaw density distribution (rupture)
- Crack size distribution (rupture)
- FCG (leakage)
- POD (rupture and leakage)
- Inspection schedule with two PODs (leakage)
- Number of realizations (rupture)
- Combination of key variables

Sensitivity to the probability of rupture, probability of leakage, or both were evaluated, where appropriate, for up to 80 years.

8.3.4.3.1 Sensitivity to Fracture Toughness

In the base case, the fracture toughness (K_{IC}) was considered normally distributed with a mean value of 200 ksi $\sqrt{\text{in.}}$ and a standard deviation of 5 ksi $\sqrt{\text{in.}}$. The probability of rupture was less than 10^{-8} per year at 80 years. The K_{IC} value was then lowered to determine at what value the acceptance criteria would be met. For this purpose, two mean values were considered (80 ksi $\sqrt{\text{in.}}$ and 100 ksi $\sqrt{\text{in.}}$) while keeping the standard deviation constant for two inspection scenarios. In the first scenario, the base case involving PSI only was considered; in the second case, an inspection scenario of PSI in addition to ISIs at 20, 40, and 60 years was evaluated. This latter case is comparable to the base case in the Reference [2] report and therefore provides a useful basis for comparison.

The rupture probabilities for the two cases are shown in Tables 8-13 and 8-14. The rupture probabilities increase with decreasing K_{IC} , as expected. It can be seen from Table 8-11 that with PSI only, the acceptance criteria are met at approximately 100 ksi $\sqrt{\text{in.}}$ (equal to half the mean value used in the base case), further demonstrating that the components are very flaw-tolerant. As can be seen from Table 8-13, below a fracture toughness of 100 ksi $\sqrt{\text{in.}}$, the probability of rupture increases (as demonstrated for the case involving 80 ksi $\sqrt{\text{in.}}$). Comparing Tables 8-13 and 8-14, it can be seen that, for the base case of PSI only and with the two mean fracture toughness values considered in the evaluation, a few locations were above the acceptance criterion; however, with the more realistic scenario of PSI in addition to ISI at 20, 40, and 60 years, all rupture probabilities met the acceptance criterion, even for a K_{IC} value as low as 80 ksi $\sqrt{\text{in.}}$. As covered previously, even at the minimum temperature of the evaluated transients,

the material of the SG vessel is on the upper shelf; therefore, the fracture toughness (K_{IC}) is at least 200 ksi√in. To address NRC concerns regarding the standard deviation on the fracture toughness in the BWRVIP-108 SER [4], a sensitivity study was performed using a standard deviation of 30 ksi√in. As can be seen from Tables 8-11 and 8-12, using a standard deviation of 30 ksi√in. and the base-case mean toughness of 200 ksi√in. did not change the results of the analysis.

The leakage probabilities were calculated for the two mean values of K_{IC} , and the results are provided in Tables 8-15 and 8-16 for the two cases analyzed. As can be seen in Tables 8-15 and 8-16, changing either K_{IC} or the standard deviation had no impact on the leakage probabilities in both cases. This result is consistent with the sensitivity analysis, where K_{IC} was not a significant parameter influencing leakage probabilities. Tables 8-15 and 8-16 also show that as rupture probabilities increase, leakage probabilities decrease; this is due to cracks rupturing instead of leaking due to the lower fracture toughness.

Table 8-13
Sensitivity of toughness on probability of rupture for 80 years (PSI only)

Item No.	Path	Probability of Rupture (per Year)			
		Base Case, $K_{IC} = 200$ ksi√in.	Base Case, $K_{IC} = 100$ ksi√in.	Base Case, $K_{IC} = 80$ ksi√in.	Base Case, $K_{IC} = 200$ SD = 30 ksi√in.
B3.130 (CE)	SGPNV-P1A(N)	1.25E-09	1.25E-09	3.00E-08	1.25E-09
	SGPNV-P1C(N)	1.25E-09	1.25E-09	1.25E-09	1.25E-09
B3.130 (B&W)	SGPNV-P2A(N)	1.25E-09	2.65E-07	2.27E-06	1.25E-09
	SGPNV-P2C(N)	1.25E-09	1.25E-09	1.25E-09	1.25E-09
B2.31	SGPTH-P4A	1.25E-09	5.01E-06	2.12E-04	3.75E-08
B2.32	SGPTH-P4C	1.25E-09	1.25E-09	1.25E-09	1.25E-09
B2.40					
C1.10	SGSSC-P9A	1.25E-09	1.25E-09	1.25E-09	1.25E-09
	SGSSC-P9C	1.25E-09	1.25E-09	2.50E-09	1.25E-09
C1.20	SGSHC-P11A	1.25E-09	1.25E-09	1.25E-09	1.25E-09
	SGSHC-P11C	1.25E-09	1.25E-09	1.25E-09	1.25E-09
C1.30	SGSTS-P12A	1.25E-09	1.25E-09	2.50E-09	1.25E-09
	SGSTS-P12C	1.25E-09	1.25E-09	1.25E-09	1.25E-09

Note: Changed values from the base case are shaded in yellow, and the limiting value is displayed in red bold text. For Paths SGPNV-P1A, SGPNV-P1C, SGPNV-P1A, and SGPNV-P2C, the results are shown for the (N)ozzle-side weld. The (S)hell-side weld results are not shown, nor are they limiting.

Table 8-14
Sensitivity of toughness on probability of rupture for 80 years (PSI + ISI at 20, 40, 60 years)

Item No.	Path	Probability of Rupture (per Year)			
		PSI, 20,40,60 K _{IC} = 200 ksi√in.	PSI, 20,40,60 K _{IC} = 100 ksi√in.	PSI, 20,40,60 K _{IC} = 80 ksi√in.	PSI, 20,40,60 K _{IC} = 200 SD = 30 ksi√in.
B3.130 (CE)	SGPNV-P1A(N)	1.25E-09	1.25E-09	1.25E-09	1.25E-09
	SGPNV-P1C(N)	1.25E-09	1.25E-09	1.25E-09	1.25E-09
B3.130 (B&W)	SGPNV-P2A(N)	1.25E-09	1.25E-09	2.50E-09	1.25E-09
	SGPNV-P2C(N)	1.25E-09	1.25E-09	1.25E-09	1.25E-09
B2.31 B2.32 B2.40	SGPTH-P4A	1.25E-09	3.75E-09	1.50E-07	2.50E-09
	SGPTH-P4C	1.25E-09	1.25E-09	1.25E-09	1.25E-09
C1.10	SGSSC-P9A	1.25E-09	1.25E-09	1.25E-09	1.25E-09
	SGSSC-P9C	1.25E-09	1.25E-09	1.25E-09	1.25E-09
C1.20	SGSHC-P11A	1.25E-09	1.25E-09	1.25E-09	1.25E-09
	SGSHC-P11C	1.25E-09	1.25E-09	1.25E-09	1.25E-09
C1.30	SGSTS-P12A	1.25E-09	1.25E-09	1.25E-09	1.25E-09
	SGSTS-P12C	1.25E-09	1.25E-09	1.25E-09	1.25E-09

Note: Changed values from the base case are shaded in **yellow**, and the limiting value is displayed in **red bold** text. For Paths SGPNV-P1A, SGPNV-P1C, SGPNV-P1A, and SGPNV-P2C, the results are shown for the (N)ozzle-side weld. The (S)hell-side weld results are not shown, nor are they limiting.

Table 8-15
Sensitivity of toughness on probability of leakage for 80 years (PSI only)

Item No.	Path	Probability of Leakage (per Year)			
		Base Case, $K_{IC} = 200 \text{ ksi}\sqrt{\text{in.}}$	Base Case, $K_{IC} = 100 \text{ ksi}\sqrt{\text{in.}}$	Base Case, $K_{IC} = 80 \text{ ksi}\sqrt{\text{in.}}$	Base Case, $K_{IC} = 200$ $SD = 30 \text{ ksi}\sqrt{\text{in.}}$
B3.130 (CE)	SGPNV-P1A(N)	1.25E-09	1.25E-09	1.25E-09	1.25E-09
	SGPNV-P1C(N)	1.25E-09	1.25E-09	1.25E-09	1.25E-09
B3.130 (B&W)	SGPNV-P2A(N)	1.25E-09	1.25E-09	1.25E-09	1.25E-09
	SGPNV-P2C(N)	1.25E-09	1.25E-09	1.25E-09	1.25E-09
B2.31 B2.32 B2.40	SGPTH-P4A	5.00E-09	1.25E-09	1.25E-09	5.00E-09
	SGPTH-P4C	1.25E-09	1.25E-09	1.25E-09	1.25E-09
C1.10	SGSSC-P9A	1.25E-09	1.25E-09	1.25E-09	1.25E-09
	SGSSC-P9C	1.25E-09	1.25E-09	1.25E-09	1.25E-09
C1.20	SGSHC-P11A	1.25E-09	1.25E-09	1.25E-09	1.25E-09
	SGSHC-P11C	1.25E-09	1.25E-09	1.25E-09	1.25E-09
C1.30	SGSTS-P12A	1.25E-09	1.25E-09	1.25E-09	1.25E-09
	SGSTS-P12C	1.25E-09	1.25E-09	1.25E-09	1.25E-09

Note: Changed values from the base case are shaded in yellow, and the limiting value is displayed in red bold text. For Paths SGPNV-P1A, SGPNV-P1C, SGPNV-P1A, and SGPNV-P2C, the results are shown for the (N)ozzle-side weld. The (S)hell-side weld results are not shown, nor are they limiting.

Table 8-16
Sensitivity of toughness on probability of leakage for 80 years (PSI + ISI at 20, 40, 60 years)

Item No.	Path	Probability of Leakage (per Year)			
		PSI, 20,40,60 K _{IC} = 200 ksi√in.	PSI, 20,40,60 K _{IC} = 100 ksi√in.	PSI, 20,40,60 K _{IC} = 80 ksi√in.	PSI, 20,40,60 K _{IC} = 200 SD = 30 ksi√in.
B3.130 (CE)	SGPNV-P1A(N)	1.25E-09	1.25E-09	1.25E-09	1.25E-09
	SGPNV-P1C(N)	1.25E-09	1.25E-09	1.25E-09	1.25E-09
B3.130 (B&W)	SGPNV-P2A(N)	1.25E-09	1.25E-09	1.25E-09	1.25E-09
	SGPNV-P2C(N)	1.25E-09	1.25E-09	1.25E-09	1.25E-09
B2.31 B2.32 B2.40	SGPTH-P4A	1.25E-09	1.25E-09	1.25E-09	1.25E-09
	SGPTH-P4C	1.25E-09	1.25E-09	1.25E-09	1.25E-09
C1.10	SGSSC-P9A	1.25E-09	1.25E-09	1.25E-09	1.25E-09
	SGSSC-P9C	1.25E-09	1.25E-09	1.25E-09	1.25E-09
C1.20	SGSHC-P11A	1.25E-09	1.25E-09	1.25E-09	1.25E-09
	SGSHC-P11C	1.25E-09	1.25E-09	1.25E-09	1.25E-09
C1.30	SGSTS-P12A	1.25E-09	1.25E-09	1.25E-09	1.25E-09
	SGSTS-P12C	1.25E-09	1.25E-09	1.25E-09	1.25E-09

Note: For Paths SGPNV-P1A, SGPNV-P1C, SGPNV-P1A, and SGPNV-P2C, the results are shown for the (N)ozzle-side weld. The (S)hell-side weld results are not shown, nor are they limiting.

8.3.4.3.2 Sensitivity to Stresses

To study the effect of cyclic stresses on failure probabilities, cyclic stresses were factored to determine what stress multipliers/factors would result in failure probabilities approaching the acceptance criterion. These stress multipliers account for the effect of geometrical variations (in terms of R/t ratios) covered in Section 4 of this report. Based on the information provided in Table 4-4, the R/t ratios for the various components can vary by as much as 33.3%, which suggests that stresses can also vary up to 33.3%. Once again, two inspection scenarios were considered—PSI only and PSI in addition to ISI at 20, 40, and 60 years. The results are presented in Tables 8-16 and 8-18 for the former case and in Tables 8-19 and 8-20 for the latter case. As can be seen in Table 8-17, for the PSI-only case, the results indicate that a stress multiplier of approximately 1.25 is required for the limiting location (Path SGPTH-P4A) to reach the acceptance criterion. As shown in Table 8-19, for the more realistic scenario of PSI in addition to ISI at 20, 40, and 60 years, a larger stress multiplier of 1.9 is required for the limiting location to reach the acceptance criterion. Based on these multipliers, an increase in the applied stress can be accommodated; under typical inspection scenarios, as much as a 90% increase in stress can be accommodated compared to a possible variation of 33% based on the varying R/t ratio.

Table 8-17
Sensitivity of stress on probability of rupture for 80 years (PSI only)

Item No.	Path	Probability of Rupture (per Year)	
		Base Case Stress Multiplier = 1	Base Case Stress Multiplier = 1.25
B3.130 (CE)	SGPNV-P1A(N)	1.25E-09	1.25E-09
	SGPNV-P1C(N)	1.25E-09	1.25E-09
B3.130 (B&W)	SGPNV-P2A(N)	1.25E-09	2.14E-07
	SGPNV-P2C(N)	1.25E-09	1.25E-09
B2.31	SGPTH-P4A	1.25E-09	4.08E-07
B2.32	SGPTH-P4C	1.25E-09	1.25E-09
B2.40			
C1.10	SGSSC-P9A	1.25E-09	1.25E-09
	SGSSC-P9C	1.25E-09	1.25E-09
C1.20	SGSHC-P11A	1.25E-09	1.25E-09
	SGSHC-P11C	1.25E-09	1.25E-09
C1.30	SGSTS-P12A	1.25E-09	1.25E-09
	SGSTS-P12C	1.25E-09	1.25E-09

Note: Changed values from the base case are shaded in yellow, and the limiting value is displayed in red bold text. For Paths SGPNV-P1A, SGPNV-P1C, SGPNV-P1A, and SGPNV-P2C, the results are shown for the (N)ozzle-side weld. The (S)hell-side weld results are not shown, nor are they limiting.

Table 8-18
Sensitivity of stress on probability of leakage for 80 years (PSI only)

Item No.	Path	Probability of Leak (per Year)	
		Base Case Stress Multiplier = 1	Base Case Stress Multiplier = 1.25
B3.130 (CE)	SGPNV-P1A(N)	1.25E-09	1.38E-08
	SGPNV-P1C(N)	1.25E-09	1.25E-09
B3.130 (B&W)	SGPNV-P2A(N)	1.25E-09	3.75E-09
	SGPNV-P2C(N)	1.25E-09	1.25E-09
B2.31	SGPTH-P4A	5.00E-09	4.13E-08
B2.32			
B2.40	SGPTH-P4C	1.25E-09	1.25E-09
C1.10	SGSSC-P9A	1.25E-09	1.25E-09
	SGSSC-P9C	1.25E-09	1.25E-09
C1.20	SGSHC-P11A	1.25E-09	1.25E-09
	SGSHC-P11C	1.25E-09	1.25E-09
C1.30	SGSTS-P12A	1.25E-09	2.50E-09
	SGSTS-P12C	1.25E-09	1.25E-09

Note: Changed values from the base case are shaded in yellow, and the limiting value is displayed in red bold text. For Paths SGPNV-P1A, SGPNV-P1C, SGPNV-P1A, and SGPNV-P2C, the results are shown for the (N)ozzle-side weld. The (S)hell-side weld results are not shown, nor are they limiting.

Table 8-19
Sensitivity of stress on probability of rupture for 80 years (PSI + ISI at 20, 40, 60 years)

Item No.	Path	Probability of Rupture (per Year)	
		PSI, 20, 40, 60 Stress Multiplier = 1	PSI, 20, 40, 60 Stress Multiplier = 1.90
B3.130 (CE)	SGPNV-P1A(N)	1.25E-09	2.50E-09
	SGPNV-P1C(N)	1.25E-09	1.25E-09
B3.130 (B&W)	SGPNV-P2A(N)	1.25E-09	4.50E-08
	SGPNV-P2C(N)	1.25E-09	1.25E-09
B2.31 B2.32 B2.40	SGPTH-P4A	1.25E-09	7.33E-07
	SGPTH-P4C	1.25E-09	1.25E-09
C1.10	SGSSC-P9A	1.25E-09	1.25E-09
	SGSSC-P9C	1.25E-09	1.25E-09
C1.20	SGSHC-P11A	1.25E-09	1.25E-09
	SGSHC-P11C	1.25E-09	1.25E-09
C1.30	SGSTS-P12A	1.25E-09	1.25E-09
	SGSTS-P12C	1.25E-09	1.25E-09

Note: Changed values from the base case are shaded in yellow, and the limiting value is displayed in red bold text. For Paths SGPNV-P1A, SGPNV-P1C, SGPNV-P1A, and SGPNV-P2C, the results are shown for the (N)ozzle-side weld. The (S)hell-side weld results are not shown, nor are they limiting.

Table 8-20
Sensitivity of stress on probability of leakage for 80 years (PSI + ISI at 20, 40, 60 years)

Item No.	Path	Probability of Leak (per Year)	
		PSI, 20, 40, 60 Stress Multiplier = 1	PSI, 20, 40, 60 Stress Multiplier = 1.90
B3.130 (CE)	SGPNV-P1A(N)	1.25E-09	1.25E-09
	SGPNV-P1C(N)	1.25E-09	1.25E-09
B3.130 (B&W)	SGPNV-P2A(N)	1.25E-09	1.25E-09
	SGPNV-P2C(N)	1.25E-09	1.25E-09
B2.31	SGPTH-P4A	5.00E-09	1.25E-09
B2.32			
B2.40	SGPTH-P4C	1.25E-09	1.25E-09
C1.10	SGSSC-P9A	1.25E-09	1.25E-09
	SGSSC-P9C	1.25E-09	1.25E-09
C1.20	SGSHC-P11A	1.25E-09	1.25E-09
	SGSHC-P11C	1.25E-09	1.25E-09
C1.30	SGSTS-P12A	1.25E-09	1.25E-09
	SGSTS-P12C	1.25E-09	1.25E-09

Note: Changed values from the base case are shaded in yellow, and the limiting value is displayed in red bold text. For Paths SGPNV-P1A, SGPNV-P1C, SGPNV-P1A, and SGPNV-P2C, the results are shown for the (N)ozzle-side weld. The (S)hell-side weld results are not shown, nor are they limiting.

8.3.4.3.3 Sensitivity to Initial Crack Depth Distribution

Starting with the base case inputs from Table 8-6, a sensitivity study was performed in which the crack depth distribution was replaced by a constant value equal to 5.2% of the wall thickness (corresponding to the ASME Code, Section XI flaw acceptance standard for these components) and an aspect ratio of 1.0, representing a semicircular crack shape. The results are shown in Tables 8-21 and 8-22 for the probabilities of rupture and leakage, respectively. The probability of rupture was not affected; however, the leakage probabilities decreased for the limiting case.

Table 8-21
Sensitivity of initial crack size on probability of rupture for 80 years

Item No.	Path	Probability of Rupture (per Year)	
		Base Case PVRUF	Base Case ASME IWB-3500 Acceptance Flaw Size (0.052t, c/a=1)
B3.130 (CE)	SGPNV-P1A(N)	1.25E-09	1.25E-09
	SGPNV-P1C(N)	1.25E-09	1.25E-09
B3.130 (B&W)	SGPNV-P2A(N)	1.25E-09	1.25E-09
	SGPNV-P2C(N)	1.25E-09	1.25E-09
B2.31 B2.32 B2.40	SGPTH-P4A	1.25E-09	1.25E-09
	SGPTH-P4C	1.25E-09	1.25E-09
C1.10	SGSSC-P9A	1.25E-09	1.25E-09
	SGSSC-P9C	1.25E-09	1.25E-09
C1.20	SGSHC-P11A	1.25E-09	1.25E-09
	SGSHC-P11C	1.25E-09	1.25E-09
C1.30	SGSTS-P12A	1.25E-09	1.25E-09
	SGSTS-P12C	1.25E-09	1.25E-09

Note: For Paths SGPNV-P1A, SGPNV-P1C, SGPNV-P1A, and SGPNV-P2C, the results are shown for the (N)ozzle-side weld. The (S)hell-side weld results are not shown, nor are they limiting.

Table 8-22
Sensitivity of initial crack size on probability of leakage for 80 years

Item No.	Path	Probability of Leakage (per Year)	
		Base Case PVRUF	Base Case ASME IWB-3500 Acceptance Flaw Size (0.052t, c/a=1)
B3.130 (CE)	SGPNV-P1A(N)	1.25E-09	1.25E-09
	SGPNV-P1C(N)	1.25E-09	1.25E-09
B3.130 (B&W)	SGPNV-P2A(N)	1.25E-09	1.25E-09
	SGPNV-P2C(N)	1.25E-09	1.25E-09
B2.31	SGPTH-P4A	5.00E-09	1.25E-09
B2.32			
B2.40	SGPTH-P4C	1.25E-09	1.25E-09
C1.10	SGSSC-P9A	1.25E-09	1.25E-09
	SGSSC-P9C	1.25E-09	1.25E-09
C1.20	SGSHC-P11A	1.25E-09	1.25E-09
	SGSHC-P11C	1.25E-09	1.25E-09
C1.30	SGSTS-P12A	1.25E-09	1.25E-09
	SGSTS-P12C	1.25E-09	1.25E-09

Note: Changed values from the base case are shaded in yellow, and the limiting value is displayed in red bold text. For Paths SGPNV-P1A, SGPNV-P1C, SGPNV-P1A, and SGPNV-P2C, the results are shown for the (N)ozzle-side weld. The (S)hell-side weld results are not shown, nor are they limiting.

8.2.4.3.4 Sensitivity to Number of Flaws

The sensitivity to the number of flaws was also investigated. In the base case, the number of flaws was assumed to be 1.0 per weld, consistent with that used in BWRVIP-108 [3]. The results of the sensitivity study are presented in Tables 8-23 and 8-24. From the tables, it can be seen that by increasing the number of flaws to 5.0, the probabilities of rupture and leakage increased marginally.

Table 8-23
Sensitivity of number of flaws on probability of rupture for 80 years

Item No.	Path	Probability of Rupture (per Year)	
		Base Case Number of Flaws = 1	Base Case Number of Flaws = 5
B3.130 (CE)	SGPNV-P1A(N)	1.25E-09	1.25E-09
	SGPNV-P1C(N)	1.25E-09	1.25E-09
B3.130 (B&W)	SGPNV-P2A(N)	1.25E-09	1.25E-09
	SGPNV-P2C(N)	1.25E-09	1.25E-09
B2.31 B2.32 B2.40	SGPTH-P4A	1.25E-09	1.25E-09
	SGPTH-P4C	1.25E-09	1.25E-09
C1.10	SGSSC-P9A	1.25E-09	1.25E-09
	SGSSC-P9C	1.25E-09	1.25E-09
C1.20	SGSHC-P11A	1.25E-09	1.25E-09
	SGSHC-P11C	1.25E-09	1.25E-09
C1.30	SGSTS-P12A	1.25E-09	1.25E-09
	SGSTS-P12C	1.25E-09	1.25E-09

Note: For Paths SGPNV-P1A, SGPNV-P1C, SGPNV-P1A, and SGPNV-P2C, the results are shown for the (N)ozzle-side weld. The (S)hell-side weld results are not shown, nor are they limiting.

Table 8-24
Sensitivity of number of flaws on probability of leakage for 80 years

Item No.	Path	Probability of Leakage (per Year)	
		Base Case Number of Flaws = 1	Base Case Number of Flaws = 5
B3.130 (CE)	SGPNV-P1A(N)	1.25E-09	1.25E-09
	SGPNV-P1C(N)	1.25E-09	1.25E-09
B3.130 (B&W)	SGPNV-P2A(N)	1.25E-09	2.50E-09
	SGPNV-P2C(N)	1.25E-09	1.25E-09
B2.31	SGPTH-P4A	5.00E-09	7.50E-09
B2.32			
B2.40	SGPTH-P4C	1.25E-09	1.25E-09
C1.10	SGSSC-P9A	1.25E-09	1.25E-09
	SGSSC-P9C	1.25E-09	1.25E-09
C1.20	SGSHC-P11A	1.25E-09	1.25E-09
	SGSHC-P11C	1.25E-09	1.25E-09
C1.30	SGSTS-P12A	1.25E-09	2.50E-09
	SGSTS-P12C	1.25E-09	1.25E-09

Note: Changed values from the base case are shaded in yellow, and the limiting value is displayed in red bold text. For Paths SGPNV-P1A, SGPNV-P1C, SGPNV-P1A, and SGPNV-P2C, the results are shown for the (N)ozzle-side weld. The (S)hell-side weld results are not shown, nor are they limiting.

8.3.4.3.5 Sensitivity to the Distribution of Number of Flaws

The sensitivity to the distribution of the number of flaws at a weld location was also investigated by replacing the constant distribution of flaws in the base case with a Poisson distribution, assuming a single flaw in each case. The results are shown in Table 8-25. A multiplier of 1.25 was applied to all stresses, and the PSI-only scenario was considered. In this case, only the probability of rupture was considered because it is the limiting condition. Table 8-23 shows that the change in the distribution of the number of flaws has only a slight effect on the probability of rupture.

Table 8-25
Sensitivity to the distribution of number of flaws on probability of rupture (Path SGPTH-P4A)

No. of Flaws	Probability of Rupture (per Year) (Stress Multiplier = 1.25)
1 flaw, constant	4.08E-07
1 flaw, Poisson distributed	3.61E-07

8.3.4.3.6 Sensitivity to Crack Size Distribution

In the base case, the PVRUF crack size distribution was used because it was the distribution recommended by the NRC in its review of BWRVIP-05 and BWRVIP-108. Two other distributions were investigated for their effect on the probability of rupture per year: the Marshall distribution and a distribution derived based on data from NUREG/CR-6817 [72, 73]. The results of the evaluation are shown in Table 8-26; they indicate that the PVRUF distribution is more conservative than either the NUREG/CR-6817 or Marshall distributions. A multiplier of 1.25 was applied to all stresses.

Table 8-26
Sensitivity of crack size distribution on probability of rupture (Path SGPTH-P4A) for 80 years

Flaw Distribution	Probability of Rupture (per Year) (Stress Multiplier = 1.25)
PVRUF	4.08E-07
Marshall	3.24E-07
NUREG/CR-6817	3.94E-07

8.3.4.3.7 Sensitivity to Crack Growth Rate

The sensitivity to crack growth rate was performed by replacing the FCG law used in the base case with the flaw growth distribution used in BWRVIP-108 [3]. In BWRVIP-108, the crack growth law was derived from data in Reference [82] at a conservative R-ratio of 0.7. This FCG law is compared to the ASME Code, Section XI FCG curve in Figure 8-8. The results are presented in Table 8-27 and show that the probability of leakage is higher for the BWRVIP-108 model compared to the ASME Code, Section XI, Appendix A, Paragraph A-4300 model used in the base case. As shown in Table 8-27, there is a difference of two orders of magnitude between the two cases. This is because Path SGPTH-P4A has a high negative K_{min} value, which results in a high crack growth rate from the BWRVIP-108 model (which considers only $R = 0.7$). Nevertheless, the ASME Code, Section XI FCG law is considered more realistic because it considers all possible R ratios.

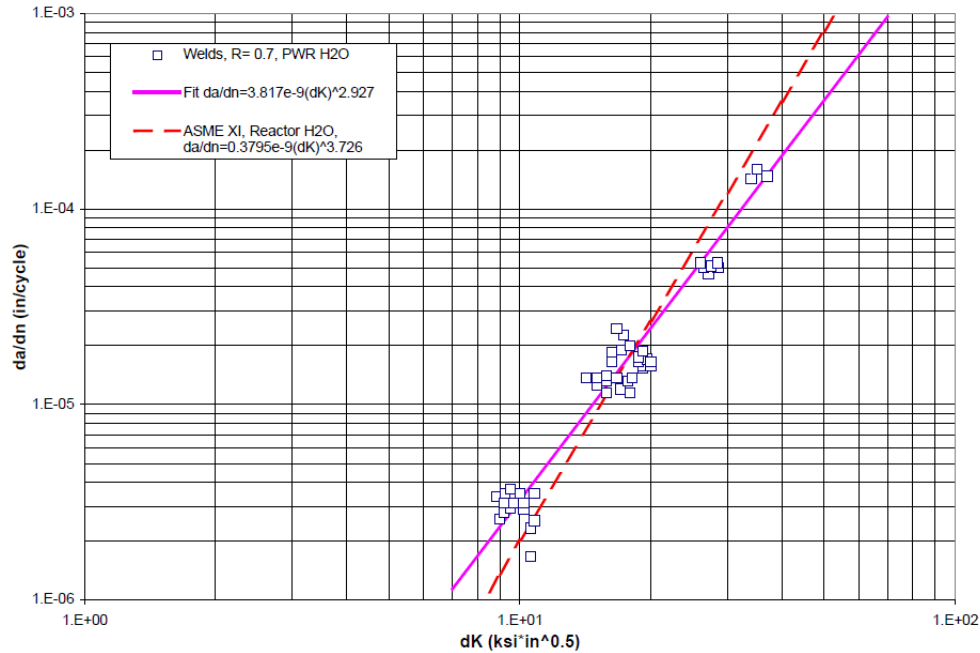


Figure 8-8
Curve fit for FCG at R-ratio of 0.7 from BWRVIP-108 and comparison to the ASME Code, Section XI FCG law [3]

Table 8-27
Sensitivity to crack growth rate on probability of leakage (Path SGPTH-P4A) for 80 years

Distribution	Probability of Leakage per Year
ASME Code Paragraph A-4300	5.00E-09
BWRVIP-108	4.36E-07

8.3.4.3.8 Sensitivity to POD Curves

To evaluate the effect of the POD curve on leakage probabilities, the BWRVIP-108 POD curve used in the base case (see Figure 8-2) was replaced with the POD curve used in the development of ASME Code, Section XI, Appendix L (see Figure 8-3). These two POD curves are compared in Figure 8-9. The probabilities of rupture and leakage for the two PODs are shown in Tables 8-28 and 8-29. Tables 8-28 and 8-29 show only slight variations between the two cases, with the probability of leakage slightly lower in the limiting case when the Appendix L POD curve is used.

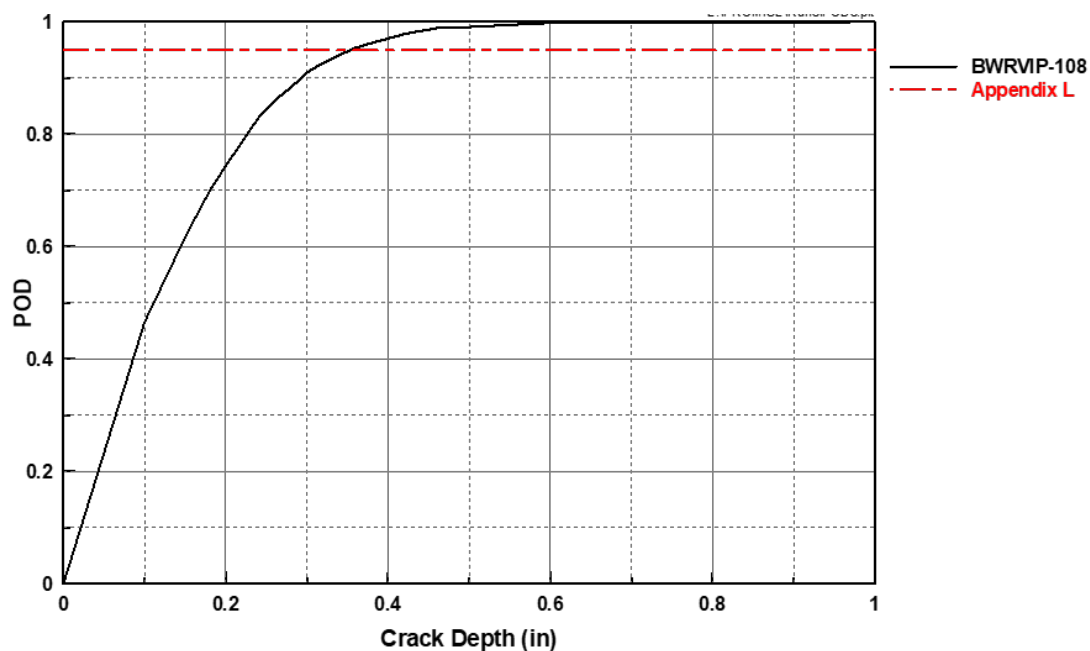


Figure 8-9
POD curves for sensitivity study

Table 8-28
Sensitivity of POD on probability of rupture for 80 years

Item No.	Case Identification	Probability of Rupture (per Year)	
		Base Case, BWRVIP-108 POD Curve	Base Case, Appendix L POD Curve
B3.130 (CE)	SGPNV-P1A(N)	1.25E-09	1.25E-09
	SGPNV-P1C(N)	1.25E-09	1.25E-09
B3.130 (B&W)	SGPNV-P2A(N)	1.25E-09	1.25E-09
	SGPNV-P2C(N)	1.25E-09	1.25E-09
B2.31	SGPTH-P4A	1.25E-09	1.25E-09
B2.32		1.25E-09	1.25E-09
B2.40		1.25E-09	1.25E-09
C1.10	SGSSC-P9A	1.25E-09	1.25E-09
	SGSSC-P9C	1.25E-09	1.25E-09
C1.20	SGSHC-P11A	1.25E-09	1.25E-09
	SGSHC-P11C	1.25E-09	1.25E-09
C1.30	SGSTS-P12A	1.25E-09	1.25E-09
	SGSTS-P12C	1.25E-09	1.25E-09

Note: For Paths SGPNV-P1A, SGPNV-P1C, SGPNV-P1A, and SGPNV-P2C, the results are shown for the (N)ozzle-side weld. The (S)hell-side weld results are not shown, nor are they limiting.

Table 8-29
Sensitivity of POD on probability of leakage for 80 years

Item No.	Case Identification	Probability of Leakage (per Year)	
		Base Case, BWRVIP-108 POD Curve	Base Case, Appendix L POD Curve
B3.130 (CE)	SGPNV-P1A(N)	1.25E-09	1.25E-09
	SGPNV-P1C(N)	1.25E-09	1.25E-09
B3.130 (B&W)	SGPNV-P2A(N)	1.25E-09	1.25E-09
	SGPNV-P2C(N)	1.25E-09	1.25E-09
B2.31	SGPTH-P4A	5.00E-09	1.25E-09
B2.32			
B2.40	SGPTH-P4C	1.25E-09	1.25E-09
C1.10	SGSSC-P9A	1.25E-09	1.25E-09
	SGSSC-P9C	1.25E-09	1.25E-09
C1.20	SGSHC-P11A	1.25E-09	1.25E-09
	SGSHC-P11C	1.25E-09	1.25E-09
C1.30	SGSTS-P12A	1.25E-09	1.25E-09
	SGSTS-P12C	1.25E-09	1.25E-09

Note: Changed values from the base case are shaded in yellow, and the limiting value is displayed in red bold text. For Paths SGPNV-P1A, SGPNV-P1C, SGPNV-P1A, and SGPNV-P2C, the results are shown for the (N)ozzle-side weld. The (S)hell-side weld results are not shown, nor are they limiting.

8.3.4.3.9 Sensitivity to Inspection Schedules Using Two Different PODs

Sensitivity studies were performed to determine the effect of several of the inspection schedules listed in Table 8-4. The evaluation was performed using the limiting component in terms of leakage (Path SGPTH-P4A), considering both the base-case POD curve and the Appendix L POD curve. Because the base-case Path SGPTH-P4A leak probabilities are very low, a stress multiplier of 1.25 with a standard deviation of 0.2 were used. These scenarios, along with the results for both POD curves, are shown in Table 8-30. The results show that the base-case (BWRVIP-108) POD curve yields conservative results when compared to the Appendix L POD curve for most inspection scenarios. The results for both POD curves are plotted as a function of time in Figure 8-10 for the case of inspections at 0 and 10 years, showing that the rupture probabilities for the base case POD are higher.

Table 8-30
Sensitivity of inspection schedule on probability of rupture (Path SGPTH-P4A) for 80 years

Probability of Rupture (per Year)		
Inspection at (years)	BWRVIP-108 POD (Stress Multiplier = 1.25, SD = 0.2)	Appendix L POD (Stress Multiplier = 1.25, SD = 0.2)
0	1.73E-05	1.54E-06
0,10	8.59E-07	7.13E-08
0, 10, 20	5.00E-09	1.25E-09
0, 10, 20, 30	1.25E-09	1.25E-09
0, 20, 40, 60	2.50E-09	3.75E-09
0, 10, 30, 50, 70	1.25E-09	1.25E-09
0, 10, 20, 40, 60	1.25E-09	1.25E-09
0, 10, 20, 30, 50, 70	1.25E-09	1.25E-09

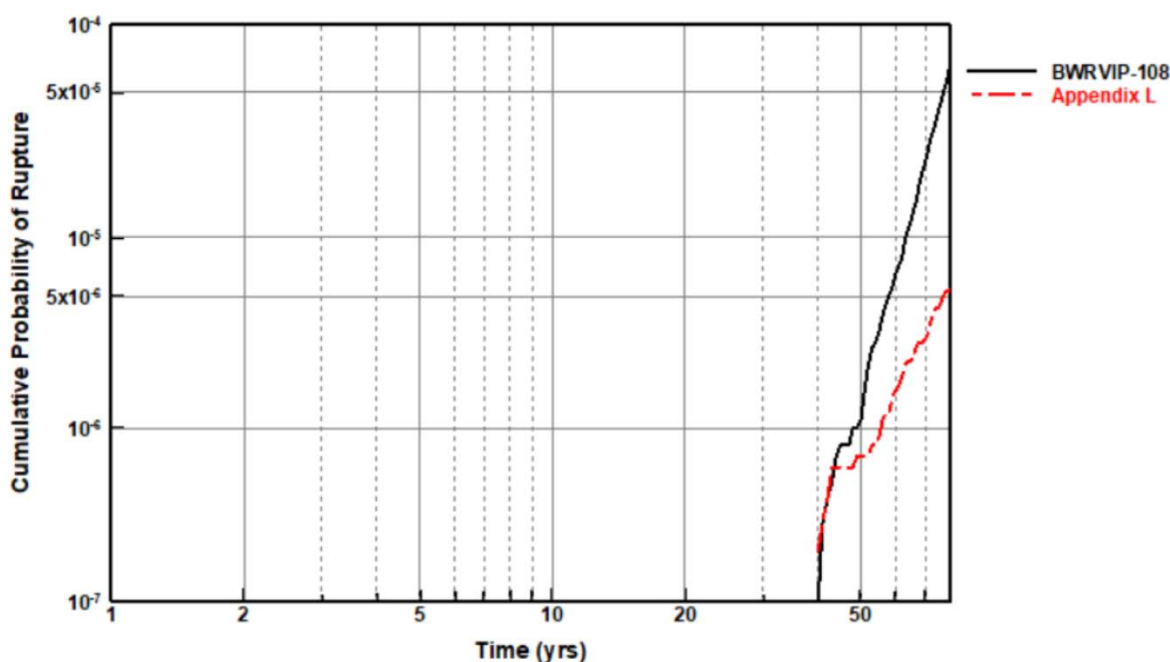


Figure 8-10
Sensitivity of inspection schedule and POD curves on probability of rupture

8.3.4.3.10 Sensitivity to Number of Realizations

A sensitivity study was performed to determine the effect of the number of realizations used in the evaluations. Path SGPTH-P4A with a stress multiplier of 1.25 was selected for this study. As shown in Table 8-31, with 10^7 and 10^8 aleatory realizations, both cases resulted in approximately the same rupture probability.

Table 8-31
Convergence test for Path SGPTH-P4A

No. of Aleatory Realizations	Probability of Rupture (per Year)
10^7	4.08E-7
10^8	4.17E-7

8.3.4.3.11 Sensitivity Study to Determine Combined Effect of Important Parameters

Based on the sensitivity studies performed in the previous sections, the most important input parameters are fracture toughness and stress. A sensitivity study was performed to determine the combined effect of these two variables. A mean fracture toughness of 200 ksi√in. with a conservative standard deviation of 30 ksi√in. and a stress multiplier of 1.33 (which corresponds to the maximum R/t ratio difference described in Section 4.3) were used. The analysis was performed assuming a realistic inspection scenario of PSI followed by two 10-year ISIs followed by two 20-year ISIs. The results of this case are shown in Table 8-32. As Table 8-32 shows, once a single 10-year ISI has been performed, prior to changing to 20-year ISI intervals, the acceptance criterion is met at all locations.

Table 8-32
Sensitivity to combined effects of fracture toughness and stress for 80 years

Item No.	Case Identification	Probability of Rupture (per Year)	
		Base Case	PSI+10+20+40+60 K _{IC} = 200 ksi√in., SD = 30 ksi√in. Stress Multiplier = 1.33
B3.130 (CE)	SGPNV-P1A(N)	1.25E-09	1.25E-09
	SGPNV-P1C(N)	1.25E-09	1.25E-09
B3.130 (B&W)	SGPNV-P2A(N)	1.25E-09	1.25E-09
	SGPNV-P2C(N)	1.25E-09	1.25E-09
B2.31	SGPTH-P4A	5.00E-09	1.88E-08
B2.32	SGPTH-P4C	1.25E-09	1.25E-09
B2.40			
C1.10	SGSSC-P9A	1.25E-09	1.25E-09
	SGSSC-P9C	1.25E-09	1.25E-09
C1.20	SGSHC-P11A	1.25E-09	1.25E-09
	SGSHC-P11C	1.25E-09	1.25E-09
C1.30	SGSTS-P12A	1.25E-09	1.25E-09
	SGSTS-P12C	1.25E-09	1.25E-09

Note: Changed values from the base case are shaded in yellow, and the limiting value is displayed in red bold text. For Paths SGPNV-P1A, SGPNV-P1C, SGPNV-P1A, and SGPNV-P2C, the results are shown for the (N)ozzle-side weld. The (S)hell-side weld results are not shown, nor are they limiting.

8.3.5 Inspection Coverage

The evaluations presented so far assumed that 100% of the inspection volume specified in ASME Code, Section XI for the SG primary- and secondary-side components could be achieved during the examinations assumed in each of the inspection scenarios. However, as explained in Section 4.4, there have been instances in which 100% coverage of the components has not been achieved during ISIs for some plants because of access restrictions and limitations. These components did receive 100% coverage during PSI through a combination of the required Section III fabrication and Section XI PSI examinations. Therefore, all components considered in this evaluation, at a minimum, were assumed to have 100% coverage during their PSI examinations, followed by at least one partial-coverage ISI, depending on the length of service of SGs/RSGs.

As covered in Section 8.3.4.1, by performing complete, 100% coverage PSI examinations, no other inspections are required for the evaluated components for 80 years to maintain safe plant operation due to the relatively low failure probabilities for rupture and leakage. Therefore, any additional ISI examinations (including limited inspections resulting from partial coverage) after the PSI examination reduces the already low probability of rupture and leakage for these components. As such, the results of the evaluations presented herein can also be applied to components with partial coverage.

A sensitivity study was performed using the combination scenario considered in Section 8.3.4.3.11 but assuming an inspection coverage of 50%. The results of this sensitivity study are presented in Table 8-33. As can be seen from Table 8-33, even with 50% coverage, the acceptance criterion is met for all locations except for the most limiting Path SGPTH-P4A, where the acceptance criterion for rupture is exceeded only slightly for this worst-case scenario.

Table 8-33
Sensitivity to combined effects of fracture toughness, stress, and 50% coverage for 80 years

Item No.	Case Identification	Probability of Rupture (per Year)	
		Base Case	PSI+10+20+40+60 K _{IC} = 200 ksi√in., SD = 30 ksi√in. Stress Multiplier = 1.33
B3.130 (CE)	SGPNV-P1A(N)	1.25E-09	4.63E-08
	SGPNV-P1C(N)	1.25E-09	1.25E-09
B3.130 (B&W)	SGPNV-P2A(N)	1.25E-09	1.24E-06
	SGPNV-P2C(N)	1.25E-09	1.25E-09
B2.31	SGPTH-P4A	5.00E-09	6.46E-06
B2.32			
B2.40	SGPTH-P4C	1.25E-09	1.25E-09
C1.10	SGSSC-P9A	1.25E-09	1.25E-09
	SGSSC-P9C	1.25E-09	1.25E-09
C1.20	SGSHC-P11A	1.25E-09	1.25E-09
	SGSHC-P11C	1.25E-09	1.25E-09
C1.30	SGSTS-P12A	1.25E-09	1.25E-09
	SGSTS-P12C	1.25E-09	1.25E-09

Note: Changed values from the base case are shaded in yellow, and the limiting value is displayed in red bold text. For Paths SGPNV-P1A, SGPNV-P1C, SGPNV-P1A, and SGPNV-P2C, the results are shown for the (N)ozzle-side weld. The (S)hell-side weld results are not shown, nor are they limiting.

8.3.6 Summary of Sensitivity Studies

The sensitivity studies performed in the previous sections show that probabilities of rupture and leakage are not significantly affected by using alternative distributions for the input variables. The key variables that affect the outcome of the analysis (fracture toughness and stress) were combined with realistic inspection scenarios, and it was concluded that the acceptance criterion for probability of rupture and leakage are still met. The results of several key sensitivity studies are summarized in Figure 8-11.

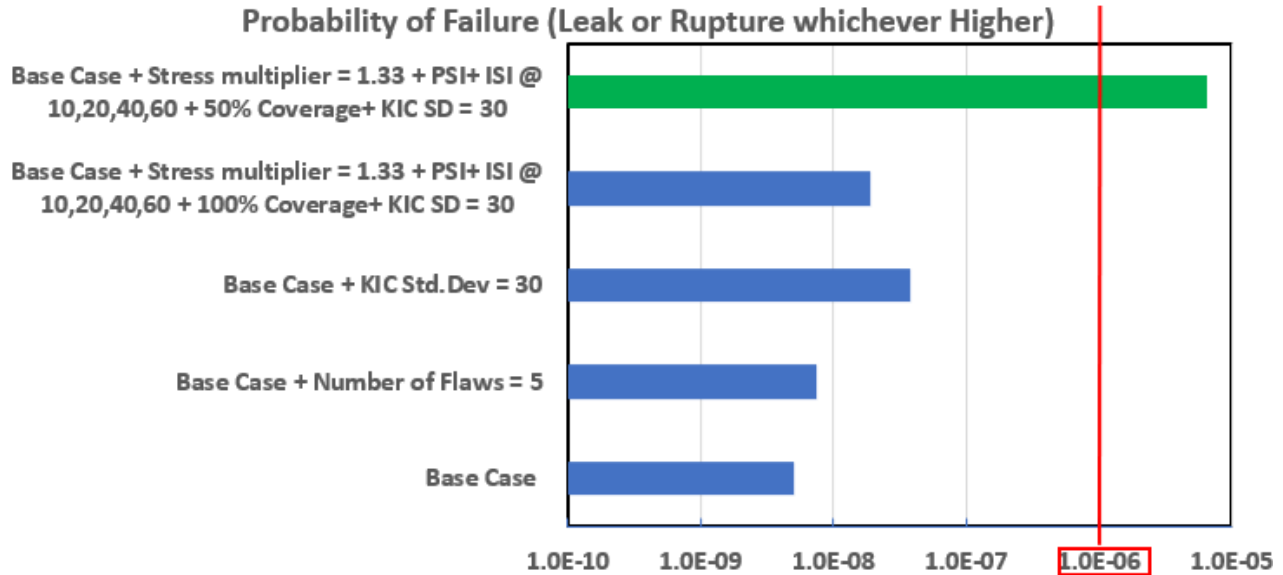


Figure 8-11
Summary of key sensitivity studies

8.4 Concluding Remarks on PFM and DFM Evaluations

From the PFM and DFM evaluations performed in this section, the following observations are made:

- The DFM evaluation demonstrated that a very long operating period (approximately 100 years) is necessary for a postulated initial flaw (with a depth equal to the ASME Code, Section XI acceptance standards) to propagate through 80% of the wall thickness (assumed as leakage for this study). After 80 years, the maximum K obtained from the analysis remains below the ASME Code, Section XI allowable fracture toughness, including the ASME Code, Section XI, Appendix G structural factor of 2.0 on primary stress, which indicates that all ASME Code, Section XI structural margins have been satisfied. This indicates that all in-scope SG primary- and secondary-side components are very flaw-tolerant.
- From the PFM evaluations, it was demonstrated that once PSI has been performed, the failure probabilities (in terms of both rupture and leakage) are significantly below the acceptance criterion of 10^{-6} failures per year after 80 years of operation.
- Sensitivity analyses were performed on most input parameters to identify the key variables that significantly affect the results of the evaluation. The most significant parameters are the fracture toughness of the SG vessel for the probability of rupture and the crack growth rate for the probability of leakage. The following items were also considered in the sensitivity studies:
 - A conservative upper shelf fracture toughness value of 200 ksi $\sqrt{\text{in.}}$ was used as the mean toughness in the PFM analysis. The sensitivity study indicated that, even if the fracture toughness was as low as 80 ksi $\sqrt{\text{in.}}$, the acceptance criterion would still be met for a realistic ISI scenario involving PSI followed by 20-year ISIs.

- With PSI only, a stress multiplier of 1.33 can be applied, and the acceptance criterion would still be met. When PSI is followed by 20-year ISI intervals, a stress multiplier of approximately 1.9 can be applied and the acceptance criterion would still be met. If the 20-year ISIs are preceded by the 10-year ISIs already performed by most plants to date, these stress multipliers could be increased further and still meet the acceptance criterion. Hence, the maximum R/t ratio variation meets the acceptance criteria.
- The PFM and DFM evaluations presented in this section incorporate many conservative inputs and, as such, the results are considered very conservative. The primary inputs and their conservatisms are summarized as follows:
 - **Stresses.** The temperature gradients and number of cycles used for this analysis are conservative. For example, typical design cycles for heatup and cooldown are 200 cycles for 40 years, which linearly projects to 300 cycles for 60 years. Typically, the actual number of operating cycles is less than the design values, making the number of cycles used conservative.
 - **Fracture toughness.** The mean fracture toughness value (200 ksi√in.) used in this analysis is a lower bound, as described in Section 8.2.2.6. In addition, a standard deviation of 5 ksi√in. was used, which produces a K_{IC} below the lower bound in 50% of the realizations.
 - **Fatigue crack growth.** The ASME Code, Paragraph A-4300 FCG law, with a 95% confidence limit on the data, was used as the median curve in this analysis, making it conservative.

Based on the evaluations performed in this section and the conservatism of the inputs, it is concluded that the current ASME Code, Section XI inspection schedules for the PWR SG components listed under Item Nos. B2.31, B2.32, B2.40, B3.130, C1.10, C1.20, and C1.30 in Tables IWB-2500-1 and IWC-2500-1 (essentially every 10 years) are conservative. The evaluations have shown that, after PSI, no other inspections are necessary for up to 80 years of plant operation to meet the NRC safety goal of 10^{-6} failures per year.

9

PLANT-SPECIFIC APPLICABILITY

The evaluations performed in this report used representative geometries, materials, and loading conditions associated with the PWR SG primary- and secondary-side components evaluated. As covered in Section 4, SG parameters vary depending on the design type as well as within each design type. Sensitivity studies were therefore performed to determine the effects of key input variables—such as geometry, materials properties, and stress—on the ability to meet the acceptance criterion. This section describes parameters that must be reviewed by a plant before using these results to confirm that the evaluation performed in this report is applicable.

9.1 Geometric Configurations

As described in Section 4, SG shell and primary inlet and outlet nozzles' geometries are similar across the various PWR designs. The stress sensitivity study performed in Section 8.3.4.3.2 (see Table 8-17) demonstrates that, for an inspection scenario of PSI followed by ISI at 20, 40, and 60 years, a stress multiplier of (at least) 1.9 can be applied to both the nozzle welds and the shell welds to account for geometric differences and the components would still meet the failure acceptance criterion. As shown in Table 4-4, the maximum variation of the R/t ratios of the components is 33.3%. Therefore, plant configurations with geometries bounded by the geometries selected and described in Section 4 are covered by this evaluation.

9.2 Materials Properties

The materials properties used to perform the stress analyses are typical of low-alloy ferritic steel pressure vessels. Most (if not all) SG nozzles and shell material are fabricated from low-alloy ferritic steel, although the B&W design might include some carbon steel; therefore, the materials properties used should be applicable to most SGs. The fracture toughness used in the evaluation is applicable to low-alloy ferritic steels and conforms to the requirements of ASME Code, Section XI, Appendix G, Paragraph G-2110. Therefore, plants with low-alloy (and carbon) ferritic steel SG nozzle and shell materials are covered by this evaluation.

9.3 Operating Transients

The operating transients and associated cycles evaluated in this report are summarized in Tables 5-6 through 5-9 and are typical of historical PWR operations, although they can vary depending on the design type as well as within each design type. As explained in Note 1 of Table 5-6, the loss-of-power transient (involving a thermal shock caused by the introduction of unheated auxiliary feedwater into a hot SG that has been boiled dry following blackout) is not considered in this evaluation due to its very low probability of occurrence. In the event that such a significant thermal event occurs, its impact on the K_{IC} value could require more frequent examinations and other plant actions outside the scope of this report's guidance.

In the fracture mechanics evaluations performed in this report, the transients that contribute the most to crack growth (absent the loss-of-power transient previously covered) are heatup and cooldown events. A total of 300 such events were evaluated during a 60-year plant life. The sensitivity study performed in Section 8.3.4.3.2 showed that for the realistic ISI scenario of PSI followed by ISI at 20, 40, and 60 years, a stress multiplier of 1.9 can accommodate small variations in the pressures and temperatures of the evaluated transients. Design transient severities were used in this evaluation, which have been shown through many years of industry fatigue monitoring experience to be conservative compared to actual transient severities experienced during plant operations. Therefore, plants with transients and cycles bounded by those shown in Tables 5-6 through 5-9 are covered by this evaluation.

9.4 Criteria for Technical Basis Applicability

Based on Sections 9.1–9.3, the following summarizes the criteria that must be met for the results of this report to be applied to a specific PWR plant.

9.4.1 General

- The loss-of-power transient (involving a thermal shock caused by the introduction of unheated auxiliary feedwater into a hot SG that has been boiled dry following blackout) is not considered in this evaluation due to its rarity. If such a significant thermal event occurs at a plant, its impact on the K_{IC} value will require more frequent examinations and other plant actions outside the scope of this report's guidance. As such, plants that have experienced such events should not use this report.
- The materials of the SG shell and nozzles must be low-alloy ferritic (or carbon) steels that conform to the requirements of ASME Code, Section XI, Appendix G, Paragraph G-2110.

9.4.2 SG Primary Inlet Nozzle-to-Vessel Welds (Item B3.130)

- The weld configurations must conform to those shown in Figures 1-3 through 1-5.
- The geometry of the piping attached to the primary inlet and outlet nozzles (that is, the RCS piping) for the various designs must be within 10% of the geometry values covered in Section 4.3.1 and listed in Table 9-1.
- The component must experience transients and cycles, over a 60-year operating life, bounded by those shown in Table 5-7 (for either a CE or Westinghouse design) and Table 5-8 (for a B&W design).

Table 9-1

Geometry values of piping attached to primary inlet and outlet nozzles

Component	Parameter	Westinghouse	CE	B&W
SG primary-side inlet nozzle	Nominal pipe size (in.)	29	42	36 / 45 ¹
SG primary-side outlet nozzle	Nominal pipe size (in.)	31	30	28

Note:

- (1) As explained in Section 4.3.1, the B&W primary-side inlet nozzle NPS is uniformly 36 in. at the nozzle inlet; the nozzle then tapers outward toward a larger diameter (identified as 45 in. based on the limited data available).

9.4.3 PWR SG Vessel (Primary Side) Welds (Item Nos. B2.31, B2.32, and B2.40)

- The weld configurations must conform to those shown in Figures 1-1 and 1-2.
- The SG vessel dimensions must be within 10% of the upper and lower bounds of the values discussed in Section 4.3.1 and listed in Table 9-2.
- The component must experience transients and cycles bounded by those shown in Table 5-7 over a 60-year operating life.

Table 9-2**Geometry values of SG vessel (primary side) components**

Component	Parameter	Westinghouse	CE	B&W
SG lower head	Diameter (in.)	127–136	164–203	149
SG upper shell	Diameter (in.)	166–178	239–244	149

9.4.4 PWR SG Vessel (Secondary Side) Welds (Item Nos. C1.10, C1.20, and C1.30)

- The weld configurations must conform to those shown in Figures 1-7 and 1-8.
- The SG vessel dimensions must be within 10% of the upper and lower bounds of the values presented in Section 4.3.1 and listed in Table 9-3.
- The component must experience transients and cycles bounded by those shown in Table 5-9 over a 60-year operating life.

Table 9-3**Geometry values of SG vessel (secondary side) components**

Component	Parameter	Westinghouse	CE	B&W
SG lower head	Diameter (in.)	127–136	164–203	149
SG upper shell	Diameter (in.)	166–178	239–244	149

10

SUMMARY AND CONCLUSIONS

This report presents the technical bases for inspection requirements of PWR SG Class 1 nozzle-to-vessel welds and the Class 1 and Class 2 vessel head, shell, tubesheet-to-head, and tubesheet-to-shell welds listed under the following item numbers in Tables IWB-2500-1 and IWC-2500-1 of ASME Code, Section XI:

- Item No. B2.31 – steam generators (primary side), head welds, circumferential
- Item No. B2.32 – steam generators (primary side), head welds, meridional
- Item No. B2.40 – steam generators (primary side), tubesheet-to-head weld
- Item No. B3.130 – steam generators (primary side), nozzle-to-vessel welds
- Item No. C1.10 – shell circumferential welds
- Item No. C1.20 – head circumferential welds
- Item No. C1.30 – tubesheet-to-shell weld

To establish the technical bases for these inspections, several topics were addressed; the findings of which are summarized as follows:

- A detailed study was performed on previous related projects that have involved ISI technical bases in the industry; it was concluded that there are several precedents in the industry for such a technical basis. Inspection requirements for many similar components, such as Class 1 PWR and BWR RPV welds, have been addressed in the past.
- A comprehensive survey was conducted for the U.S. and international PWR fleet to collect the number of examinations performed and associated examination results for the PWR SG item numbers listed previously. The survey results showed that, out of a total of 1,374 examinations identified by the plants that responded to the survey that have been performed on the previous item numbers, two PWR units reported flaws in Item No. B2.40 components and two PWR units reported flaws in Item No. C1.20 components that exceeded the acceptance criteria of ASME Code, Section XI. However, none of these flaws was considered service-induced, and flaw evaluations were performed to justify leaving the flaws in service. No other indications were identified in any of the in-scope components.
- PWR SG designs and operating experience were reviewed. Information was also reviewed regarding variability among SG designs in terms of dimensions, design pressures and temperatures, and ASME Code design considerations, as well as information on configurations with known limitations. The main conclusion was that, although variations exist among SG designs, the configurations are similar enough from a stress standpoint that

any differences could be addressed in the PFM and DFM evaluations through sensitivity analyses using stress multipliers. Therefore, representative components were selected for evaluation based on the plants that responded to the EPRI survey, the factors covered in Section 4.3, and a set of related criteria.

- SG operating transients were reviewed, and a set of representative transients with design basis severities and conservative numbers of occurrences for 60 years was established for the SG primary- and secondary-side components evaluated in this report. The operating transients were then used in stress analyses to determine through-wall stresses at critical weld locations. The stress analyses included the evaluation of representative SG primary inlet nozzle configurations for two plant design types and a bounding SG shell geometry. Additional sensitivity analyses were performed to address variations in nozzle and SG shell geometries across the fleet.
- A degradation mechanism evaluation was performed for all PWR SG primary- and secondary-side components evaluated in this report. It was concluded that the only potential degradation mechanism for these components is fatigue (that is, corrosion fatigue, mechanical fatigue, and/or thermal fatigue). Therefore, this mechanism was considered in the PFM and DFM evaluations for these components.
- Comprehensive DFM and PFM evaluations were performed. DFM evaluations were performed to determine the time for a postulated flaw to reach the minimum of 80% of the wall thickness in depth (assumed as leakage for this study) or the allowable fracture toughness with an applied structural factor and to help establish critical locations to be considered in the PFM evaluations. The PFM evaluations were performed using the NRC safety goal of 10^{-6} failures per year as the acceptance limit for various inspection scenarios. The results of the DFM and PFM evaluations showed the following:
 - The DFM evaluation demonstrated that it would take a very long operating period (approximately 100 years) for a postulated initial flaw (with a depth equal to the ASME Code, Section XI acceptance standards) to propagate to 80% through-wall (assumed as leakage). After 80 years, the maximum K obtained from the analysis remained below the ASME Code, Section XI allowable fracture toughness, including the Section XI, Appendix G structural factor for primary stress. This indicates that ASME Code, Section XI structural margins have been met and all components are very flaw-tolerant.
 - From the PFM studies, once PSI has been performed, both the probability of rupture and probability of leakage are below the NRC safety goal of 10^{-6} failures per year after 80 years of plant operation. Therefore, from a safety viewpoint, no other inspections are required through 80 years of plant operation. The evaluation also considered limited coverage during subsequent ISIs to address components for which full examination coverage cannot be obtained due to physical obstructions present for some components in some plants.
 - For an inspection scenario consisting of PSI followed by 20-year ISIs, the failure probabilities (both in term of rupture and leakage) are significantly below the acceptance criterion of 10^{-6} failures per year after 80 years of operation. The results are even more favorable if previous 10-year inspections are combined with the 20-year inspection interval.

- A sensitivity analysis was performed to identify key input parameters that have a significant effect on the results of the evaluation. Sensitivity studies were then performed on all key parameters. The most significant input parameters that affect the probabilities of failure and leakage were determined to be the fracture toughness of the SG vessel (for the probability of rupture) and the crack growth rate (for the probability of leakage). Other key results included the following:
 - A conservative upper shelf toughness value of 200 ksi√in. was used as a mean value with a standard deviation of 5 ksi√in. in the PFM analysis. A sensitivity study indicated that, even if the fracture toughness was as low as 150 ksi√in. or the standard deviation was increased to 30 ksi√in., the acceptance criterion would still be met.
 - An alternative crack growth rate that was investigated in BWRVIP-108 was used to evaluate the effect of crack growth rate on the probability of leakage. The alternative crack growth rate resulted in lower probabilities of leakage compared to the ASME Code, Section XI, Appendix A crack growth rate relationship.
 - With only PSI, a stress multiplier of 1.25 can be applied to the stresses considered in this evaluation and still meet the acceptance criterion. Using a more realistic scenario of PSI followed by three 20-year ISI intervals, stress multipliers of 1.9 can be applied and still meet the acceptance criterion. If the 20-year ISIs are preceded by the 10-year ISIs already performed by most plants to date, this stress multiplier would increase further.
- The evaluations presented in this report incorporate conservative inputs and, as such, the results are considered conservative. The two primary conservatisms are the following:
 - Fracture toughness: The mean fracture toughness, K_{IC} , value of 200 ksi√in. was used in this analysis. This value is a reasonable lower bound value, as described in Section 8.2.2.6. In addition, a standard deviation of 5 ksi√in. was used, which produced a K_{IC} of less than the lower bound in 50% of the realizations. Sensitivity studies were performed for K_{IC} values as low as 80 ksi√in. and a standard deviation of 30 ksi√in. that still showed acceptable results.
 - Fatigue crack growth: The ASME Code, Section XI, Paragraph A-4300 fatigue crack growth curve was used. This relationship, which represents a 95% confidence limit on the data, was assumed to be a median curve in this analysis.

Based on the evaluations performed and described in this report, technical bases were developed for various ASME Code, Section XI inspection schedules for all seven items (B2.31, B2.32, B2.40, B3.130, C1.10, C1.20, and C1.30) in Tables IWB-2500-1 and IWC-2500-1 (essentially every 10 years). These results can be used by PWR plants, using the plant-specific applicability requirements in Section 9, to establish optimized inspection schedules for these SG components.

11

REFERENCES

1. ASME Boiler and Pressure Vessel Code, Section XI, 2017 Edition.
2. *Technical Bases for Inspection Requirements for PWR Steam Generator Feedwater and Main Steam Nozzle-to-Shell Welds and Nozzle Inside Radius Sections*. EPRI, Palo Alto, CA: 2019. 3002014590.
3. *BWRVIP-108: BWR Vessels and Internals Project, Technical Basis for the Reduction of Inspection Requirements for the Boiling Water Reactor Nozzle-to-Shell Welds and Nozzle Blend Radii*. EPRI, Palo Alto, CA: 2002. 1003557.
4. Safety Evaluation of Proprietary EPRI Report, “BWR Vessel and Internals Project, Technical Basis for the Reduction of Inspection Requirements for the Boiling Water Reactor Nozzle-to-Vessel Shell Welds and Nozzle Inner Radius (BWRVIP-108).” U.S. Nuclear Regulatory Commission, Washington, D.C. December 19, 2007, ADAMS Accession Number ML073600374.
5. *BWRVIP-241: BWR Vessels and Internals Project, Probabilistic Fracture Mechanics Evaluation for the Boiling Water Reactor Nozzle-to-Shell Welds and Nozzle Blend Radii*, EPRI, Palo Alto, CA: 2010. 1021005.
6. Safety Evaluation of Proprietary EPRI Report, “BWR Vessel and Internals Project, Probabilistic Fracture Mechanics Evaluation for the Boiling Water Reactor Nozzle-to-Shell Welds and Nozzle Blend Radii (BWRVIP-241).” U.S. Nuclear Regulatory Commission, Washington, D.C. April 19, 2013, ADAMS Accession Number ML13071A240 and ML13071A233.
7. Code Case N-702, “Alternate Requirements for Boiling Water Reactor (BWR) Nozzle Inner Radius and Nozzle-to-Shell Welds,” ASME Code Section XI, Division 1, Approval Date: February 20, 2004. American Society of Mechanical Engineers, New York, NY.
8. Regulatory Guide 1.147, Revision 17, “Inservice Inspection Code Case Acceptability, ASME Code Section XI, Division 1,” dated August 2014. U.S. Nuclear Regulatory Commission, Washington, D.C.
9. B. Bishop, C. Boggess, and N. Palm, “Risk-Informed extension of the Reactor Vessel In-Service Inspection Interval,” WCAP-16168-NP-A, Rev. 3, October 2011.
10. Code Case N-691, “Application of Risk-Informed Insights to Increase the Inspection Interval for Pressurized Water Reactor Vessels,” ASME Code, Section XI, Division 1, Approval Date: November 18, 2003. American Society of Mechanical Engineers, New York, NY.
11. “Revised Safety Evaluation by the Office of Nuclear Reactor Regulation; Topical Report WCAP-16168-NP-A, Revision2, ‘Risk-Informed Extension of the Reactor Vessel In-service Inspection Interval,’ Pressurized Water Reactor Owners Group, Project No. 694,” July 26, 2011, ADAMS Accession Number ML111600303.

12. Code Case N-706-1, “Alternate Examination Requirements of Table IWB-2500-1 and IWC-2500-1 for PWR Stainless Steel Residual and Regenerative Heat Exchangers,” ASME Code Section XI, Division 1, Approval Date: January 10, 2007. U.S. Nuclear Regulatory Commission, Washington, D.C.
13. W. Bamford, B. Bishop, R. Haessler, and M. Bowler, “Technical Basis for Revision of Inspection Requirements for Regenerative and Residual Heat Exchangers,” Paper No. PVP2006-ICPVT-11-93892. Presented at ASME 2006 Pressure Vessels and Piping Division Conference (Vancouver, British Columbia, Canada, July 23–27, 2006).
14. *BWRVIP-05: BWR Vessels and Internals Project, Technical Basis for the Reduction of Inspection Requirements for the Boiling Water Reactor Nozzle-to-Shell Welds and Nozzle Blend Radii*, EPRI, Palo Alto, CA 2002. 1003557.
15. Information Notice 97-63 “Status of NRC Staff’s review of BWRVIP-05.” U.S. Nuclear Regulatory Commission, Washington, D.C., August 7, 1997.
16. Information Notice 97-63, Supplement 1, Status of Review of BWRVIP-05,” U.S. Nuclear Regulatory Commission, Washington, D.C., May 7, 1998.
17. “Final Safety Evaluation of the BWR Vessel and Internals Project BWRVIP-05 (TAC No. M93925),” U.S. Nuclear Regulatory Commission, Washington, D.C., July 28, 1998.
18. Generic Letter 98-05, “Boiling Water Reactor Licenses Use of the BWRVIP-05 Report to Request Relief from Augmented Examination Requirements on Reactor Pressure Vessel Circumferential Shell Welds,” U.S. Nuclear Regulatory Commission, Washington, D.C., November 10, 1995.
19. “Supplement to Final Safety Evaluation of BWR Vessel and Internals Project BWRVIP-05 Report (TAC No. MA3395),” U.S. Nuclear Regulatory Commission, Washington, D.C., March 7, 2000.
20. *BWRVIP-74-A: BWR Vessels and Internals Project, BWR Reactor Pressure Vessel Inspection and Flaw Evaluation Guidelines for License Renewal*. EPRI, Palo Alto, CA: 2003. 1008872.
21. P. Purtscher, S. Sheng, and T. Dickson, “Analysis of Circumferential Welds in BWRs for Life Beyond 60,” Paper No. PVP2015-45836. In Proceedings of the ASME 2015 Pressure Vessels and Piping Conference, Volume 7: Operation, Applications and Components (Boston, Massachusetts, July 19–23, 2015).
22. Code Case N-560-2, “Alternate Inspection requirements for Class 1, B-J Piping Welds,” ASME Code, Section XI, Division 1, Approval Date: March 28, 2000. American Society of Mechanical Engineers, New York, NY.
23. *Revised Risk-Informed Inservice Inspection Evaluation Procedure*. EPRI, Palo Alto, CA: 1999. TR-112657, REVB-A.
24. Regulatory Guide 1.193, Revision 5, “ASME Code Cases Not Approved for Use.” U.S. Nuclear Regulatory Commission, Washington, D.C.: August 2017.
25. Code Case N-577-1, “Risk-Informed Requirements for Class 1, 2 or 3 Piping. Method A,” ASME Code, Section XI, Division 1, Approval Date: March 28, 2000. American Society of Mechanical Engineers, New York, NY.

26. Code Case N-578-1, "Risk-Informed Requirements for Class 1, 2 or 3 Piping. Method B," ASME Code, Section XI, Division 1, Approval Date: March 28, 2000. American Society of Mechanical Engineers, New York, NY.
27. WCAP-14572, "Westinghouse Owners Group, Application of Risk-Informed Methods to Piping Inservice Inspection Topical Report," Revision 1-NP-A, February 1999.
28. Code Case N-716-1, "Alternative Piping Classification and Examination Requirements," ASME Code, Section XI, Division 1, Approval Date: January 27, 2013. American Society of Mechanical Engineers, New York, NY.
29. Report No. 2002-02A-01, "Risk-Informed / Safety Based (RIS_B) Technology, A Blended Approach to Defining Examination Requirements, ASME Section XI, Working Group on the Implementation of Risk-Based Examinations, Whitepaper in Support of Code Case N-716 (Item Nos. RI-02-02A, SGWCS 0301, BC04-318)," Revision 0, October 2005.
30. Report No. 2002-02A-01, "Risk-Informed / Safety Based (RIS_B) Technology, A Blended Approach to Defining Examination Requirements, ASME Section XI, Working Group on the Implementation of Risk-Based Examinations, Whitepaper in Support of Revision 1 to Code Case N716 (Item Nos. RI-02-02A, SGWCS 0301, BC04-318)," Revision 1, October 2010.
31. Code Case N-613-2, "Ultrasonic Examination of Full Penetration Nozzles in Vessels, Examination Category B-D, Reactor Nozzle-to-Vessel Welds and Nozzle Inside Radius Section, Figs. IWB-2500-7(a), (b), (c) and (d)," ASME Code, Section XI, Division 1, Approval Date: December 20, 2010. American Society of Mechanical Engineers, New York, NY.
32. *Nondestructive Evaluation: Reactor Pressure Vessel Threads in Flange Examination Requirements*. EPRI, Palo Alto, CA: 2016. 3002007626.
33. Letter from M. T. Markley (NRC) to C. R. Pierce (Southern Nuclear Operating Co. Inc.), "Vogtle Electric Generating Plant, Units 1 And 2, And Joseph M. Farley Nuclear Plant, Unit 1 -Alternative to Inservice Inspection Regarding Reactor Pressure Vessel Threads In-Flange Inspection (CAC Nos. MF8061, MF8062, MF8070)," dated January 26, 2017, ADAMS Accession Number ML17006A109.
34. Letter from J. G. Danna (NRC) to D. G. Stoddard (Dominion Nuclear Connecticut Inc.), "Millstone Power Station, Unit Nos. 2 And 3 - Alternative Requests RR-04-24 And IR-3-30 For Elimination of the Reactor Pressure Vessel Threads in Flange Examination (CAC Nos. MF8468 AND MF8469)," dated May 25, 2017, ADAMS Accession Number ML17132A187.
35. Letter from D. J. Wrona (NRC) to B. C. Hanson (Exelon Generating Company, LLC), "Braidwood Station, Units 1 and 2; Byron Station, Unit Nos. 1 and 2; Calvert Cliffs Nuclear Power Plant, Units 1 and 2; Clinton Power Station, Unit No. 1; Dresden Nuclear Power Station, Units 2 and 3; Limerick Generating Station, Units 1 and 2; Nine Mile Point Nuclear Station, Units 1 and 2; Peach Bottom Atomic Power Station, Units 2 and 3; Quad Cities Nuclear Power Station, Units 1 and 2; R. E. Ginna Nuclear Power Plant; And Three Mile Island Nuclear Station, Unit 1 – Proposed Alternative to Eliminate Examination of Threads In Reactor Pressure Vessel Flange (CAC Nos. MF8712-MF8729 and MF9548)," dated June 6, 2017, ADAMS Accession Number ML17170A013.

36. Letter from U. Shoop (NRC) to S. Capps (Duke Energy), “Brunswick Steam Electric Plant, Unit No. 1; Catawba Nuclear Station, Unit No. 2; Shearon Harris Nuclear Power Plant, Unit 1; McGuire Nuclear Station, Unit Nos. 1 and 2; Oconee Nuclear Station, Unit Nos. 1, 2 and 3; and H.B. Robinson Steam Electric Plant, Unit No. 2 - Alternative to Inservice Inspection Regarding Reactor Pressure Vessel Threads In Flange Inspection (CAC Nos. MF9513-MF9521; EPID L-2017-LLR-0019),” dated December 26, 2017, ADAMS Accession Number ML17331A086.
37. Code Case N-864, “Reactor Vessel Threads in Flange Examinations,” ASME Code, Section XI, Division 1, Approval Date: July 28, 2017. American Society of Mechanical Engineers, New York, NY.
38. *Evaluation of Basis for Periodic Visual Examination of Accessible Areas of Reactor Vessel Interior per Examination Category B-N-1 of ASME Section XI, Division 1*. EPRI, Palo Alto, CA: 2018. 3002012966.
39. Code Case N-885, “Alternative Requirements for Table IWB-2500-1, Examination Category B-N-1, Interior of Reactor Vessel, B-N-2, Welded Core Support Structures and Interior Attachments to Reactor Vessels, Category B-N-3, Removable Core Support Structures,” ASME Code, Section XI, Division 1, Approval Date: December 4, 2018. American Society of Mechanical Engineers, New York, NY.
40. *Identification and Assessment of Low-Value Nondestructive Evaluation Examinations with High Outage Impacts*. EPRI, Palo Alto, CA: 2018. 3002012965.
41. Letter from F. A. Kearney (Exelon) to U.S. Nuclear Regulatory Commission, “Byron Station Unit 2 90-Day Inservice Inspection Report for Interval 3, Period 3, (B2R17),” dated July 29, 2013, Docket No. 50-455, ADAMS Accession Number ML13217A093.
42. Letter from J. M. Sorensen (NMC) to U.S. Nuclear Regulatory Commission, “Unit 1 Inservice Inspection Summary Report, Interval 3, Period 3 Refueling Outage Dates 1-19-2001 to 2-25-2001 Cycle 20 / 05-26-99 to 02-25-2001,” dated May 29, 2001, Docket Nos. 50-282 and 50-306, ADAMS Accession Number ML011550346.
43. Letter from J. P. Solymossy (NMC) to U.S. Nuclear Regulatory Commission, “Response to Opportunity For Comment On Task Interface Agreement (TIA) 2003-01, “Application of ASME Code Section XI, IWB-2430 Requirements Associated With Scope of Volumetric Weld Expansion at the Prairie Island Nuclear Generating Plant” (Tac Nos. MB7294 and MB7295),” dated April 4, 2003, Docket Nos. 50-282 and 50-306, ADAMS Accession Number ML031040553.
44. NUREG-1841, “U.S. Operating Experience with Thermally Treated alloy 690 Steam Generator Tubes.” U.S. Nuclear Regulatory Commission, Washington, D.C.: 2007.
45. N. Cofie et al, “Management of Steam Generator Feedwater Nozzle Cracking in PWRs, ASME PVP-Vol. 286, pp. 31–43, 1994.
46. ASME Boiler and Pressure Vessel Code, Section III, 1998 Edition. American Society of Mechanical Engineers, New York, NY.
47. ASME Boiler and Pressure Vessel Code, Section II Materials, Part D – Properties, 2013 Edition. American Society of Mechanical Engineers, New York, NY.

48. Arkansas Nuclear One – Unit 1, SAR Amendment 28, Facility Operating License Number DPR-51, Docket Number 50-313, ADAMS Accession Number ML18323A147.
49. *Materials Reliability Program: Characterization of U.S. Pressurized Water Reactor (PWR) Fleet Operational Transients (MRP-393)*. EPRI, Palo Alto, CA: 2014. 3002003085.
50. *Component Life Estimation: LWR Structural Materials Degradation Mechanisms*. EPRI, Palo Alto, CA: 1987. NP-5461.
51. Information Notice No. 82-37, “Cracking in the Upper Shell to Transition Cone Girth Weld of a Steam Generator at an Operating Pressurized Water Reactor.” U.S. Nuclear Regulatory Commission, Washington, D.C. September 16, 1982.
52. Information Notice No. 85-65, Crack Growth in Steam Generator Girth Welds.” U.S. Nuclear Regulatory Commission, Washington, D.C. July 31, 1985.
53. C. Czajkowski, “Evaluation of Transgranular Cracking Phenomenon on the Indian Point 3 Steam Generator Vessel.” *International Journal of Pressure Vessels and Piping*, Vol. 26, 1986, pp. 97–110.
54. Regulatory Guide 1.36, Revision 1, “Nonmetallic Thermal Insulation for Austenitic Stainless Steel.” U.S. Nuclear Regulatory Commission, Washington, D.C.: May 2015.
55. ANSYS Mechanical APDL (UP20170403) and Workbench (March 31, 2017), Release 18.1, SAS IP, Inc.
56. T. Slot, “Stress Analysis of Thick Perforated Plates,” *Technomics*, 1972.
57. Letter from B. Sheron (NRC) to D. Mims, Acceptance for Referencing of Report SIR-94-080 - Relaxation of Reactor Coolant Pump Flywheel Inspection Requirements, May 21, 1997.
58. WCAP-15666, “Extension of Reactor Coolant Pump Motor Flywheel Examination,” July 2001.
59. W. Bamford, B. Bishop, D. Kurek, N. Closky, G. Stevens, L. Becker, and S. Ranganath, “Technical Basis for Elimination of Reactor Vessel Nozzle Inner Radius Inspections,” Proceedings of ASME 2001 Pressure Vessels and Piping Conference, Atlanta, Georgia.
60. T. Gilman, A. Alleshwaram, and T. Satyan-Sharma, “Industry First NRC Approved Appendix L Flaw Tolerance Evaluation to Manage Fatigue in a Surge Line,” PVP2015-45194, *Proceedings of the ASME 2015 Pressure Vessels and Piping Conference* (July 19–23, Boston, MA).
61. *Materials Reliability Program: Technical Basis for Reexamination Interval Extension for Alloy 690 PWR Reactor Vessel Top Head Penetration Nozzles (MRP-375)*. EPRI, Palo Alto, CA: 2014. 3002002441.
62. F. Simonen and K. Johnson, “Effects of Residual Stresses and Underclad Flaws on the Reliability of Reactor Pressure Vessels,” PVP-Vol. 251, *Reliability and Risk in Pressure Vessels and Piping*, ASME PVP Conference, 1993.
63. API Standard 579-1/ASME FFS-1, Fitness-for-Service, Second Edition, June 2016.
64. SI-TIFFANY 3.1 (software). Structural Integrity Associates, September 2018.

References

65. NRC Branch Technical Position MTEB 5-2, “Fracture Toughness Requirements,” Rev. 1, July 1981.
66. M. Kirk and M. Erickson, “Assessment of the Fracture Toughness of Ferritic Steel Fracture Toughness on or near the Lower Shelf,” Paper No. PVP2015-45850. In *Proceedings of the ASME Pressure Vessels and Piping Conference* (July 19–23, 2015, Boston, MA).
67. *Application of Master Curve Fracture Toughness Methodology for Ferritic Steels*. EPRI, Palo Alto, CA: 1999. TR-108390, Revision 1.
68. A. Der Kiureghian and O. Ditlevsen, “Aleatory or Epistemic? Does it Matter?” *Structural Safety*, Vol. 31, pp. 105–112, 2009.
69. Letter from B. Sheron (NRC) to C. Terry (BWRVIP), Transmittal of NRC Staff’s Independent Assessment of the Boiling Water Reactor Vessel and Internals Project BWRVIP-05 Report and Proprietary Request for Additional Information (TAC NO. M93925), August 14, 1997, ADAMS Legacy Library Accession Number 9709090456.
70. W. Marshall, “An Assessment of the Integrity of PWR Pressure Vessels.” Study Group Report, Service Branch, UKAEA, London, June 1982.
71. G. Schuster et al., “Characterization of Flaws in U.S. Reactor Pressure Vessels.” NUREG/CR-6471, Volumes 1–3.
72. F. Simonen, S. Doctor, G. Shuster, and P. Heasler, *A Generalized Procedure for Generating Flaw-Related Inputs to the FAVOR Code*. NUREG/CR-6817. U.S. Nuclear Regulatory Commission, Washington, D.C.: August 2013.
73. Structural Integrity Associates Calculation Package 1700313.301, Fabrication Flaw Size Distribution, Revision 0.
74. G. Stevens, S. Gosselin, and J. Davis, “Technical Basis Document for Section XI Nonmandatory Appendix L Revisions,” Appendix L Technical Basis Document, 9/21/2006.
75. xLPR Version 2.0: Technical Basis Document PWSCC and Fatigue Crack Growth and Coalescence Module Development, June 26, 2016.
76. M. Erickson and T. Dickson, “Recommended Screening Limits for Pressurized Thermal Shock,” NUREG/CR-1874, March 2010.
77. Letter from B. Thomas (NRC) to J. Lubinski (NRC), Acceptance Criteria to Use with xLPR Code, Version 2.0, dated November 7, 2016, ADAMS Accession Number ML16271A436.
78. Structural Integrity Associates Report DEV1806.401, *Software Project Plan, Software Requirements, Functional Specification, and Software Verification and Validation Plan for PROMISE Version 2.0*, Revision 1.
79. Structural Integrity Associates Report DEV1806.403, *PROMISE 2.0 Verification and Validation Report*, Revision 1.
80. Structural Integrity Associates Report DEV1806.402, *PROMISE 2.0 Theory and User’s Manual*, Revision 1.
81. SI Calculation 1600481.302, “Verification of Software VIPERNOZ,” Version 1.1, Revision 1.

82. Structural Integrity Associates Calculation Package, “Stress Intensity Factors (SIFs) for Nozzle Corner Cracks,” DEV1801.302, 3/12/2018.
83. W. Bamford, “Application of Corrosion Fatigue Crack Growth Rate Data to Integrity Analysis of Nuclear Reactor Vessels,” *Journal of Engineering Material and Technology*, Volume 101, 1979.
84. Sensitivity Analysis—Comparison Studies, DEI, EMC2, SIA, Version 5, September 2018.

The Electric Power Research Institute, Inc. (EPRI, www.epri.com) conducts research and development relating to the generation, delivery and use of electricity for the benefit of the public. An independent, nonprofit organization, EPRI brings together its scientists and engineers as well as experts from academia and industry to help address challenges in electricity, including reliability, efficiency, affordability, health, safety and the environment. EPRI also provides technology, policy and economic analyses to drive long-range research and development planning, and supports research in emerging technologies. EPRI members represent 90% of the electricity generated and delivered in the United States with international participation extending to 40 countries. EPRI's principal offices and laboratories are located in Palo Alto, Calif.; Charlotte, N.C.; Knoxville, Tenn.; Dallas, Texas; Lenox, Mass.; and Washington, D.C.

Together...Shaping the Future of Electricity

Programs:

Nuclear Power

Nondestructive Evaluation

© 2019 Electric Power Research Institute (EPRI), Inc. All rights reserved. Electric Power Research Institute, EPRI, and TOGETHER...SHAPING THE FUTURE OF ELECTRICITY are registered service marks of the Electric Power Research Institute, Inc.

3002015906

Electric Power Research Institute

3420 Hillview Avenue, Palo Alto, California 94304-1338 • PO Box 10412, Palo Alto, California 94303-0813 USA
800.313.3774 • 650.855.2121 • askepri@epri.com • www.epri.com